



**THE DETERMINATION OF THE RETROFITTING
STRATEGIES ON THERMAL COMFORT AND
ENERGY EFFICIENCY OF MOSQUES:
YAŞAMKENT MOSQUE EXAMPLE**

**2022
MASTER THESIS
ARCHITECTURE ENGINEERING**

Hosam Mohamed Abdulsalam DWELA

**Thesis Advisor
Assist.Prof.Dr. Merve TUNA KAYILI**

**THE DETERMINATION OF THE RETROFITTING STRATEGIES ON
THERMAL COMFORT AND ENERGY EFFICIENCY OF MOSQUES:
YAŞAMKENT MOSQUE EXAMPLE**

Hosam Mohamed Abdulsalam DWELA

**T.C.
Karabuk University
Institute of Graduate Programs
Department of Architecture
Prepared as
Master Thesis**

**Thesis Advisor
Assist.Prof.Dr. Merve TUNA KAYILI**

**KARABUK
January 2022**

I certify that in my opinion the thesis submitted by Hosam Mohamed Abdulsalam DWELA titled “THE DETERMINATION OF THE RETROFITTING STRATEGIES ON THERMAL COMFORT AND ENERGY EFFICIENCY OF MOSQUES: YAŞAMKENT MOSQUE EXAMPLE” is fully adequate in scope and quality as a thesis for the degree of Master of Science.

Dr. Öğr. Üyesi Merve TUNA KAYILI
Thesis Advisor, Department of Architecture

This thesis is accepted by the examining committee with a unanimous vote in the Department of Architecture as a Master of Science thesis. January 20, 2022

<u>Examining Committee Members (Institutions)</u>	<u>Signature</u>
Chairman : Doç. Dr. Arzuhan Burcu GÜLTEKİN (GU)
Member : Dr. Öğr. Üyesi Merve Tuna KAYILI (KBU)
Member : Dr. Öğr. Üyesi Tuğba İnan GÜNAYDIN (OHU)
Member : Dr. Öğr. Üyesi Ahmet Emre DİNÇER (KBU)
Member : Dr. Öğr. Üyesi Bahar Sultan QURRAIE (KBU)

The degree of Master of Science by the thesis submitted is approved by the Administrative Board of the Institute of Graduate Programs, Karabuk University.

Prof. Dr. Hasan SOLMAZ
Director of the Institute of Graduate Programs

“I declare that all the information within this thesis has been gathered and presented in accordance with academic regulations and ethical principles and I have according to the requirements of these regulations and principles cited all those which do not originate in this work as well.”

Hosam Mohamed Abdulsalam DWELA

ABSTRACT

M. Sc. Thesis

THE DETERMINATION OF THE RETROFITTING STRATEGIES ON THERMAL COMFORT AND ENERGY EFFICIENCY OF MOSQUES: YAŞAMKENT MOSQUE EXAMPLE

Hosam Mohamed Abdulsalam DWELA

Karabük University

Institute of Graduate Programs

The Department of Architecture

Thesis Advisor:

Assist. Prof. Dr. Merve TUNA KAYILI

January 2022, 161 pages

Reducing heating loads in buildings located in cold climates and thus increasing the efficiency of energy performance consumption is an issue that is dismissed, especially in buildings of worship. This research examines the effects of proposals for improvement such as insulation thickness, transparency ratio, glazing type, and green roof on thermal comfort and energy performance of a building located in a cold-semi-arid climate region. In the research, Yaşamkent Mosque in Ankara, Turkey, was determined as a contemporary architectural example as a case study. Firstly, the thermal comfort and energy consumption of the mosque were determined. Then the indoor temperature and relative humidity were observed, and then the simulation program outputs and observed data used in the study were verified. The effects of retrofitting scenarios on thermal comfort and energy consumption in the building were examined by the simulation program. As a result, it was found that the

best retrofitting scenario for building envelope is establishing a green roof on the roof with a 30% transparency ratio with Low-E glazing and an insulation thickness of 15 cm on the external walls and roof and 7.5 cm thermal insulation for the floor. With these improvements, indoor thermal comfort increased by 6%. And annual energy consumption decreased by 23%. The study is expected to have a role in guiding improvements to existing buildings of worship in colder climate regions.

Key Words : Mosque, Thermal comfort, Energy performance, Low-E window, Green roof, Thermal insulation.

Science Code : 80103

ÖZET

Yüksek Lisans Tezi

CAMİLERİNİN ISIL KONFOR VE ENERJİ PERFORMANSINA YÖNELİK İYİLEŞTİRME ÖNERİLERİNİN BELİRLENMESİ: YAŞAMKENT CAMİİ ÖRNEK

Hosam Mohamed Abdulsalam DWELA

Karabük Üniversitesi

Lisansüstü Eğitim Enstitüsü

Mimarlık Anabilim Dalı

Tez Danışmanı:

Dr.Öğr.Üyesi. Merve TUNA KAYILI

Ocak 2022, 161 sayfa

Soğuk iklimde yer alan yapıların ısıtma yüklerinin azaltılması ve buna bağlı olarak enerji performansının artırılması, özellikle ibadet yapılarında göz ardı edilen bir durumdur. Tez çalışması Soğuk-Yarı kurak iklim kuşağında bulunan bir ibadet yapısı üzerinden yalıtım kalınlığı, şeffaflık oranı, cam tipi ve yeşil çatı gibi iyileştirme önerilerinin yapının ısı konfor ve enerji performansına etkilerini irdelemektedir. Çalışmada, alan çalışması olarak çağdaş mimari örneği Ankara Yaşamkent Cami seçilmiştir. İlk olarak caminin ısı konfor ve enerji tüketimi belirlenmiş, sonrasında ise iç mekanda yapılan sıcaklık ve nem ölçümleri ile çalışmada kullanılan simülasyon programları ve çıktıları doğrulanmıştır. Yalıtım kalınlığının artırılması, uygun şeffaflık oranının ve cam tipinin tespit edilmesi ve yeşil çatı entegrasyonu senaryolarının yapının ısı konfor ve enerji performansına etkisi belirlenmiştir. Sonuç olarak en iyi iyileştirmenin, Low-E cam ile %30 şeffaflık oranı ve kabukta ve çatıda

15 cm yalıtım kalınlığı ile ve zeminde 7,5 cm yalıtım kalınlığı ile çatıda yeşil çatı kurgusunun olduğu tespit edilmiştir. Bu iyileştirmeler ile ısı konforunda %6 artarken, yıllık enerji tüketiminde ise %23 azalma gözlenmiştir. Çalışmanın soğuk iklim bölgesinde yer alan mevcut ibadet yapılarının iyileştirmelerinde yol gösterici olması beklenmektedir.

Anahtar Kelimeler : Cami, Isıl konfor, Enerji performansı, Low-E pencere, Yeşil çatı, Isı yalıtımı.

Bilim Kodu : 80103

ACKNOWLEDGMENT

I thank heaven Allah for my success in completing this mission.

I would like to thank:

Foremost my thesis advisor Assist. Prof. Dr. Merve TUNA KAYILI head of the architecture department at Karabük University. The door to Prof. Merve's office was always open whenever I ran into a trouble spot or had a question about my research or writing. She consistently allowed this research to be my own work but steered me in the right direction whenever she thought I needed it.

My parents for their care and prayer for me to achieve the best throughout all my life.

My wife and children for their suffering with me for all the late nights and early mornings over the past three years.

I would also like to thank Yaşamkent mosque Imam Mr. Muharrem for allowing me to carry out the study requirements inside the mosque.

CONTENTS

	<u>Page</u>
APPROVAL.....	ii
ABSTRACT.....	iv
ÖZET.....	vi
ACKNOWLEDGMENT.....	viii
CONTENTS.....	ix
LIST OF FIGURES	xii
LIST OF TABLES	xvii
ABBREVIATIONS INDEX	xx
PART 1	1
INTRODUCTION	1
1.1. ARGUMENT	1
1.2. OBJECTIVES	3
1.3. PROCEDURE	3
1.4. DISPOSITION	4
PART 2	5
THERMAL COMFORT AND ENERGY EFFICIENCY	5
2.1. CLIMATE AND BUILT ENVIRONMENT	5
2.2. THERMAL COMFORT	11
2.2.1. The Concept of Thermal Comfort	11
2.2.2. Factors Affecting Thermal Comfort	12
2.2.3. Thermal Comfort Standards	19
2.2.3.1. ASHRAE 55.....	19
2.2.3.2. ISO 7730	20
2.2.3.3. EN 15251	21
2.2.4. Thermal Comfort Models	23
2.2.4.1. Predicted Mean Vote (PMV)	23
2.2.4.2. Predicted Percentage of Dissatisfied (PPD).....	25

	<u>Page</u>
2.3. PASSIVE SOLAR DESIGN STRATEGIES	27
2.3.1. Thermal Mass	34
2.3.2. Glazing.....	37
2.3.3. Insulation	45
2.4. THERMAL COMFORT AND ENERGY EFFICIENCY IN MOSQUES	50
PART 3	58
MATERIAL AND METHOD	58
3.1. MATERIAL	58
3.1.1. Case Study	58
3.1.2. Climate Analysis of Ankara	68
3.1.3. Simulation Program	73
3.1.3.1. Grasshopper	74
3.1.3.2. Building Performance Simulation in Grasshopper	75
3.1.3.3. LadyBug Tools.....	77
3.1.3.4. HoneyBee Tools.....	79
3.1.4. Data Logger	80
3.2. METHOD	81
3.2.1. Data Collection and Calibration	81
3.2.2. Data Evaluation	82
3.2.3. Determination of the Retrofitting Scenarios.....	85
3.2.3.1. Scenario 1.....	86
3.2.3.2. Scenario 2.....	87
3.2.3.3. Scenario 3.....	89
3.2.3.4. Scenario 4.....	90
3.2.3.5. Scenario 5.....	91
PART 4	92
RESULTS AND DISCUSSION	92
4.1. CASE STUDY ANALYSIS.....	92
4.2. THE RESULT OF SCENARIO 1	94
4.3. THE RESULT OF SCENARIO 2	105

	<u>Page</u>
4.4. THE RESULT OF SCENARIO 3	109
4.5. THE RESULT OF SCENARIO 4	113
4.6. THE RESULT OF SCENARIO 5	117
PART 5	120
CONCLUSION	120
REFERENCES.....	126
APPENDICES	137
APPENDIX A: OBSERVED AND SIMULATED TEMPERATURE DATA	137
APPENDIX B: WORKFLOW TO CREATE ENERGY MODEL IN THE SIMULATION SOFTWARE	145
APPENDIX C: TABLES OF MONTHLY AVERAGE OF PMV&PPD	149
APPENDIX D: PHOTOGRAPHS OF SOME OF THE MODERN MOSQUES IN TURKEY	158
RESUME	161

LIST OF FIGURES

	<u>Page</u>
Figure 1.1. The structure of the thesis.....	4
Figure 2.1. Schematic Bioclimatic Index by Olgyay (Freire Castro, 2019).....	8
Figure 2.2. Factors affecting thermal comfort (Hegger et al., 2008).	13
Figure 2.3. Predicted mean vote (PMV).	24
Figure 2.4. CBE tool to calculate the PMV based on ASHRAE 55 (URL8).....	25
Figure 2.5. The relationship between PPD and PMV (Ekici, 2013).	26
Figure 2.6. Total primary energy supply by source, Turkey, 2000-19 (IEA, 2021).	28
Figure 2.7. Passive house principles (Passive house institute).	30
Figure 2.8. Elements of passive solar design (Energy.gov, 2010).	34
Figure 2.9. Structure of double glazed window (Lohia and Dixit, 2015).	39
Figure 2.10. Structure of triple glazed window (Lohia and Dixit, 2015).....	41
Figure 2.11. A sketch describes electrochromic evacuated glazing. (Fang et al., 2010).....	42
Figure 2.12. Comparison of the insulation value of window types (Donn and Thomas, 2010).....	43
Figure 2.13. Insulation in conjunction with thermal mass and glazing (Donn and Thomas, 2010).....	45
Figure 2.14. Turkey's thermal zones (TS 825).	47
Figure 2.15. Qibla direction in Turkey (Ilçi et al., 2018).	55
Figure 2.16. Mihrab wall of TBMM mosque (URL9).	56
Figure 3.1. Location of Yaşamkent mosque (Google Earth).	59
Figure 3.2. (a) The ground floor of the mosque, (b) The mosque during construction (URL10).....	60
Figure 3.3. The mosque model through Revit 2020.....	60
Figure 3.4. The ground floor of the mosque.	61
Figure 3.5. SNDWAY SW-T60 Laser distance meter.	61
Figure 3.6. External walls layers.	62
Figure 3.7. Workflow for preparing external walls, a. Construction materials, b. Establishing the wall, c. Properties of the wall.	62
Figure 3.8. Roof layers.	63

	<u>Page</u>
Figure 3.9. Workflow for preparing the roof, a. Construction materials, b. Establishing the roof, c. Properties of the roof.....	64
Figure 3.10. Floor layers.	65
Figure 3.11. Workflow for preparing the floor, a. Construction materials, b. Establishing the floor, c. Properties of the floor.....	65
Figure 3.12. A view inside the prayer hall showing the glazing façade.	66
Figure 3.13. South façade of Yaşamkent mosque.....	66
Figure 3.14. Double glazing window.	67
Figure 3.15. Workflow for preparing the window, a. Material properties, b. Establishing the window, c. Properties of the window.	67
Figure 3.16. Cold semi-arid climate regions according to Köppen World Map (Köppen, W).	69
Figure 3.17. Annual air temperature in Ankara by LadyBug Tools	70
Figure 3.18. Annual relative humidity in Ankara by LadyBug Tool.....	70
Figure 3.19. The wind rose for Ankara by LadyBug Tools.	71
Figure 3.20. Hourly wind speed for Ankara by LadyBug Tools.....	71
Figure 3.21. Psychometric Chart for Ankara during cold months. The yellow polygon is the comfort zone without any passive or active systems, and the green polygon is the comfort zone with the passive solar heating system.....	72
Figure 3.22. Comfortable hours of comfort zone for Ankara. (a) for comfort zone without any passive or active systems, (b) for comfort zone with the passive solar heating system by LadyBug Tools.....	72
Figure 3.23. Monthly heating and cooling loads (HDD&CDD) for Ankara by LadyBug Tools.	73
Figure 3.24. The process for drawing a sine curve within python and in Grasshopper (Mode Lab, 2015).....	74
Figure 3.25. Building Performance Simulation tools in Grasshopper (URL2).....	75
Figure 3.26. Complexity of preparing energy model for the case study.....	76
Figure 3.27. The relationship between Rhino, Grasshopper, Ladybug, Honeybee, and the simulation engines (URL3).....	76
Figure 3.28. Outputs of Ladybug tools (URL4).....	77
Figure 3.29. The Ewpmap for Turkey (URL5).	78
Figure 3.30. Steps to analyze sun-path for the case study by Ladybug tools.....	78
Figure 3.31. 3D diagram of sun-path visualizations for the case study.	79
Figure 3.32. HoneyBee working methodology (URL6).	79
Figure 3.33. RC-51H data logger.	80

	<u>Page</u>
Figure 3.34. Hourly observed and simulated temperature data.....	85
Figure 3.35. Creating opaque materials by HoneyBee components.	87
Figure 3.36. HoneyBee Glazing based on ratio component.....	88
Figure 3.37. The building with 75% glazing ratio (WWR-0,75).	88
Figure 3.38. The building with 50% glazing ratio (WWR-0,50).	89
Figure 3.39. The building with 30% glazing ratio (WWE-0,30).	89
Figure 3.40. Creating windows by HoneyBee components.	90
Figure 3.41. Green roof layers were used in the study (URL7).	90
Figure 4.1. Annual heating and cooling loads for the existing model by floor area (Kwh/m ²).	93
Figure 4.2. PMV and PPD values for the existing building.	94
Figure 4.3. Annual PMV and PPD chart for the existing building.	94
Figure 4.4. Heating and cooling loads for wall insulation by floor area (Kwh/m ²)...	95
Figure 4.5. PMV and PPD values for the wall with 80 mm insulation.	96
Figure 4.6. Annual PMV and PPD chart for the wall with 80 mm insulation.	96
Figure 4.7. PMV and PPD values for the wall with 100 mm insulation.	97
Figure 4.8. Annual PMV and PPD chart for the wall with 100 mm insulation.	97
Figure 4.9. PMV and PPD values for the wall with 150 mm insulation.	98
Figure 4.10. Annual PMV and PPD chart for the wall with 150 mm insulation.	98
Figure 4.11. PMV and PPD values for the wall with 200 mm insulation.....	99
Figure 4.12. Annual PMV and PPD chart for the wall with 200 mm insulation.	99
Figure 4.13. Heating and cooling loads for the floor by floor area (Kwh/m ²).	101
Figure 4.14. PMV and PPD values for the floor with 75 mm insulation.	101
Figure 4.15. Annual PMV and PPD chart for the floor with 75 mm insulation. ...	102
Figure 4.16. PMV and PPD values for the floor with 100 mm insulation.	102
Figure 4.17. Annual PMV and PPD chart for the floor with 100 mm insulation. .	103
Figure 4.18. PMV and PPD values for the roof with 150 mm insulation.	104
Figure 4.19. Annual PMV and PPD chart for the roof with 150 mm insulation....	104
Figure 4.20. Heating and cooling loads for WWR values by floor area (Kwh/m ²).	105
Figure 4.21. PMV and PPD values for WWR 75%.	106
Figure 4.22. Annual PMV and PPD chart for WWR 75%.	106

	<u>Page</u>
Figure 4.23. PMV and PPD values for WWR 50%.	107
Figure 4.24. Annual PMV and PPD chart for WWR 50%.....	107
Figure 4.25. PMV and PPD values for WWR 30%.	108
Figure 4.26. Annual PMV and PPD chart for WWR 30%.....	108
Figure 4.27. Heating and cooling loads for WWR values by floor area (Kwh/m ²).	110
Figure 4.28. PMV and PPD values for triple glazing system.	111
Figure 4.29. Annual PMV and PPD chart for triple glazing system.....	111
Figure 4.30. PMV and PPD values for double glazing system with low-E panels.....	112
Figure 4.31. Annual PMV and PPD chart for double glazing system with low-E panels.....	112
Figure 4.32. Heating and cooling loads for the green roof by floor area (Kwh/m ²). ...	114
Figure 4.33. PMV and PPD values for the green roof with 100 mm insulation. ...	114
Figure 4.34. Annual PMV and PPD chart for the green roof with 100 mm insulation.	115
Figure 4.35. PMV and PPD values for the green roof with 150 mm insulation. ...	115
Figure 4.36. Annual PMV and PPD chart for the green roof with 150 mm insulation.	116
Figure 4.37. PMV and PPD values for the green roof without insulation.	116
Figure 4.38. Annual PMV and PPD chart for the green roof without insulation...	117
Figure 4.39. Heating and cooling loads for the retrofitted model by floor area (Kwh/m ²).	118
Figure 4.40. PMV and PPD values for the best scenario.	119
Figure 4.41. Annual PMV and PPD chart for the best scenario.....	119
Figure 5.1. Annual heating and cooling loads for each scenario.	122
Figure Appendix A.1. Hourly observed and simulated temperature data on 28 Nov 2020.	141
Figure Appendix A.2. Hourly observed and simulated temperature data on 29 Nov 2020.....	141
Figure Appendix A.3. Hourly observed and simulated temperature data on 30 Nov 2020.....	142
Figure Appendix A.4. Hourly observed and simulated temperature data on 01 Dec 2020.....	142
Figure Appendix A.5. Hourly observed and simulated temperature data on 02 Dec 2020.....	143

	<u>Page</u>
Figure Appendix A.6. Hourly observed and simulated temperature data on 03 Dec 2020.....	143
Figure Appendix A.7. ElitechLogWin software.....	144
Figure Appendix B.1. Creating Honeybee Zone: a. Creat surfaces, b. Set the window, c. Set glazing ratio, d. United all components to make HB Zone.....	145
Figure Appendix B.2. Creating the Honeybee energy model, a. Creat building zones, b. unite and adjoin all zones to create the energy model.	146
Figure Appendix B.3. Preparing the energy model to be simulated, a. Creat energy model, b. simulation parameters, c. Construction materials, d. Weather file.	147
Figure Appendix B.4. Preparing the energy model to be simulated, a. Creat energy model, b. Running the simulation and presenting the results.	148
Figure Appendix D.1. Alacaatlı Uluyol Mosque, Ankara, Turkey.	158
Figure Appendix D.2. Mogan Gölü Mosque, Ankara, Turkey.....	158
Figure Appendix D.3. Fatih Üniversitesi Mehmet Hasircilar Mosque, Istanbul, Turkey.	159
Figure Appendix D.4. Şakirin Mosque, Istanbul, Turkey.	159
Figure Appendix D.5. Marmara Theology Mosque, Istanbul, Turkey.....	159
Figure Appendix D.6. GOSB Mosque, Kocaeli, Turkey.....	160
Figure Appendix D.7. Alaçatı Süreyya ve Muzaffer Baskıcı Mosque, Izmir, Turkey.. ..	160
Figure Appendix D.8. Pezberg Mosque, Penzberg, Germany.....	160

LIST OF TABLES

		<u>Page</u>
Table 2.1.	Sustainable design principles (Brophy and Lewis, 2011).....	10
Table 2.2.	Metabolic Rates for Typical Task, Based on ANSI/ASHRAE Standard 55-2013.....	17
Table 2.3.	Thermal insulation value of clothing components (ASHRAE 55, 2013).	18
Table 2.4.	ASHRAE thermal comfort index (ASHRAE 55, 2013).....	20
Table.2.5.	Categories of thermal comfort environment. Percentage of dissatisfaction due to general comfort and local discomfort (ISO 7730).	21
Table.2.6.	Categories of buildings with the level of expectations of occupants (EN 15251).....	22
Table.2.7.	Recommended criteria according to the building category (EN 15251).	22
Table 2.8.	Heat storage properties of materials (U.S. Department of Energy).	35
Table 2.9.	Comparison of different types of glazing systems in terms of thermal performance (Ghosha and Neogi, 2014).	44
Table 2.10.	Recommended U-values to be considered as maximum value by region (TS 825).....	48
Table 3.1.	External walls materials and their properties (Revit library).....	61
Table 3.2.	Roof materials and their properties (Revit library).....	63
Table 3.3.	Floor materials and their properties (Revit library).	64
Table 3.4.	Properties of the glass material (Revit library).....	67
Table 3.5.	Thermal properties of the building constructions (By author).	67
Table 3.6.	Heating and cooling degree-day limits (IEA, 2008).....	68
Table 3.7.	Heating degree-day for Ankara (Büyükalaca et al. 2001).	69
Table 3.8.	Cooling degree-day for Ankara (Büyükalaca et al. 2001).	69
Table 3.9.	Calibration criteria of IPMVP, FEMP, and ASHRAE Guideline 14 (Ruiz and Bandera, 2017).....	84
Table 3.10.	Calibration data of the case study.	85
Table 3.11.	U-value of the wall with different thermal insulation thicknesses.	86
Table 3.12.	U-value of the floor with different thermal insulation thicknesses.	86
Table 3.13.	U-value of the roof with different thermal insulation thicknesses.....	87

	<u>Page</u>
Table 3.14. Glazing ratio scenario.	88
Table 3.15. Properties of glazing types in the study (By author).	89
Table 3.16. U-value of green roofs examined in the study.	91
Table 3.17. U-value of building envelope in the retrofitted model (By author).	91
Table 4.1. Annual heating and cooling loads for the existing model by floor area (Kwh/m ²).	93
Table 4.2. Annual heating and cooling loads for each thickness of external walls by floor area (Kwh/m ²).	95
Table 4.3. Annual heating and cooling loads for the ground floor by floor area (Kwh/m ²).	100
Table 4.4. Annual heating and cooling loads for the roof by floor area (Kwh/m ²).	103
Table 4.5. Annual heating and cooling loads for each supposed glazing ratio by floor area (Kwh/m ²).	105
Table 4.6. Annual heating and cooling loads for each glazing type (Kwh/m ²). ..	109
Table 4.7. Annual heating and cooling loads for the green roof (Kwh/m ²).	113
Table 4.8. Annual heating and cooling loads for the retrofitted model by floor area (Kwh/m ²).	118
Table 5.1. Comparing the results.	120
Table 5.2. Comparing the best performance of retrofitting strategies with the existing model and 1,2,3,4 scenario.	121
Table 5.3. Comparing the annual consumption of retrofitting strategies with the existing model and 1,2,3,4 scenario.	123
Table Appendix A.1. Observed temperature data.	137
Table Appendix C.1. Monthly average PMV&PPD the existing model.	149
Table Appendix C.2. Monthly average PMV&PPD wall with 80mm insulation. ..	149
Table Appendix C.3. Monthly average PMV&PPD wall with 100mm insulation.	150
Table Appendix C.4. Monthly average PMV&PPD wall with 150mm insulation.	150
Table Appendix C.5. Monthly average PMV&PPD wall with 200mm insulation.	151
Table Appendix C.6. Monthly average PMV&PPD floor with 75mm insulation.	151
Table Appendix C.7. Monthly average PMV&PPD floor with 100mm insulation.	152
Table Appendix C.8. Monthly average PMV&PPD roof with 150mm insulation.	152
Table Appendix C.9. Monthly average PMV&PPD WWR 75%.	153
Table Appendix C.10. Monthly average PMV&PPD WWR 50%.	153

	<u>Page</u>
Table Appendix C.11. Monthly average PMV&PPD WWR 30%.	154
Table Appendix C.12. . Monthly average PMV&PPD triple glazing with 6mm cavity.	154
Table Appendix C.13. Monthly average PMV&PPD triple glazing with 10mm cavity.	155
Table Appendix C.14. Monthly average PMV&PPD double glazing with low-E panels.....	155
Table Appendix C.15. Monthly average PMV&PPD Green roof with 100 mm insulation.	156
Table Appendix C.16. Monthly average PMV&PPD Green roof with 150 mm insulation.	156
Table Appendix C.17. Monthly average PMV&PPD Green roof without insulation.	157
Table Appendix C.18. Monthly average PMV&PPD Retrofitted model (SC5).....	157

ABBREVIATIONS INDEX

ALCA	: Average Linkage Cluster Analysis
ASHRAE	: American Society of Heating, Refrigerating, and Air Conditioning Engineers
CBE	: The Center for the Built Environment
CEN	: Comité Européen de Normalisation (European Committee for Standardization)
CLO	: Clothes thermal insulation unit
CO ₂	: Carbon dioxide
CVRMSE	: Coefficient of Variation of the Root Mean Square Error
EPBD	: The Energy Performance of Buildings Directive
EVO	: Efficiency Valuation Organization
EPW	: Energyplus weather file
FEMP	: The Federal Energy Management Program
GHG	: Greenhouse Gas
HVAC	: Heating, ventilation, and air conditioning
IEA	: International Energy Agency
IPCC	: Intergovernmental Panel on Climate Change
IPMVP	: The International Performance Measurement and Verification Protocol
ISO	: The International Organization for Standardization
Low-E	: Low Emissivity
MET	: Metabolic Equivalent unit
MRT	: Mean Radiant Temperature
NEMV	: The North American Energy Measurement and Verification Protocol
NMBE	: Normalized Mean Bias Error
PMV	: Predicted Mean Vote
PPD	: Predicted Percentage of Dissatisfied
R-value	: Thermal resistance

SHGC	: The solar heat gain coefficient
TS 825	: The Turkish Standards Manual for Thermal Insulation for Buildings
TÜİK	: Türkiye İstatistik Kurumu (Turkish Statistical Institute)
U-value	: Thermal transmittance
WWR	: Window-to-wall ratio
ρ	: Correlation coefficient
ε	: Vacuum permittivity unit

PART 1

INTRODUCTION

In this chapter, the argument and objectives related to the research will be presented, and then the stages of the research will be defined, and the chapter will conclude with a review of the thesis disposition.

1.1. ARGUMENT

Buildings are envelopes designed primarily to protect their occupants from many risks, the most important of which are extreme climate conditions. In ancient times, man built his shelter from materials available in his environment and by methods that fit with the actual climate to provide sufficient thermal comfort. After the Industrial Revolution and the discovery of fossil fuels, man has wholly relied on the machine and adapted it to meet the thermal comfort requirements of buildings through air conditioning and heating systems regardless of outdoor climatic conditions.

The building sector, directly and indirectly, accounts for 30 percent of global final energy consumption, or around 3,100 Mtoe, including nearly fifty-five percent of global electricity consumption. Furthermore, building operations (heating and cooling systems) account for approximately twenty-eight percent of global CO₂ emissions, making decarbonization a top priority in the fight against global warming. (Abergel and Delmastro, 2020).

In order to minimize the demand for fossil fuel burning, new buildings must be responsible and respect the environment. New buildings must decrease the amount of energy demanded to perform and emphasize using energy from sustainable sources (Lentz, T. R, 2010).

Unfortunately, most building designers and builders around the world ignore the thermal performance of their structures. Existing knowledge about design solutions that create thermal comfort conditions in a building is hesitantly applied. Architects must recognize that they must design buildings with low heating and cooling loads and provide thermal comfort to their occupants.

Several studies have been conducted to assess the impact of building envelope design on energy consumption and thermal comfort separately. Nevertheless, the number of studies that have examined both energy consumption and thermal comfort remains very few (Atmaca et al., 2021).

Mosques are among the buildings that consume energy. They are places of worship for Muslims, the demand for implementing more mosques is constantly increasing. In Turkey, until 2021, there are 89,445 mosques (TÜİK).

Many studies examined the possibilities of improving the performance of mosques in terms of thermal comfort and energy consumption. Most of these studies were in hot-arid, hot-humid, and temperate climates (Azmi et al., 2021). Some of them followed the numerical approach by using simulation tools (Al-Homoud et al., 2009; Al-Homoud, 2009; Faghih and Bahadori, 2011; Alabdullatief and Omer, 2017). Others utilized a numerical approach supported by field measurements (Al Anzi and Al-Shammeri, 2010; Budaiwi et al., 2012; Ibrahim et al., 2014; Maarof, 2014; Bughrara et al., 2017; Yüksel et al., 2020; Atmaca and Gedik, 2020; Diler et al., 2021). No studies were found that examined the effect of passive solar design strategies in mosques located in cold climates.

During the early design stages, the best decision must be made by architects. They can control the building envelope components such as building materials, glazing, thermal insulation, etc., to achieve the best thermal comfort for users of their designs (Çakır, 2006).

There is no choice for architects beyond utilizing techniques that help the success of buildings' role in fighting climate change by addressing excessive energy

consumption in buildings while guaranteeing an adequate degree of comfort for users. Therefore, architects seek inspiration and incorporate advances from other sectors, including engineering, sophisticated computers, and building science. Building performance is gaining relevance in the architectural industry as an integrated design approach that simultaneously addresses environmental issues and comfort (Hong et al., 2000).

1.2. OBJECTIVES

The main objective of this research is to investigate the extent to which some passive solar design strategies reduce heating loads in cold semi-arid climates and achieve the comfort of users. The research also aims to analyze the design approach that followed in the implementation of the Yaşamkent Mosque and its effect on the users' thermal comfort and energy consumption. Another objective of this research is to examine the impact of the thickness of the thermal insulation on the thermal loads inside the mosque. According to the geographical location of Turkey, the direction of the Qiblah is approximately on the south. Thus the southern facade will be utilized to get the appropriate amount of direct solar. Hence, the study will evaluate the glazing ratio on the south facade. Also, the study will consider three types of glazing. Finally, the research will examine the effect of adding GreenRoof to the mosque's roof.

1.3. PROCEDURE

This research focused on assessing the impact of passive solar design strategies on thermal comfort in the cold climate by evaluating retrofitting scenarios done in Salih Bezci Mosque in Yaşamkent neighborhood in the city of Ankara capital the Turkish Republic. The first stage of the research was measuring indoor temperature degrees in the case study for six days by using Datalogger, with the help of drawings obtained from the Internet. A mosque survey was carried out, and the model was prepared by Revit 2020. Then in the second stage, the energy model was prepared in Rhino7 and Grasshopper, and the simulation process and retrofitting was conducted

by Ladybug Tools and HoneyBee tools. In the third stage, data from the previous two stages were collected, extracted, and presented in tables and graphs to be discussed.

1.4. DISPOSITION

This thesis consists of five parts. The first part explains the purposes and the objectives of the research and the stages taken to do it. The second part is concerned with previous studies. This part presents a literature review of the relationship between climate and built environment, as well as about thermal comfort and the factors affecting it and the standards and models used to measure it. It also provides information on the most important passive solar design strategies used in this study. The third part provides detailed information about the materials and method of the research. The fourth part includes the results and findings collected from the analysis software. The fifth part states the conclusion of the research by summarizing its findings and submitting recommendations.

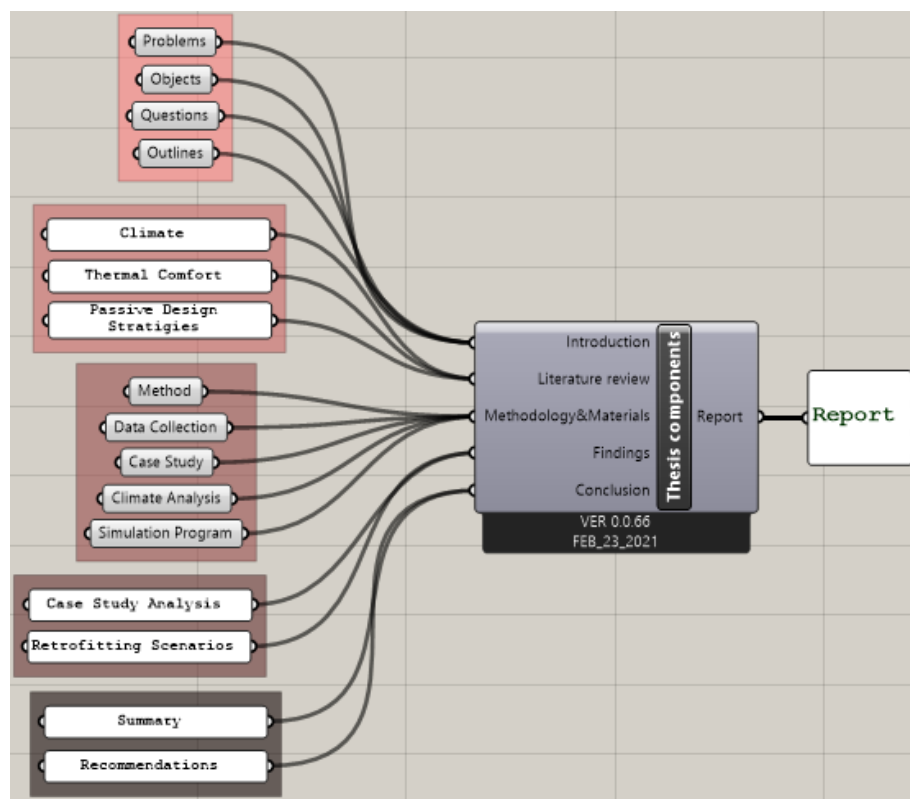


Figure 1.1. The structure of the thesis.

PART 2

THERMAL COMFORT AND ENERGY EFFICIENCY

This part provides a comprehensive overview of the climate and its relationship to the built environment, thermal comfort, passive solar architecture, and energy efficiency in mosques. The scientific literature in this part was derived from more than a hundred sources, including scientific articles, master's and Ph.D. theses, and websites. This part consists of four sections. The first section discusses the relationship between climate and the built environment and trends based on the compatibility between climate and architecture. In the second section, the concept of thermal comfort, the factors affecting it, and the standards used to monitor it are defined in detail. The third section explains the passive design strategies related to the case study in the research, as it covered in detail three passive design strategies: thermal mass, glazing, and thermal insulation. The fourth section presents the previous studies' results related to the thermal comfort and energy efficiency in mosques.

2.1. CLIMATE AND BUILT ENVIRONMENT

Climate is described as specific conditions to the factors of temperature, drought, humidity, etc., of a specific region. The world consists of many regions. Each region has its own distinct climatic characteristics. This climate is influenced by both natural and human-made factors throughout the region (Energy.gov). The natural factors contain the atmosphere, geosphere, hydrosphere, and biosphere, while the human-made factors involve the consumption of natural resources such as oil, natural gas, water, etc., and the built environment. Any defect in these factors will lead to a change in the local, regional and global climate, and this is what actually happened. The Intergovernmental Panel on Climate Change (IPCC) in the Fifth Assessment Report (AR5) defined climate as average statistical data on the state of the weather

over a long period that extends from months to thousands and millions of years (IPCC, 2014).

The relationship between climate, people, and buildings is unpredictable and interdependent (Crosbie, 2008). The built environment (for example, a city) has an effect on the climate within the geographical area over which this city extends, which makes this area has a climate that differs greatly from the climate of the region where the city is located. City components such as facades, roofs of buildings, and the surface of roads can affect the flow of wind and solar radiation, which leads to a change in temperature patterns. Moreover, the consumption of energy and natural resources in cities can produce considerable changes in the temperature.

The climate-appropriate design and using construction methods and materials that are compatible with the environment and the climate is the most important strategy for constructing low-energy buildings (Voss et al., 2007). Generally, when designing buildings, the climate of the implementation site is not taken into account, and the climatic and environmental characteristics of the site are not considered. And this is happening especially in developing countries. Accordingly, this will lead to a decrease in the quality of the indoor environment of the buildings, and perhaps its absolute absence, which makes these buildings uncomfortable and unsuitable for a healthy life for their users (HSE.gov). To solve this issue, people resort to installing mechanical heating systems and air-conditioning equipment (HVAC) to make the building environment more comfortable (Voss et al., 2007).

Buildings offer a safe indoor environment from uncontrollable outside environments and purpose to provide comfortable spaces for the occupants. Mostly, in the indoor environment, climate control is not successful with a direct impact in comfort conditions on the health of their users (Wagner et al., 2007).

The climate and architecture are always complex reactive conditions and dynamic dialogue. The climate plays a significant role in designing a building. Architecture attempts to modify the climate and create a comfortable environment. Day by day, paying attention to the potential impacts of climate on built environments is

increasing. At present, approximately fifty-five percent of the population throughout the world lives in cities. However, it is predicted to grow to more than sixty-eight percent over thirty years (United Nations Population Division, 2019).

Vitruvius is one of the most prominent architects in the ancient world. Vitruvius mentioned in his book that architecture has three basic features: firmness, commodity, and delight. And his book "Ten Books on Architecture" was the guide for Roman Empire projects. Vitruvius was aware that the climate has a deep impact on the buildings, especially that the wide geographical area of the Roman Empire was characterized by the diversity of climates that differ from one region to another, which is obvious from what he stated in his book "designs for homes ought to conform to diversities of climate" (Pearlmutter, 2007).

Butti and Perlin provided detailed building recommendations. In temperate regions such as the Italian peninsula, buildings should face the south to be warmer by gaining the most direct solar radiation from the sun. In contrast, the hot regions such as North Africa should direct buildings to the north to avoid more heat from the direct solar sun. Butti and Perlin explained that solar strategies had been rediscovered since the classical period (Pearlmutter, 2007).

Olgay stated that the way to control the environment is through acting with the climate rather than acting against it. Also, To achieve this, Olgay created the "schematic bioclimatic index," which is based on outdoor climate and not on just indoor practices. Following this method makes it possible to determine the relationship between climate and indoor thermal comfort for any climatic conditions (Freire Castro, 2019).

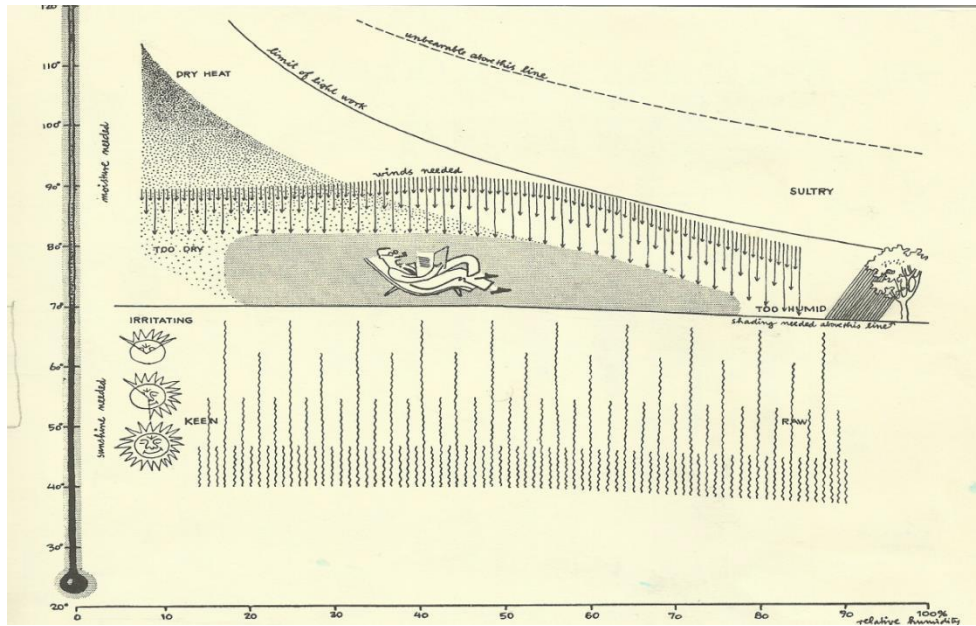


Figure 2.1. Schematic Bioclimatic Index by Olgyay (Freire Castro, 2019).

The idea of this index is based on determining the outdoor comfort zone without being affected by wind or direct solar radiation. The index covers a wide range of temperatures, relative humidity, wind velocity, and solar radiation.

Giovani was one of the first researchers in the 20th century to raise new possibilities for the use of thermal mass, thermal insulation, night ventilation, evaporative cooling, and direct and indirect solar heating. Givoni placed out the physical base of the relationship between climate and architecture with a rigorous knowledge of the physiological processes that drive uncomfortable (Kumar et al., 2018).

Mazria (2003) stated that if it was to be considered the impact of architects on building materials industries carefully, it could be easily concluded that the sector of architecture is responsible for more greenhouse gas emissions than any other sector. It is also the fastest-growing sector in energy consumption (Marzia, 2003). According to Mazria, architecture is destroying the world, and it is also the key to stopping this destruction. One of the solutions to stop this destruction may be instructing architects and other building professionals about designing and building more efficient buildings and compatible with the environment and the climate.

Metz. et al. (1982) explained that, although perfectly designed passive solar buildings can provide thermal comfort in addition to their positive impact on reducing energy consumption, they may have a significant impact on the decreasing indoor air quality. This effect occurs due to reduced air infiltration between indoors and outdoors and air movement in passive solar buildings. Due to the mechanism of work of passive solar systems that depend on the provisions of closing the spaces to maintain the thermal stability of the space, there is no air exchange between the interior and the exterior, which causes air to stagnate and thus deteriorates the indoor air quality. And this will have a negative effect on the health of the occupants. In addition to that, the noticeable rise in temperatures at the solar radiation collecting point (near the windows), as well as the possibility of increased humidity, etc., will have a significant impact on the decrease in indoor air quality (Metz et al., 1982).

Building materials are the main source of air pollution inside a building. The most important pollutants resulting from building materials in passive solar buildings include 1- Formaldehyde: It is one of the most common indoor air pollutants. Formaldehyde is a component of many building materials, including; Particleboard, which is used in flooring, furniture, etc., Plywood paneling which is widely used in the furniture industry, and interior decoration work, Resin-treated upholstery, Foam insulation, and Carpet (Metz et al., 1982). With formaldehyde in many materials inside the building, how much of this invisible gas we breathe every day is unimaginable, and the resulting health problems can cause. Constant exposure to formaldehyde can cause health problems such as skin sensitivity, eye irritation, headache, fainting, asthma, and respiratory diseases (Harris et al., 1981).

2- Radon: It is one of the compounds that contribute to lowering indoor air quality. The presence of high levels of radon causes cancerous diseases, especially lung cancer. They are mainly found in soil and groundwater. Moreover, many building materials contain radon, such as granite, bricks, concrete blocks, and gypsum boards (Metz et al., 1982).

Solar direct gain is the basis for the work of passive solar systems. Solar will transfer through the windows directly to the indoor. Continuous exposure to strong solar at

points near the collection elements (windows) will increase the temperature of building materials and furnishings at those points, causing the emission of formaldehyde and radon. Also, the increase in humidity in indoor spaces is related to the formation of fungus and bacteria, which causes a decline indoor air quality.

Agreeing with Mazria, Brophy and Lewis announced that architects have the key to making buildings compatible with the environment. According to Table 2.1, the design process is categorized into six stages: inception, design, tender, construction, operation, and refurbishment (Brophy and Lewis, 2011).

Table 2.1. Sustainable design principles (Brophy and Lewis, 2011).

Inception	<ul style="list-style-type: none"> • Considering sustainability first. • Agreeing to the building to be compatible with the environment. • Analyze the site thoughtfully. • Study further good practices.
Design	<ul style="list-style-type: none"> • Use passive heating and cooling possibilities. • Use available local materials. • Analysis expected building energy performance. • Finalize architectural plans. • Determine construction techniques.
Tender	<ul style="list-style-type: none"> • Define green design requirements for contractors.
Construction	<ul style="list-style-type: none"> • Protect the environment from damages during working on the site. • Ensure contractors are observant of the implementation of the specifications. • Examine building envelope implementation quality.
Operation	<ul style="list-style-type: none"> • Evaluate the performance of the building with the environment. • Assessment indoor air quality.
Refurbishment	<ul style="list-style-type: none"> • Check energy performance before performing any retrofit. • Verify the possibility and quality of retrofitting.

The planning stage of the implementation of the building is one of the most critical stages. During this stage, determining the costs of construction and the environmental performance of the building can be obtained (Lechner, 2014). In

addition, the possibility of determining the environmental impact of the building is up to ninety percent during the early design stage (Hosey, 2012).

Thermal comfort is one of the issues that is becoming one of the priorities of architects, designers, and researchers curious about building physics. Many studies have been conducted in this field to determine thermal comfort. So, what is the concept of thermal comfort?. How it is measured?. And how to make buildings more comfortable for their occupants?. All these questions will be answered in detail in the next section.

2.2. THERMAL COMFORT

People can stay in a range of environments. This capacity of humans to adapt to varied environments has led to different conceptions of the perfect climate. Hence, what may be regarded as an excellent climate in one place might be deemed unpleasant in another region. Therefore, thermal comfort varies from place to region. Over the past several decades, researchers have been investigating the physical, physiological, and psychological reactions of humans to their surroundings with the objective of building an effective model to define and predict comfort temperature. (Gabril, 2014).

2.2.1. The Concept of Thermal Comfort

Thermal comfort is a personal condition related to an individual. It cannot be definitely defined. However, various researchers have made many efforts to define thermal comfort. Nevertheless, there are some differences in the definitions. Still, the most internationally accepted definition of thermal comfort has been stated by International standard ASHRAE 55 (American Society of Heating, Refrigerating and Air-Conditioning Engineers) defined thermal comfort as “that condition of mind which expresses satisfaction with the thermal environment.” (ANSI/ASHRAE Standard 55, 2013).

But, this definition was questioned by Heije. Within the view of definition, it clearly adopts factors beyond the physical/physiological, and it indicates that thermal comfort will be affected by individual differences in mood, personality, culture, and other individuals, organizational as well as social factors. Heije stated that “This description seems to be quite precise but it is not, when comfort is regarded as solely as a subjective mental state it seems elusive, both because it cannot be measured objectively and because it is continuously changing” (Gabril, 2014).

Fanger clarified that the compatibility of the thermal environment of any building with the requirements of thermal comfort for users is the main goal in any artificial environment built in any climate. As also claimed that if a set of people is subjected to the climatic conditions of the same room, satisfying all at the same time would be unachievable because of physical differences. Consequently, if one desires to create ideal thermal comfort for the group, thermal comfort for the maximum proportion of the group should indeed be targeted (Fanger, 1970). Fanger stated that the fundamental purpose of the heating and air conditioning industry is to ensure thermal comfort for occupants. Also, he said that from a more profound viewpoint, the main purpose of buildings is to offer comfortable places for their occupants, which depend on these thermal surroundings. This approach produced a radical influence on the construction sector, the selection of materials, and the whole building industry.

2.2.2. Factors Affecting Thermal Comfort

Many researchers in various fields such as physiologists, psychologists, sociologists, physicists, and environmental engineers were interested in studying the intricate interactions between humans and the environment. This interest led to the conducting of many studies in this respect (Nicol et al., 2012). These studies make it possible to conclude that thermal comfort depends on the human perception of external influences such as physiological, psychological, physical, and environmental factors. This approach can be considered as a comprehensive context for the concept of thermal comfort. The factors influencing thermal comfort have been summarized as shown in Figure 2.2.

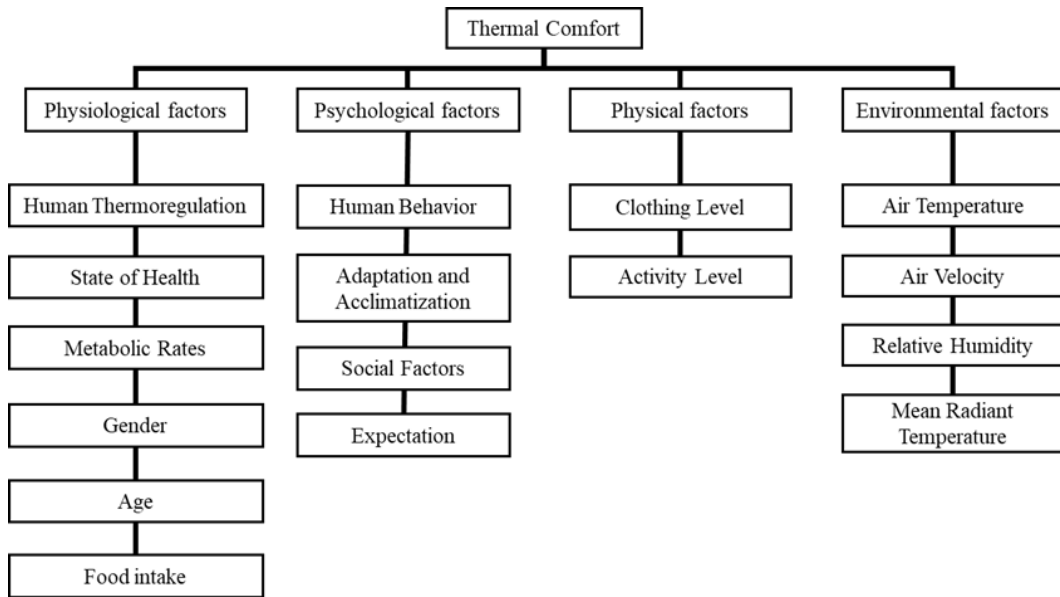


Figure 2.2. Factors affecting thermal comfort (Hegger et al., 2008).

Environmentally, four parameters have an enormous effect on the thermal comfort of any occupied space, air temperature, mean radiant temperature of the surrounding, air velocity, and relative humidity (Kılıçarslan, 2013). Air temperature determines the heat loss rate in the air mainly due to convection and thermal conductivity. But in fact, it does not affect the evaporation rate of water from the skin, which mainly relies on the amount of relative humidity in the air (Arens and Zhang, 2006). The mean radiant temperature of the surroundings (including people, furniture, landscape, etc.) influences the rate of radiant heat transfer between the body and the surrounding environment. Typically, surface temperatures change continually from location to location inside a space. Due to this, the radiant heat exchange will change according to the position in space. When measuring the temperature of any point inside a space, consideration must be given to the radiation effect on this point according to the distance between it and the radiating surface. The air motion influences heat transfer rate among skin and air through convection and evaporation from the body as well. The air motion influences heat transfer rate among skin and air through convection and evaporation from the body as well. If the moisture content of the air is reduced, the increase in air velocity becomes undesirable (Gabril, 2014).

According to Fanger, thermal comfort is affected by six factors: Two physical factors; the activity level of occupants, the thermal resistance of the clothing, and

four environmental factors; air temperature, mean radiant temperature, air velocity, and relative humidity (Fanger, 1970). In fact, thermal comfort has been defined differently in many studies. However, there is a common rule among all these studies, which is that there are many environmental and personal factors that must be recognized for humans to reach a state of thermal comfort (Parsons, 2002).

Çengel mentioned in his book that thermal comfort, in addition to environmental factors like temperature, air motion, and relative humidity, depends on metabolism rate and clothing insulation. Also, he stated that 23 to 27 °C is accepted as operative temperatures for normal clothed people who are resting or doing light works. The relative humidity affects the heat, and increasing relative humidity leads to decreasing heat by evaporation slowing down. The normal level of relative humidity is accepted as 30-70%, so the best level is 50%. Excessive air motion can cause thermal discomfort by generating partial cooling on the human body. Moreover, asymmetric thermal radiation can cause thermal discomfort. The wide glazed surfaces and uninsulated walls/floor can cause asymmetric thermal radiation (Çengel, 2002).

Physiological factors are the first reaction of the human body when a change in the thermal state happens. There are six physiological factors that have a great influence on the feeling of thermal comfort: Human thermoregulation, state of health, metabolic rates, gender, age, and food intake.

The human body is distinguished by its tremendous ability to regulate the body's internal temperature. The internal temperature of a healthy person is around 37 degrees Celsius. Due to the continuous changes in the ambient temperature, heat loss occurs from the human body to the surrounding environment. In order to maintain the thermal balance between the lost heat and the heat produced by the body, the brain works like a thermostat to maintain a constant internal temperature continuously. When the temperature in human skin decreases at a rate faster than 0.004 degrees Celsius per second, the cold receptors begin to produce a cold sensation, while the warm receptors begin to produce warm sensations if the

temperature increases by more than 0.001 degrees Celsius per second approximately (Olesen and Parsons, 2002).

Physiologically, when the body temperature changes. The body restores the heat balance using the blood to transfer large amounts of heat, as the blood has a high heat capacity and high thermal conductivity. When the temperature decreases, the human body begins to contract the vessels. By this process, blood circulation to the peripheral part of the body is reduced, which reduces the loss of heat in the surrounding areas. In contrast, when the temperature increases, the body begins to widen the vessels. Then, blood flow to the extremities of the body increases, which leads to blood flow to the skin and increased heat loss in the surrounding environment (Gabril, 2014). In addition, the body can decrease the temperature by evaporation, as the body begins to sweat when the temperature rises. Also, heat can be reduced by convection from the body to the air. And by direct contact of the body on things (floor, furniture, etc.), in addition to radiating heat to nearby surfaces inside the room (Nicol et al., 2012).

Metabolic rate plays an important role in the process of thermal comfort of the body. It is defined as the rate of energy expended by the body per unit of time (Lou et al., 2018). It is also defined as the energy that the body uses both for performing its normal functions, such as maintaining the body itself, and performing external functions such as physical work (Parsons, 2010).

In the thermal comfort aspect, according to field studies, there is no difference between males and females, and even if it is found, it is a small difference and has no significance, as men and women prefer almost the same thermal environments (ANSI/ASHRAE 55, 2013). In contrast to these studies, other studies have observed significant differences in thermal comfort between males and females (Erlandson et al., 2005). In addition, many studies have observed that in the same thermal conditions, females express more dissatisfaction than males. Thus it is suggested that females should be taken in the first place when examining indoor thermal comfort requirements because if females are satisfied, it is very likely that males are satisfied as well (Karjalainen, 2012). Some studies have found that with aging, the

metabolism rate decreases slightly. This decrease is compensated for by less evaporation loss in the elderly. And this is due to the lack of activity in the elderly. These studies have also discovered that older males and females prefer roughly the same thermal conditions (Karwowski, 2010).

Psychologically, there are four factors that affect a person's thermal comfort: Human behavior, Acclimatisation, social and culture, and expectation. In addition to the human physiological system of thermoregulation that reacts and responds involuntarily to the changes of the surrounding environment, human behavior is an important and influential system in order to restore the thermal balance of the body. Parsons stated in his study that the most powerful form of human thermoregulation is personal behavior. For example, dressing or undressing, changing position, and moving are human behavior that comes in response to uncomfortable feelings (Parsons, 2010).

Acclimatization is another psychological factor that influences the thermal comfort of humans. When the human body is exposed regularly for a long time to the same climatic conditions, the human body will naturally adapt to this condition. Koenigsberger et al. said that when the human body is exposed to new climate conditions, it will take 30 days to regain its acclimatization state again (Gabril, 2014). Geographical location and climate type are the main factors that influence the time the human body needs to adapt. Studies have shown that people exposed to warm and humid climates over a long period spanning several generations have better tolerance to higher temperatures than people in cold climates (Yamtraipat et al., 2005).

Social and cultural factors have an important role in terms of the thermal comfort of humans. The thermal perception and preferences of people are influenced by culture as well as climate. Culture has been shown to have a great influence on clothing type, human behavior, and technology (Andamon et al., 2006). Generally, people are inspired by culture to create designs for buildings as well as clothing that helps adapt to the outdoor thermal conditions (Cole and Lorch, 2003).

There are two physical factors (personal factors) that influence the conditions of thermal comfort: Activity level and clothing level. The level of activity is the factor that affects the level of metabolic energy. The heat produced by the body is measured in the Metabolic Equivalents unit (MET), which can be expressed as energy density per unit body surface area (W/m^2). The metabolic rate level was determined for each activity level based on values developed through laboratory studies to determine MET rates for specific activities and professions (ANSI/ASHRAE 55, 2013; ISO 7730, 2005).

Table 2.2. Metabolic Rates for Typical Task, Based on ANSI/ASHRAE Standard 55-2013.

Activity	MET	W/m^2	W(av)
Sleeping	0.7	40	70
Reclining, lying in bed	0.8	46	80
Seated, at rest	1	58	100
Standing, sedentary work	1.2	70	120
Very light work (shopping, cooking, light industry)	1.6	93	160
Medium-light work (house, machine tool)	2	116	200
Steady medium work (jackhammer, social dancing)	3	175	300
Heavy work (sawing, planning by hand, tennis) up to	6	350	600
Very heavy work (squash, furnace work) up to	7	410	700

On the other hand, the rate of MET can be influenced by body type, body mass, fitness, hormone levels, and blood flow. Furthermore, performing mental tasks could raise activity levels up to 1,3 MET, and periods of stressful activity resulting in greater muscle tension could raise the MET rates of typical office tasks up to 1,5 MET ((Lou et al., 2018).

Since ancient times, humans began to wear clothes to protect their bodies from the climate conditions (heat, sun, rain, cold, etc.) They mainly used animal skins and plants as clothing to cover their bodies. The clothes act as thermal insulation for the body it can control the level of heat loss from the body to the surrounding environments. The thermal insulation value of the clothing is expressed in the CLO unit, where CLO is the value of thermal resistance that is necessary to keep thermal comfort in a sitting position in a well-ventilated room.

Previous studies relied on season and climate to estimate the CLO values. They set the thermal insulation value of clothing at 0,35-0,6 CLO in summer and 0,8-1,2 CLO in winter. Table 2.3 shows the CLO values estimated by using tables developed from clothing insulation studies conducted in laboratory studies (ANSI/ASHRAE 55, 2013; ISO 7730, 2005)

Table 2.3. Thermal insulation value of clothing components (ASHRAE 55, 2013).

Male	Clo	Female	Clo
Underwear: singlets	0,06	Underwear: bra + panties	0,05
T-shirt	0,09	half slip	0,13
Briefs	0,05	Full slip	0,19
long, upper	0,35	Long upper	0,35
long, lower	0,35	Long lower	0,35
Shirt: light, short sleeve	0,14	Blouse: light	0,20
light, long sleeve	0,22	Heavy	0,29
heavy, short sleeve	0,25	Dress: light	0,22
heavy, long sleeve	0,29	Heavy	0,70
+5% for tie or turtle-neck			
Vest: light	0,15	Skirt: light	0,10
Heavy	0,29	Heavy	0,22
Trousers: light	0,26	Slacks: light	0,26
Heavy	0,32	Heavy	0,44
Pullover: light	0,20	Pullover: light	0,17
Heavy	0,37	Heavy	0,37
Jacket: light	0,22	Jacket: light	0,17
Heavy	0,49	Heavy	0,37
Socks: ankle length	0,04	Stockings: any length	0,01
knee length	0,10	Panty hose	0,01
Footwear: sandals	0,02	Footwear: sandals	0,02
shoes	0,04	Shoes	0,04
boots	0,08	boots	0,08

However, the values described in the previous table are the result of studies conducted on a standing person wearing Western-style clothing. Therefore, when conducting studies in places with different cultures in the type and shape of clothing,

these values are useless when using them. Nicole has described that clothes that can be considered thick in one climate can be considered thin in another (Nicol et al., 2012).

In terms of physical and psychological factors, Nicol explained that there is no temperature at which everyone will be comfortable: comfort is a psychological situation determined by climate, culture, and economics (Nicol, 2004). It can be said that physiological and psychological factors are difficult to predict or measure, as they differ from one person to another. On the contrary, it is possible to control the physical and environmental factors to provide a comfortable environment.

2.2.3. Thermal Comfort Standards

People spend most of their time indoors. More than ninety percent of people spend more than twenty hours a day in closed environments, at home, at work, in shopping centers, in cafes, etc. Therefore, the indoor environment has a great influence on the conditions of the occupants and the quality of life, since the rising importance of analyzing and understanding the impact of the internal environment on people. Numerous local and international standards have been developed related to indoor environmental quality (Allen and Macomber, 2020).

In this research, the criteria for thermal comfort within the indoor environment will be clarified. Regarding the measurement of thermal comfort, there are three widely used international standards: Standard ASHRAE 55 developed in 2004, ISO Standard 7730 developed in 2005, and CEN Standard EN15251 developed in 2007. However, In this study, ASHRAE 55 standard will be used to monitor indoor thermal comfort because the component that calculates thermal comfort in the simulation tools that will be utilized in the study is designed according to ASHRAE 55 standard.

2.2.3.1. ASHRAE 55

ASHRAE is an abbreviation for the American Society of Heating, Refrigerating and Air-Conditioning Engineers, which was established in New York City, US, in 1894

(ASHRAE, 2004). ASHRAE 55 is based on the predicted average votes PMV and the expected percentage of dissatisfied PPD measurement methods to determine comfort zone. The feeling of satisfaction or dissatisfaction varies according to the state of the occupants within the space. The standard assumes that people are considered to be in a comfortable thermal environment when voting with zero on a 7-point scale of ASHRAE. The standard establishes conditions adequate to the majority of occupants subjected to the same conditions within a specified space (Olesen and Brager, 2004). A “majority” was defined as the general acceptance of 80% of occupants for a given level on a scale of ASHRAE. The ideal temperature is calculated by the following formula:

$$T_{comf} = 0.31T_o + 17.8 \quad (2.1)$$

Where: “ T_{comf} ” is the ideal temperature for comfort.

“ T_o ” is the mean outdoor temperature for the collected data.

Table 2.4. ASHRAE thermal comfort index (ASHRAE 55, 2013).

Question	Scale	Thermal sensation	Vote
How do you feel about the thermal environment in this room?	3	Hot	
	2	Warm	
	1	Slightly warm	
	0	Comfortable, neutral	
	-1	Slightly cool	
	-2	Cool	
	-3	Cold	

2.2.3.2. ISO 7730

The abbreviation “ISO” stands for the International Standards Organisation, which was established in Geneva, Switzerland, in 1947. ISO developed a European thermal standard that is known as ISO 7730, which is related to human physiology and heat transfer. ISO 7730 standard is based on both thermal comfort indices the predicted average votes PMV, and the expected percentage of dissatisfied PPD. The standard

has classified buildings into categories according to the PMV inside these buildings, as shown in the Table 2.5 (Arens et al., 2010).

Table.2.5. Categories of thermal comfort environment. Percentage of dissatisfaction due to general comfort and local discomfort (ISO 7730).

Category	Thermal state of the body as a whole		Operative temperature C ⁰		Max. mean air velocity m/s	
	PPD %	PMV	Summer (0,5 clo) cooling	Winter (1 clo) heating	Summer (0,5 clo) cooling	Winter (1 clo) heating
A	< 6	-0,2<PMV<+0.2	23,5 – 25,5	21 – 23	0,18	0,15
B	< 10	-0,5<PMV<+0.5	23 – 26	20 – 24	0,22	0,18
C	< 15	-0,7<PMV<+0.7	22 – 27	19 – 25	0,25	0,21

The standard states that variations in the PMV and PPD index can occur due to age, racial, geographical deviations, and sick or disabled people. In addition, it is also dedicated to interior contexts where steady thermal comfort or modest deviations from comfort occur (Olesen and Parsons, 2002).

2.2.3.3. EN 15251

EN 15251 is a European standard established by the European Committee for Standardization (Comité Européen de Normalisation CEN). It is one of the standards developed as part of The Energy Performance of Buildings Directive (EPBD), which was founded in 2002 with the objective to enhance the energy performance of buildings. The standard demands interior thermal comfort conditions to be assessed and to come through a category system for varying degrees of expectation and building function. It defines four categories of buildings according to the occupants' level of expectations, as shown in Table 2.6. Moreover, the standard defines interior environmental parameters, which affect the energy efficiency of buildings, including indoor air quality, lighting, and acoustic performance (Nicol and Wilson, 2011).

Table.2.6. Categories of buildings with the level of expectations of occupants (EN 15251).

Category	Description
I	High level of expectation, recommended for spaces occupied by very sensitive and fragile persons with special requirements, like the disabled, the sick, very young children, and the elderly.
II	A normal level of expectation should be used for new buildings and renovations.
III	An acceptable, moderate level of expectation may be used for existing buildings.
IV	Values outside the criteria for the above categories. This category should only be accepted for a limited part of the year.

The standard uses the Smart Controls and Thermal Comfort (SCATS) database for its adaptive standard, and data were collected from five European countries during the same period in the same way and using a standard set of tools (Nicol and Humphreys, 2004).

The PPD index is used to determine the estimated number of unsatisfied occupants according to the PMV. For example, the comfort zone for category II (Normal level of thermal comfort expectation) is determined by restricting the PMV between $-0,5$ and $0,5$, with less than 10 percent of occupants being unsatisfied with the interior environment (CSN EN 15251). Table 2.7 shows the recommended levels of PPD and PMV according to the building category that has been classified by EN 15251 standard.

Table.2.7. Recommended criteria according to the building category (EN 15251).

Category	Predicted Percentage of Dissatisfied PPD	Predicted Mean Vote PMV
I	$< 6\%$	$-0,2 < PMV < 0,2$
II	$< 10\%$	$-0,5 < PMV < 0,5$
III	$< 15\%$	$-0,7 < PMV < 0,7$
IV	$> 15\%$	$PMV < -0,7$ or $PMV > 0,7$

2.2.4. Thermal Comfort Models

Many indexes have been proposed for the assessment of thermal comfort in interior environments. More than 80 indexes have been proposed during the previous several decades (Carlucci, 2013).

How can it be scientifically determined whether a certain indoor climate is satisfactory or not? This is the question that Fanger discussed to determine a method to achieve any meaningful findings from practical observations. It is also an essential requirement for the establishment of standards in this field. Fanger mentioned that lots of thermal indices had been established to enable predicting a human's thermal environment or thermal state (Fanger, 1970). The following is an explanation of three of these indices in more detail.

2.2.4.1. Predicted Mean Vote (PMV)

Fanger (1973) defined predicted mean vote (PMV) as “the index that predicts, or represents, the mean thermal sensation vote on a standard scale for a large group of persons for any given combination of the thermal environmental variables, activity and clothing levels” (Fanger, 1973).

Fanger developed a set of relationships that giving the PMV as a function of six variables: four environmental parameters and two personal parameters:

1. Air temperature
2. Mean radiant temperature
3. Air velocity
4. Relative humidity
5. Clothing level
6. Activity level

The PMV model was used as an international standard. ISO7730 recommends that the PMV should be preserved to zero (0) with a tolerance of $\pm 0,5$ in the seven-point

index of ASHRAE, which represents the average thermal perception felt by a large group of people in both naturally ventilated buildings and air-conditioned buildings (ASHRAE, 2017). The recent edition of ASHRAE Standard 55 applied PMV as an indicator of thermal comfort instead of the SET index (Nicol et al., 2012).

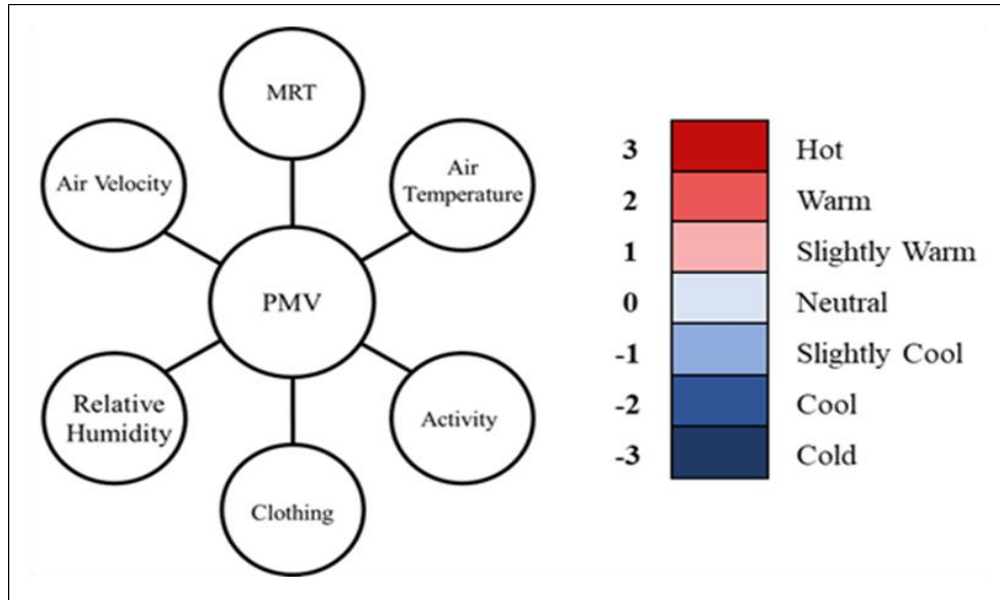


Figure 2.3. Predicted mean vote (PMV).

The PMV model is generally connected with a static model since it is dependent on a steady-state energy balance. It cannot estimate the particular reaction to a step change. Moreover, it is a sophisticated mathematic formulation integrating all ambient aspects in addition to the activity and clothes. The PMV model which Fanger Established has indicated via the vote of comfort on a scale ranging from -3 (very cold) to +3 (very hot), and the difference between the heat created and the heat expelled by the human body, according to the following formula (Gameiro da Silva, 2013):

$$\text{PMV equation} = (0.303e^{-2.1M} + 0.028) [(M-W) - H - R - E_c - C_{res} - E_{res}] \quad (2.2)$$

Where the symbols indicate, respectively:

M - the metabolic rate, in Watt per square meter (W/m²).

W - the effective mechanical power, in Watt per square meter (W/m^2).

H - the sensitive heat losses.

E_c - the heat exchange by evaporation on the skin.

C_{res} - heat exchange by convection in breathing.

E_{res} - the evaporative heat exchange in breathing.

Nowadays, PMV can be calculated by computer software, programming code provided by ISO Standard 7730, and the Center for the Built Environment (CBE) website based on ASHRAE 55 developed by the University of California, Berkeley.

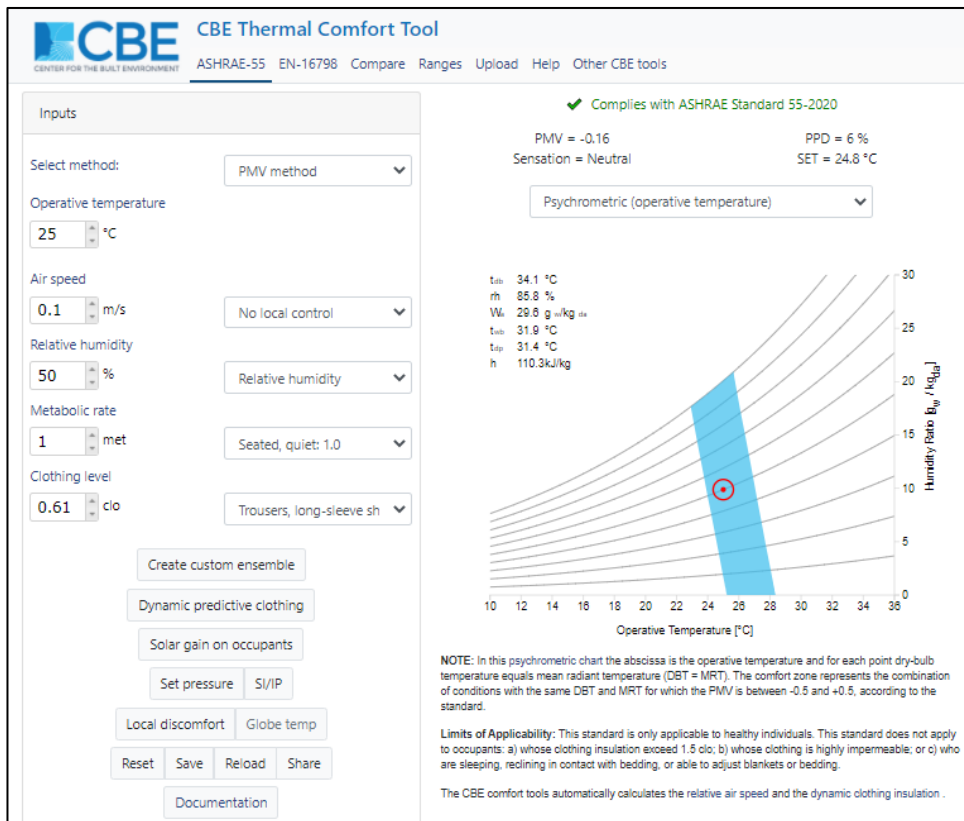


Figure 2.4. CBE tool to calculate the PMV based on ASHRAE 55 (URL8)

2.2.4.2. Predicted Percentage of Dissatisfied (PPD)

According to Fanger, even during the best conditions of comfortable in which PMV is at zero (0) levels, some 5% of the population would be dissatisfied. The PPD index (Predicted Percentage of Dissatisfied) has been established to estimate how many people are dissatisfied in a specific thermal environment (Ekici, 2013). According to

ASHRAE, the thermal comfort zone is specified as the zone where 90% of occupants feel satisfied. The approximate relationship between PPD and PMV is shown in Figure 2.5.

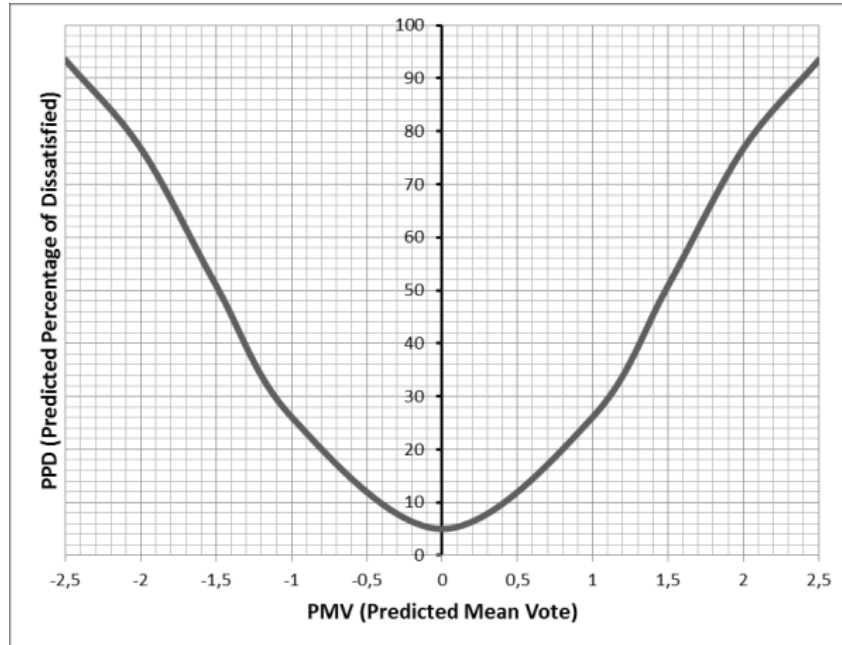


Figure 2.5. The relationship between PPD and PMV (Ekici, 2013).

Fanger found in his experiments that the link between the PMV index and the PPD may be inferred through an analytical equation corresponding to a curve whose appearance matches an inverted Gaussian distribution. Therefore, thermal comfort zones (classes A, B, and C) are determined by the ranges of PMV values from -0, 2 to 0,2, -0,5 to 0,5, and -0,7 to 0,7, which correspond respectively to PPD values below 6, 10, and 15%. (Figure 2.5) describes how concluding that. Because of individual differences between people, even in which $PMV = 0$, the percentage of dissatisfaction PPD is 5%. PPD index can be calculated by the following formula (Gameiro da Silva, 2013):

$$PPD = 100 - 95 \cdot e^{(0.03353 PMV^4 + 0.2179 PMV^2)} \quad (2.3)$$

2.3. PASSIVE SOLAR DESIGN STRATEGIES

Due to the increasing development of cities as a result of continuous population growth, the energy demand is increasing rapidly. To meet this demand, more fossil fuels will be burned, which means higher CO₂ rates. Unfortunately, according to this scenario, the world is going for the worst. In order to avoid the disaster, the world is urging to reduce energy consumption. Moreover, the search for alternative, clean and renewable sources is inevitable.

Heating is one of the largest of global energy use. Providing heating is responsible for about half of global energy consumption. The buildings sector accounts for more than a third of global energy consumption. The source of most of the energy consumed is fossil fuels, and they are responsible for most of the carbon dioxide emissions CO₂ that are harmful to the environment. The buildings sector represents about 40% of the volume of CO₂ emissions. The volume of CO₂ emissions increased to 10 gigatons during 2019 (IEA).

In Turkey, the consumption of fossil fuels is increasing year by year. Since 2000 energy supply in Turkey has expanded by 92%, which mostly depends on fossil fuels. The building sector is rapidly growing in Turkey. Turkstat data (TÜİK) in October 2019 clarified that "there were 9,5 million buildings in Turkey". According to occupancy permit statistics, more than 100,000 new structures are being built every year. The building sector is responsible for the usage of 21% of energy consumption. As a result of the steady increase in the number of buildings, the energy demand will increase, and consequently, carbon dioxide emissions will increase. Total greenhouse gas (GHG) emissions in Turkey were 520,9 million tonnes of carbon dioxide equivalent in 2018, of which energy-related emissions were considered for 72% (IEA, 2021).

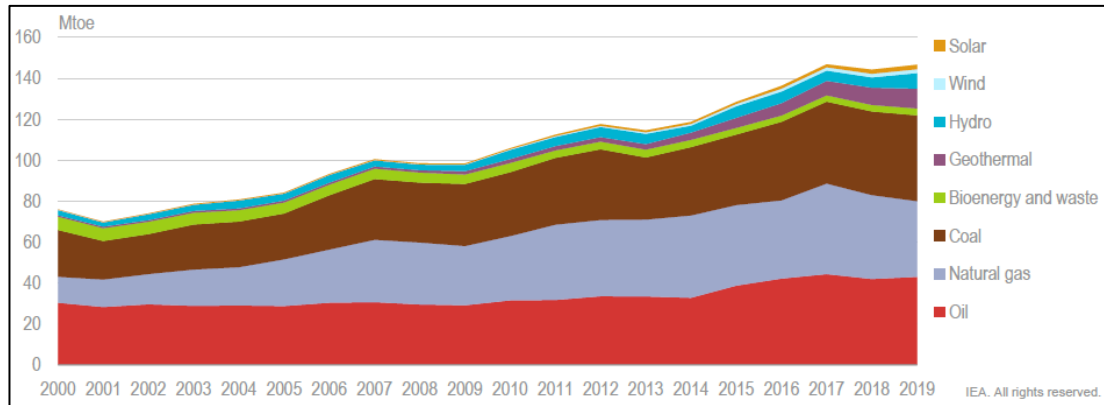


Figure 2.6. Total primary energy supply by source, Turkey, 2000-19 (IEA, 2021).

Many people believe that fossil fuels are unlimited. But the fact that is unknown or is known and is not wanted to be believed is that fossil fuels are running out. Moreover, the gases emitted by burning fossil fuels cause what is known as “global warming.” Thus, finding solutions that reduce energy consumption in buildings has become an issue of great importance by architects, designers, and others. One of the treatments is examining and developing techniques that can benefit and adapt to the climate.

After the energy crisis in the year 1973, thinking of solutions and strategies that reduce energy consumption became inevitable. Passive design systems have become a step in the right direction. “Passive space-conditioning applications are possibly the most cost-effective, most efficient, and most comfortable strategy to global solar energy use.” Wright believed that most areas on the planet obtain quality and amount of solar energy that is adequate for maintaining human existence (Wright, 2008).

Within the sustainable architecture and green building approach, the passive solar design thought emerged as one of the ideas supporting the voices demanding to reduce buildings-energy consumption generated from fossil fuels. Passive solar design is an inventive method to use the sun for both heating and cooling, based on the design of buildings. The use of HVAC systems for indoor comfort has increased the consumption of energy generated from fossil fuels and thus increased environmental pollution (Pudke et al., 2017).

According to Cofaigh et al., there are three reasons (political, economic, and environmental) that encourage to support passive solar design: 1) Politically to reduce dependency on oil. 2) Economically to saving money. 3) Environmentally to reduce greenhouse gas emissions (Boeri et al., 2015).

Marzia explained that a conventional building depends largely on, if not entirely on, mechanical air-conditioning systems to control the indoor environment. He also stated that “we have become prisoners of complicated mechanical systems. A minor power or equipment failure can make these buildings uninhabitable”. On the contrary, passive systems can make the indoor environment comfortable without the need for mechanical systems. (Fugate, 2018). Bainbridge and Haggard stated that people are insecure as long as they live in conventional buildings which depend on mechanical systems. “People are too often hot in summer, cold in winter, and face real danger if the power goes off.” On the other hand, the passive solar building is highly dependent on natural resources and techniques adapted in its design, so the building is more adaptable to changing environments. “The benefits of sustainable design include comfort, health, economy, security, and safety during power outages.” (Bainbridge and Haggard, 2011).

Passive systems are described as systems that allow energy gaining and reusing, for example: Using it for heating interior spaces through the heat transfer characteristic. These systems have been used by architects, as they believe that passive systems can be integrated into buildings to meet thermal needs. Using these systems can create buildings that are thermally comfortable and able to reduce the level of dependence on fossil fuels. This approach lets buildings use less energy than the conventional approach. Furthermore, using passive systems have a positive role in reducing greenhouse gas emissions, which contributes to protecting the environment. (Nahar et al., 2003).

Passive solar design systems are techniques used to collect, store, and distribute thermal energy by direct radiation, thermal conductivity, and convection. Thus, this can only be done through an innovative and developed architectural design and an appropriate selection of building materials. The Passivhaus Institute defined five

basic principles of passive design: buildings should be high-insulated, glazed with well-insulated windows, designed with the lowest thermal bridges, airtight, and operated with heat recovery ventilators (Trubiano, 2013).

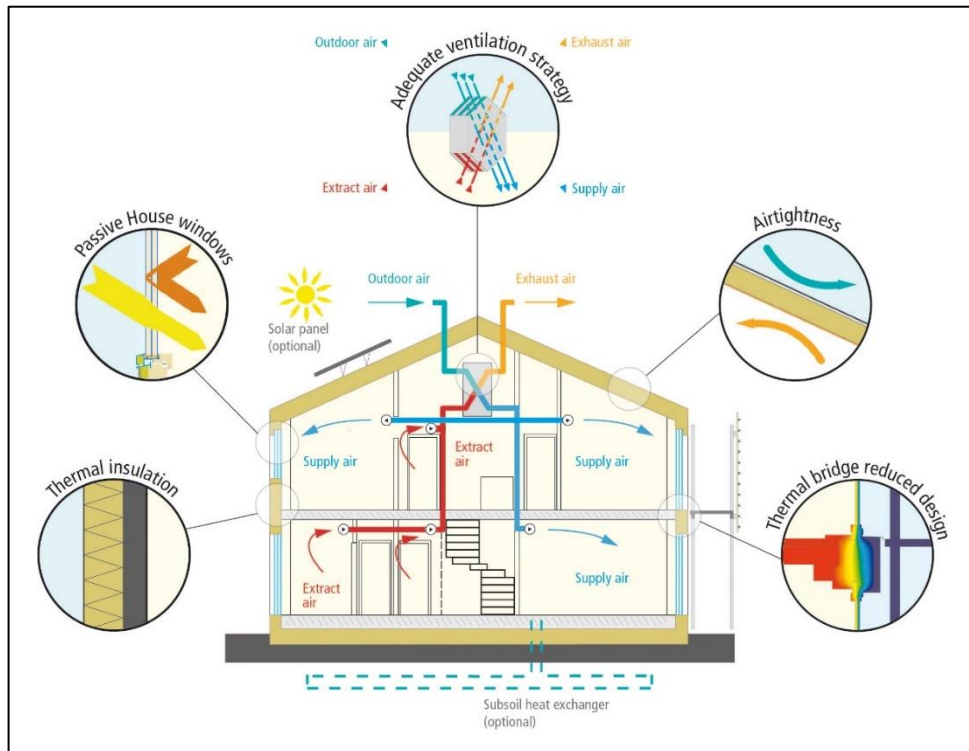


Figure 2.7. Passive house principles (Passive house institute).

1. High insulation: Most of the heat is lost (or gained) through the building envelope (external walls and external roof), so it must be well insulated to reduce heat loss in winter or gain in summer.
2. High-performance window: Well-insulated windows and equipped with low-E glass panels can prevent heat loss.
3. Absence of thermal bridges: The intersection points of the building elements such as the corners and edges create voids or bridges cause to lose energy through, so it must be ensured to closed tightly.
4. Airtightness building envelope: The building envelope must be tightly closed to prevent and resist air leakage due to climatic factors.
5. Heat recovery ventilation: This mechanical system allows exchanging air indoors and outdoors to maintain a good level of indoor air quality.

Passive design systems have several advantages. One advantage of passive systems is that they are easy to design, operate, and maintain. This is due to the fact that these systems are composed of common building components and have a long service life. Furthermore, passive design systems eliminate the need for mechanical equipment such as fans, pumps, compressors, tubes, and ducts. For example, a passive solar system cannot significantly reduce the heating load. However, it can be incorporated into the building at the early design stage or added later at little or no additional budget. During the 1980s, the energy market returned to stability again, which led to a loss of focus on using passive solar design techniques. Yet, insulation and glazing technologies have witnessed remarkable progress, as some of those interested in this field have experimented with using these technologies, and according to their experiences, making buildings tighter and better insulated is more efficient than designing methods for capturing and storing solar energy and distributing it within space (Fugate, 2018).

Lstiburek (2014) argued that with the passive solar design, we would not be disturbed. Our homes will be heated in the winter. The solar heat gain coefficient (SHGC) has a significant effect on heat gain through windows. We should use glazing with a low solar heat gain coefficient to obtain high efficiency (Lstiburek, 2014).

Holladay built a solar building in Northern Vermont in 1974 in order to evaluate passive solar design techniques. He argues that the use of glazing southern facade techniques is insufficient and useless without insulation. As glazing facades facing the south and with large surfaces help to gain enough solar heat to heat the building when needed, but what when there is no need for heating? Usually, a building with passive solar design techniques can gain too much or too little solar heat as it is lost a lot of it. However, with the improvement of the thermal performance of buildings by using insulation, buildings these days had become less energy-consuming than buildings in the seventies when there was no use of insulation. Holladay confirms that the large areas of glazing facing the south are the main reason for gaining more heat than necessary, especially in the afternoon during sunny days, while it is the main reason for losing a lot of heat, especially at night or during cloudy days. Lots of

heat will be lost through large glazing surfaces facing the south when compared to insulated walls (Holladay, 2016).

Many studies have proven that passive solar design techniques can reduce energy consumption and damage to the environment, but how can passive solar design systems heat the building without the intervention of mechanical systems?. To answer this question, there is a need to understand how passive solar design systems work. Physically, heat transfers from hot materials to cooler materials, and heat transfer continues until the temperature differences vanish and become equal. According to this phenomenon (Heat transfer between materials), passive solar design systems operate. Thus the flow of heat from hot spaces to cold spaces allows heating the building spaces. In buildings, heat transfer occurs by convection, conduction, and radiation of heat through roofs, walls, floors, and windows. Passive solar design systems work through three basic principles:

1. Convection: In indoor spaces, hot air rises while cold air stays down because hot air is lighter than cold air. Passive solar design systems use convection to transfer solar heat from the south walls to the interior spaces.
2. Radiation: Solar radiation occurs mostly through windows. Heat radiate and move through the air from hot surfaces to cooler surfaces. The south facades are the best for capturing the most solar radiation in the northern hemisphere. South glazing facades are the most effective technique in passive solar systems.
3. Heat capacity: Passive solar design systems use many materials with high heat storage capacity to store heat. Materials with high thermal mass can be used as a passive solar technique to absorb direct solar radiation and redistribute it inside the building.

Generally, a passive solar system consists of five basic elements:

1. Collection: Windows are utilized to absorb solar. In the northern hemisphere, windows should face south. East and west windows can also capture solar energy, but considerably less than south windows.

2. Storage: Passive solar systems are used in cold climates. During the night, temperatures drop significantly and rapidly, and thus there is a need to store the collected energy of solar radiation during daylight hours to redistribute it at night inside the space. Materials that have high thermal mass absorb heat either by direct radiation from the sun (Direct gain) or convection (Indirect gain).
3. Absorbed: it is the hard, darkened exposed surface of the storage element. This surface could be a masonry or concrete wall, floor, or partition (phase change material) that remains in the direct path of the sunlight. When sunlight falls on the surface then is absorbed as heat (Energy.gov, 2010).
4. Distribution: Usually, any building consists of several spaces, and all of these spaces cannot face the southern windows, so there is a need to redistribute the heat gained within the southern space of the building to the rest of the spaces to promote comfort level of the occupants in the whole building, the heat will be transferred either through convection by the movement of air, either naturally or mechanically (Fans), or by conduction or radiation: by the occupants themselves when they move between the spaces of the building, where their bodies absorb heat from warm sunny spaces and move through them to the less warm spaces.
5. Control: The biggest issue that occupants of passive solar buildings face is wide fluctuations in the indoor temperature. When the outdoor air temperature rises during hot days, an uncomfortable increase in the indoor temperature of the occupants occurs. During the peak of the solar radiation period (often at noon), the solar sun must be blocked out to enter the building by control devices such as overhangs, awnings, curtains, shutters, and blinds, as well as external openings in the roof or exterior walls can allow overheated air to escape.

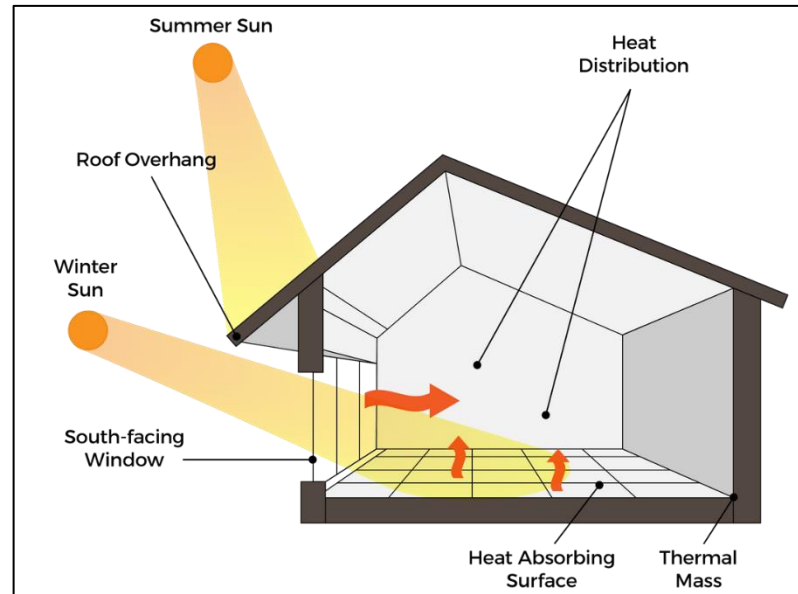


Figure 2.8. Elements of passive solar design (Energy.gov, 2010).

Donn and Thomas (2010) mentioned six major principles of passive solar design systems. The most important three principles are thermal mass, glazing, and insulation.

2.3.1. Thermal Mass

Thermal mass relates to materials that can store heat for lengthy times. The thermal mass may be employed successfully to collect heat obtained from the sun during day hours and release the heat during the night hours.

Thermal mass operates in two ways. First, when the sunlight passes inside the building through windows, the solar radiation will be absorbed directly by high thermal mass surfaces. Second, when the air within the building is hotter than the surfaces, thermal mass absorbs heat from the air. The heat stored by the two mentioned ways is transferred back into the space when the space temperature falls below the surface's temperature (Donn and Thomas, 2010).

Thermal mass (concrete, brick, stone, and tile) in a passive solar building collects heat from the sun during the cold season and heat from the heated air within the building during the hot season. The thermal storage capacities of a given material are

determined by its conductivity, specific heat, and density. The majority of the concrete and masonry materials often utilized in passive solar have comparable specific heat. Conductivity rises as density rises. Thus density is the most important element influencing performance. In general, the higher the density, the better. (U.S. Department of Energy).

Table 2.8. Heat storage properties of materials (U.S. Department of Energy).

Material	Density (kg/m ³)	Heat Capacity (J/kg·K)
Poured Concrete	1920 - 2400	8370 - 10460
Clay Masonry		
Molded Brick	1920 - 2100	8370 - 9200
Extruded Brick	2000 - 2160	8790 - 9620
Pavers	2080 - 2160	9200 - 9620
Concrete Masonry		
Block	1280 - 2240	5440 - 9620
Brick	1840 - 2240	7950 - 9620
Pavers	2080 - 2400	9200 - 10460
Gypsum Wallboard	800	3470
Water	1000	21,770

All materials have thermal mass, but thermal mass varies from one substance to another. The material must have sufficient heat capacity to store enough heat to be useful as a heat storage component in a passive solar system, as well as the ability to release heat at an ideal level to manage indoor temperature flux. Most metals have a large heat capacity, but due to their high conductivity, they are useless as passive solar thermal mass. On the contrary, wood has good heat capacity, but it has too low conductance. The use of phase change materials (PCMs) can offer the possibility of lightweight alternatives for thermal mass. (Mathews, 2013).

Concrete, masonry, and stone are the most common form of thermal mass. To receive solar radiation directly, the thermal mass must be coordinated with the solar collector (glass) in a direct-gain system. This may be accomplished by using a concrete floor and a masonry or concrete wall on the north side of the area and a glazed facade on the south side. The solar radiation will be collected by the thermal mass as the sun passes across its path.

Thermal mass can positively affect the Mean Radiant Temperature (MRT) of a space where Mean Radiant Temperature (MRT) is the average temperature of the surfaces that surround a certain place and exchange thermal radiation. This point is affected by all surfaces in the space includes floors, ceilings, walls, doors, windows, and even furniture. The radiant temperature of the surface has more effect on thermal comfort inside space than the indoor air temperature. When exposed to cold surfaces, radiant heat will be absorbed from the body through emissivity. On the contrary, when exposed to warm surfaces, the body will absorb radiant heat. Regardless of the air temperature. “As a matter of fact, warm surfaces may cause a person to feel warmer than the surrounding air temperature would indicate and likewise cold walls or windows may make one feel cold even though the surrounding air may be at a comfortable level” (d’Ambrosio Alfano et al., 2013).

Thermal mass must be precisely constructed; otherwise, it might be more damaging than beneficial. A structure with a lot of thermal mass on both the inside and outside is most successful if it is located in a diurnal climate, which is an environment with a lot of temperature volatility during the day and night. When the temperature rises during the day, the thermal mass absorbs a large portion of the heat, preventing the indoor temperature from rising too high. The thermal mass will then gently release the accumulated heat throughout the cool night to keep the interior temperature from dropping too low. However, in cold climate regions, the external temperature is unlikely to achieve the thermal comfort threshold. As a result, the thermal mass will never be able to absorb enough heat energy. Furthermore, the thermal mass's conductance will constantly pull heat from the interior to the exterior. In this scenario, insulation is more important than thermal mass since thermal mass will work against the occupants' thermal comfort (Holladay, 2013).

Peter Yost, a building performance researcher, stated that “during the winter, I have concluded that it is best to expand your thermal comfort zone quite a bit in the early mornings until the sun catches up on that mass.” The way to solve this issue is to install a supplementary heating system that can warm up the building in the early morning (Holladay, 2013).

The following is some advice from Martin Halland for embedding thermal mass in a direct passive solar building:

1. For direct gain systems, the thermal mass area should be three to six times that of the south-facing window.
2. The thermal mass (commonly concrete) should have a maximum thickness of roughly 4 inches (10 cm). Thicker concrete will not absorb heat rapidly enough for direct gain systems.
3. Darker-colored concrete floors outperform lighter-colored flooring.
4. Carpets should not be used to cover concrete floors (Holladay, 2013).

For several reasons, the thermal mass of the building will not be examined in the study:

1. The building envelope is constructed from precast concrete, which has a high thermal mass.
2. The external walls are designed with a thickness of 40 cm, which multiplication the ability of the external walls to conserve the heat energy gained.
3. Preserve the architectural style followed by the designer by utilizing precast concrete as a basic construction material for the building envelope.
4. Finally, the study follows the approach of retrofitting, which aims to improve the building after the implementation, and any modification to the building's structure will mean the demolition of the building in whole or in part.

2.3.2. Glazing

The building envelope is the most influential factor in the energy performance of the buildings. It is the main barrier to prevent the flow of thermal energy from/to the building. The glazing system is one of the components of the building envelope and is the most important component in passive solar buildings. In addition to allowing the solar to cross inside the building, it is also responsible for the energy loss through

it. Improving the glazing system has a great potential to improve the performance of buildings (Ali et al., 2017).

Glazing is an essential component in any building to transmit daylight and heating energy. The efficiency of the glazing depends on many factors such as orientation, type, size, etc. In the past two decades, there have been significant advances in glazing technology. Nowadays, windows are applicable with double and triple panels. Also, in order to prevent heat transfer through the window, panels were coated by a metal layer which is well known as "Low-E glass." Double and triple glazing systems contain air gaps between the panels filled with air or gas to reduce heat transfer through the glass. Additionally, windows have enhanced frames to reduce thermal bridging and leaking. However, even high-efficiency windows have a much greater heat loss potential than walls with thermal insulation.

Windows are a major component of the building envelope. In addition to their aesthetic role, they also perform an essential function in the building's interaction with the surrounding environment, where the windows provide the building with solar (Aldawoud, 2017). The size of the windows significantly affects the quantity of heat intake and loss through the building envelope. The larger the windows, the greater amount of heat loss (in winter) which leads to increasing the need for heating, and heat gain (in summer), which leads to increasing the need for cooling. Windows are considered to have the lowest thermal performance among the components of the building envelope.

There are three main factors that affect the performance of windows: thermal transmittance (U-value), solar transmittance (SHGC), and airtightness of windows. In addition to other factors that have a significant impact on the performance of windows, such as location, orientation, building materials, building design, and climatic factors (Sadineni et al., 2011).

The amount of energy lost through windows is about a third of the energy lost through the building envelope. Energy losses through windows can be decreased by the following strategies: increasing the number of panels in the window (double

glazing or triple glazing). Moreover, energy savings can also be increased by filling the air gap between the panels with an inert gas such as argon, krypton, or xenon. Also, coating the panels with low-emission materials can reduce heat loss by radiation through windows (Arıcı and Karabay, 2010).

Arıcı and Karabay (2010) in their study, specified the optimal thickness of the air cavity between the glass panels in double-glazed windows in the four climate regions of Turkey by using the degree-days method. The study was based on measuring the cost of heating using five types of fuels and at three levels of a base temperature (18-20- 22 °C). The study concluded that the optimum thickness of the air cavity ranges between 12 to 15 mm depending on climate zone, fuel type, and base temperature. In cold climates, there is no effect for fuel type and base temperature on the optimum air cavity thickness. The study showed that about 60% of energy could be saved by using well-improved glass windows (Arıcı and Karabay, 2010).

Double glazing is presently the most common. In addition to increasing energy efficiency, double glazing decreases condensation on windows and noise transmission. The greater the performance of the double glazing, the higher the temperature of the inside glass, making people feel warmer while approaching it. The most effective windows lose less than half the heat of typical double glazing and less than a quarter of the heat of typical single glazing (Donn and Thomas, 2010).



Figure 2.9. Structure of double glazed window (Lohia and Dixit, 2015).

In a study carried out by Almarzouq and Sakhrieh (2018) a building envelope was improved by replacing single windows with double windows with low emissivity glass. They found that using double glazing windows achieved savings in energy consumption by 24,7%, but it led to a deterioration in thermal comfort by 1% (Almarzouq and Sakhrieh, 2018).

Brdnik (2021) in her study, investigated the use of a double glazing system with low-emissivity and high-emissivity panels. She proved that in low-solar gains buildings, low-emissivity panel placement on the outer side reduces energy consumption, while in high-solar gains buildings, the low-emissivity panel should be placed on the inner side (Brdnik, 2021).

The latest innovation in the field of glazing is "the multilayer glazing window," which is known as "triple glazed window." It is a window that consists of three panels of glass separated by an air cavity that is mostly filled by gas. Compared with double glazing, it contains an additional layer of glass, which makes heat loss slower and enhances the possibility of maintaining the temperature of the indoor space longer. Manz et al. conducted a study to evaluate heat transfer through triple glazed windows using two methods: 1- an analytical thermal network model and 2- a numerical finite-difference model. Three panels of untempered soda-lime glass with a thickness of 6/4/6 mm and four low-emittance coatings ($\epsilon = 0,03$) were used. The study proved that the use of triple-glazed windows reduces heat transmittance with a U-value of less than $0,2 \text{ W/m}^2 \cdot \text{K}$ (Manz et al., 2006).

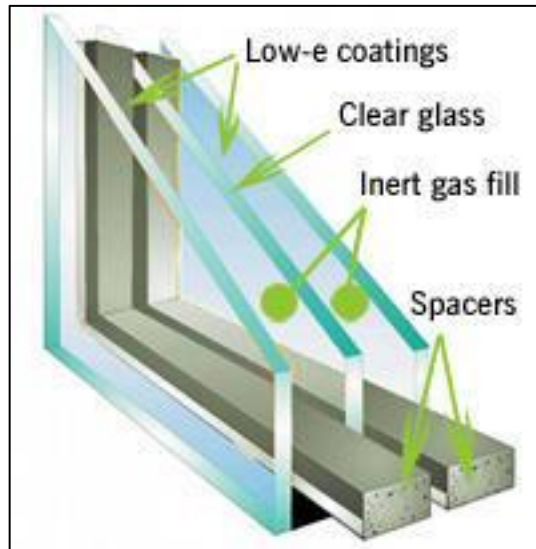


Figure 2.10. Structure of triple glazed window (Lohia and Dixit, 2015).

According to Lohia and Dixit (2015) triple glazed windows provide the same tasks as double glazed windows but with more efficiency and effectiveness. Triple glazed windows can provide 28% to 30% more insulation than double glazed windows. Also, it can reduce heat transfer by 75% to 80% (Lohia and Dixit, 2015).

Triple glazing windows can contribute to reducing energy consumption if at least two low-emissivity panels are used, provided that the emissivity value is at ($\epsilon = 0,03$) in buildings with low-solar gains. While in buildings with high-solar gains, the emissivity value should be lower (Brdnik, 2021).

Nikoofard et al. (2012) proved in their study that using triple windows with low emissivity panels in the south facade in buildings in Calgary, Canada, (cold climate) could reduce heating loads to 13,7% compared to buildings without windows in the south façade (Nikoofard et al., 2012).

In addition to the performance of windows in visual communication between the inside and outside, they can reduce the need for artificial heating and lighting, provided that the appropriate type, size, and position are chosen within the building. Otherwise, the results will be an adverse impact on the comfort of the space. Reflective, selective, low-E coatings, electrochromic coatings, thermochromic

coatings, and photochromic coatings windows are some conceivable advanced technologies in material glass that can be the answer for receiving the advantage of natural illumination without severe heat loss or gain. These advanced technologies can prevent the undesired waves from accessing the space while allowing desired ones to penetrate (Doğrusoy, 2001).

Fang et al. (2010) conducted a study on the thermal performance of electrochromic glass. They noticed that the white electrochromic glass layer could absorb about 10% of solar, while the opaque layer could absorb about 60 to 80%. The thermal performance was examined in two cases: 1- When the electrochromic glass layer faces the outer side, 2- When the electrochromic glass layer faces the inner side. When the electrochromic layer is towards the inner side, the temperature differential between the inner and outside layers is too high. Thus, it is recommended in all cases that the electrochromic layer has to face the inner side (Fang et al., 2010).

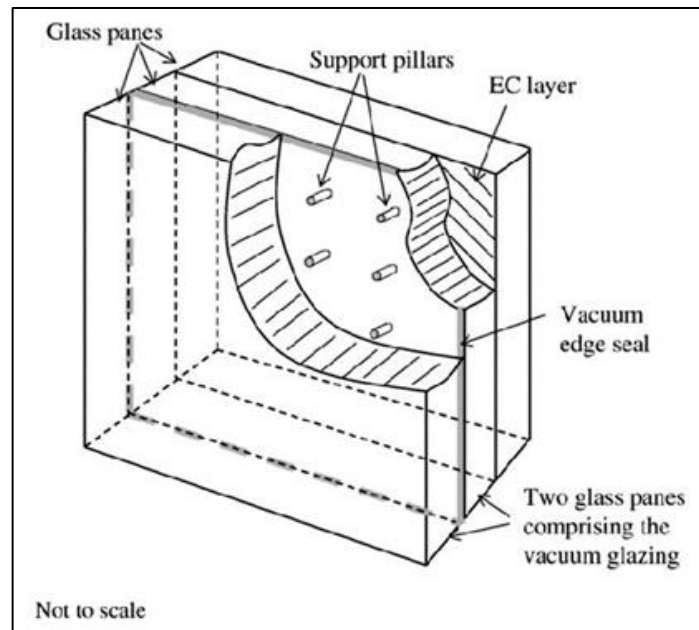


Figure 2.11. A sketch describes electrochromic evacuated glazing. (Fang et al., 2010).

In their study, Sbar et al. (2012) examined the performance of electrochromic windows compared to ordinary windows in commercial office buildings in several climatic zones and proved that using electrochromic windows can reduce energy consumption by up to 45% (Sbar et al., 2012).

Detsi et al. (2020) examined a triple glazing system with different coated glass panels (electrochromic, thermochromic, and low-E) in their study. The study proved that this glazing system could reduce energy consumption in cold and hot climates (Detsi et al.2020).

Thermally fractured metal frames outperform ordinary metal frames by 20%. Wooden as well as other low heat conduction frames, such as PVC sections, can exceed typical metal frames by 40%; 'low-E coating on the inner panel of double glazing can give up to a 30% advantage, and argon gas between the panels in double windows adds an extra benefit. According to Figure 2.12, typical double glazing is just half as effective as the best double glazing.

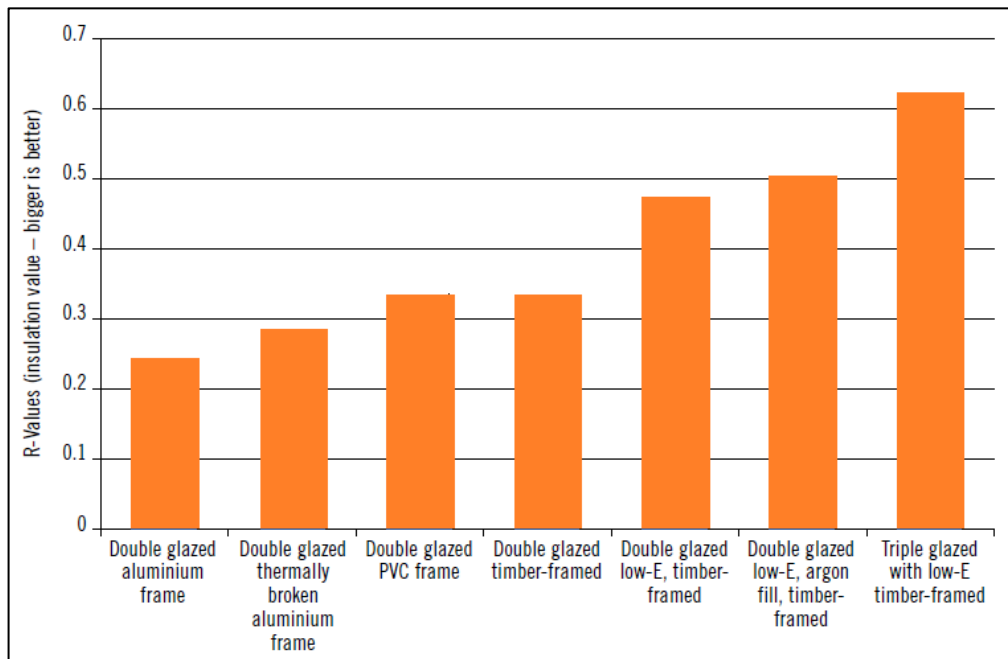


Figure 2.12. Comparison of the insulation value of window types (Donn and Thomas, 2010).

Ghoshal and Neogi (2014) discussed the various types of glazing systems and their thermal efficiency. The study concluded by comparing different glazing systems according to their thermal properties. The following table shows the thermal performance of various types of glazing systems (Ghosha and Neogi, 2014).

Table 2.9. Comparison of different types of glazing systems in terms of thermal performance (Ghosha and Neogi, 2014).

Glazing system	Window components.	U-Value (W/(m ² ·K))
Single glazing	One glass panel	5,79 – 6,3
Double glazing	Two glass panels with an air-filled cavity	2,78 – 3,24
Double glazing	Two glass panels with argon filled cavity	2,61 – 2,95
Double glazing	Two glass panels with argon filled cavity and having night insulation	1,5 – 1,99
Double glazing	Two glass panels with evacuated space in between	0,86
Double glazing	Two glass panels with monolithic aerogel	0,63
Double glazing	Two glass panels with granular aerogel in	1,69
Electrochromic evacuated glazing	Two glass panels form evacuated glazing with a third panel having an EC layer	Slightly < 1
Triple evacuated glazing	Three glass panels with two evacuated	0,26

On the other hand, Wilson (2012) explained that excessive use of glazing does not always have positive results. When the sun is in a low position, especially in the morning and evening, it causes severe glare that can make the place uncomfortable. This issue can be solved by reducing glazing on the eastern and western facades. Also, when the outside air temperature is too high, large glass surfaces can increase the indoor air temperature and thus make the place uncomfortable. This problem issue can be solved by using shading devices (Wilson, 2012).

In addition to the possibility of heat loss through the windows, glass is considered one of the most components of the building that conflict with privacy, as the transparent surface of the glass allows revealing the interior and the transmission of external noise to the inside of the building, so these factors may affect the choice of the type and size of glazing. Landscape can play an important role in addressing the issue of privacy and noise.

Three types of glazing systems will be examined in this study: a triple glazing system with an air cavity of 6 mm thickness, a triple glazing system with an air cavity of 10 mm thickness, and a double glazing system with low emissivity panels and an air cavity of 12 mm thickness.

2.3.3. Insulation

The quantity of thermal mass is a vital issue in terms of being able to store adequate heat, and it is deeply significant to either not leak the heat to the incorrect side of the thermal mass. For example, the concrete floor must have insulation under it. Instead, most of the heat energy absorbed by the concrete will be transferred to the surface below as the earth is continuously colder than the interior temperature, and heat pass from warm to cold.

Insulation is one of the most important influencing factors in passive solar design. In order to maintain the energy efficiency and thermal comfort of a building in both summer and winter seasons, adequate levels of insulation must be implemented. By reducing heat transfer in and out of a building, insulation works in conjunction with thermal mass and glazing to reduce both heating and cooling demands (Donn and Thomas, 2010).

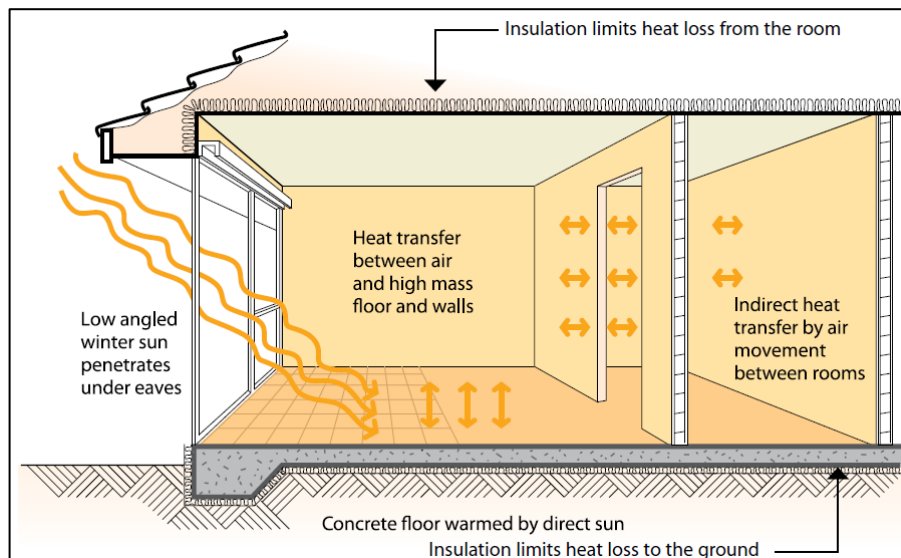


Figure 2.13. Insulation in conjunction with thermal mass and glazing (Donn and Thomas, 2010).

Insulation is aimed at addressing the conductivity property of the building's envelope. Heat loss through the building envelope is closely related to the quality of thermal insulation. Conductive heat loss is measured by the U factor. The lower the value of U-value for any material, this indicates the ability to retain heat, and on the

contrary, the R-value, which indicates the resistance of the material to heat transfer. The higher R-value, the better the material can resist the transfer of thermal energy. Climate has a great influence on the performance of insulation. In a cold climate, the purpose of insulation is to preserve the gained heat inside the building frame for the longest potential time, while in a hot climate, insulation aims to prevent or stop heat transfer to the inside. In a passive solar building, during the night, the internal temperatures begin to decrease then the heat collected and stored in the thermal mass during the day will flow. When the thermal conductivity value of the external wall and roof materials is too high, the heat released from the thermal mass will be immediately lost, which will lead to indoor discomfort. In poorly insulated buildings, there will be no benefit from the heat energy gained during the day. Therefore, the storage of thermal energy inside the building is very important for the effectiveness of the effective passive solar system. However, this will not occur without perfect insulation. "For passive design, the motto should be 'Insulate before you insolate.'" (Brondzik and Kwok, 2014).

There are many various insulation products, R-values vary depending on the kind of insulating material, certain materials are better insulators than others although with the same thickness, and some need to be thicker to attain the necessary R-value. Density is the main factor that determines R-value, hence in certain circumstances, insulating materials of the same kind and thickness may have varying R-values (smarterhomes.org.nz).

Donn and Thomas (2010) recommended that "always try to use higher levels of insulation than Building Code minimum requirements." It would be better to do the best the first time. Also, insulation must be installed correctly to obtain optimum performance. For instance, pinching the insulation over places thinner or fewer than its area greatly reduces its efficiency (Donn and Thomas, 2010).

In Turkey, 27% of energy consumption is spent on heating. This number is considered a large number for a country that depends mainly on fossil fuels for energy production. Therefore, Turkey has paid great attention to the thermal insulation of buildings to reduce energy consumption and make buildings more

efficient. The Turkish Standards Manual for Thermal Insulation for Buildings TS 825 was developed and entered into force in 2000. This standard is applied as a mandatory standard in all licensed buildings to be constructed in Turkey (Ertas, 2000). The objective of applying this standard revolves around three objectives:

1. To save energy by reducing the amount of energy used to heat buildings.
2. To specify the standard calculation method and the value to be used while calculating the energy requirement.
3. Ensuring the production of high-rise buildings with comfortable and energy-saving conditions.

Based on TS 825, Turkey is categorized into four thermal zones due to different weather conditions, as shown in Figure 2.14. The daily degree calculation method was used to determine the heating requirements, or in other words, determine the U values that can be accepted, as shown in Table 2.10.

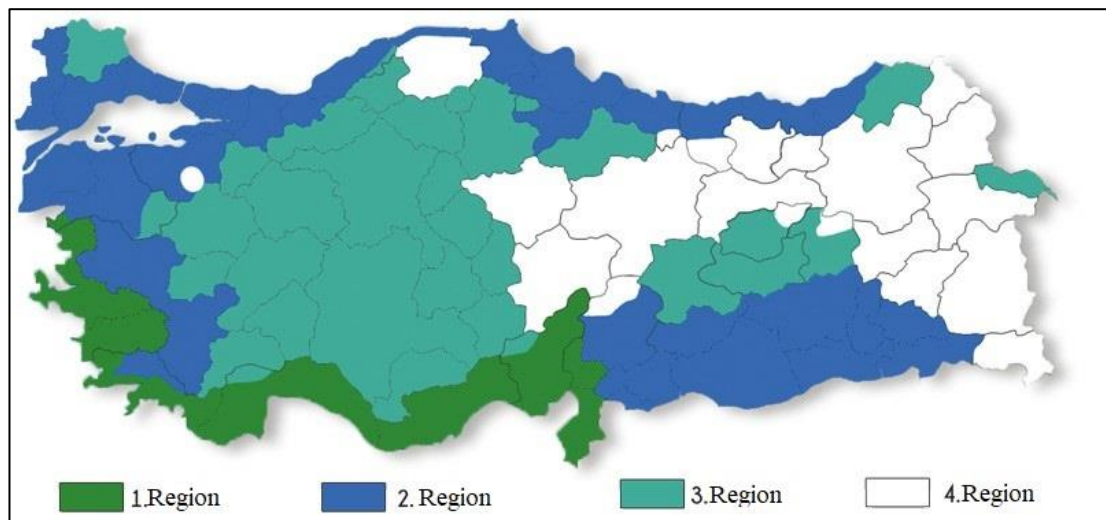


Figure 2.14. Turkey's thermal zones (TS 825).

Table 2.10. Recommended U-values to be considered as maximum value by region (TS 825).

	U-value (W/(m ² ·K)) Walls	U-value (W/(m ² ·K)) Ceilings	U-value (W/(m ² ·K)) Floors	U-value (W/(m ² ·K)) Windows
Region1	0,70	0,45	0,70	2,4
Region2	0,60	0,40	0,60	2,4
Region3	0,50	0,30	0,45	2,4
Region4	0,40	0,25	0,40	2,4

Ucar and Balo (2009) conducted a study to determine the optimal thickness of thermal insulation of the walls. The study included four different cities within the four climate regions of Turkey. In this study, extruded polystyrene, fiberglass, foam board 3500, and foam board 1500 were considered as insulation materials. The study showed that the optimum thicknesses of thermal insulation for walls range between 1,06 and 7,64 cm, depending on the climate (Ucar and Balo, 2009).

Bolattürk (2008) conducted a study to determine the optimal insulation thickness in several cities located in the first climate zone in Turkey by calculating the annual heating and cooling loads using the degree-hours method. The study proved that using a constant value of U-value for external walls according to the Turkish standard of thermal insulation (TS825) in all cities of the region is not the accurate method to calculate the thickness of thermal insulation. Instead, Bolattürk suggested calculating the thermal insulation thickness for each city separately. In addition, the calculations have to be done based on cooling degree-hour (Bolattürk, 2008).

Kaynaklı and Kaynaklı (2016) concluded in their study that solar radiation falling on the external walls has a significant effect on the insulation thickness. They clarified that solar radiation could reduce heating loads. On the other hand, it can increase cooling loads. Furthermore, they proved in their study conducted on four cities in the four climate zones of Turkey that the optimal insulation ranges from 3,9 to 7,5 cm thick and can achieve annual savings in energy consumption at a rate of 44 to 63% (Kaynaklı and Kaynaklı, 2016).

Kaynakli (2008) investigated the best thickness of thermal insulation in Bursa, Turkey. He calculated the annual heating requirements based on Hour-degree values

for a long period and then determined the best insulation thickness for different types of fuel used for heating. He found the optimal thickness varies between 5,3 and 12,4 cm depending on the fuel type. Furthermore proved that the suitable fuel for heating is natural gas to achieve the lowest cost (Kaynakli, 2008).

Al-Sanea and Zedan (2001) conducted a study to determine the effect of the thermal location of the external walls on energy consumption. They compared the thermal performance of a building with an external insulation layer to that with an internal insulation layer in January and July in Riyadh city, Saudi Arabia. The results showed that the location of the insulation layer does not have a significant impact on the performance of the building (Al-Sanea and Zedan, 2001).

Atmaca et al. (2021) in their study, proved that increasing the thickness of the thermal insulation in buildings has a significant effect on energy saving, except for the floor insulation, where they proved that increasing the thickness of the floor insulation has a weak effect on reducing energy consumption (Atmaca et al., 2021).

Installing thermal insulation perfectly will have environmental benefits: Consumption of fossil fuels used for energy generation will decrease, and thus the rate of harmful gas emissions will decrease. And economic benefits: Thermal insulation will contribute to reducing energy consumption. Moreover, thermal insulation plays a great role in maintaining comfortable levels in indoor environments (Ertaş, 2000).

Increasing the thickness of the thermal insulation of the building envelope (external walls, floor, and roof) will be examined in this study. According to the literature above, increasing the thickness of the insulation has a positive effect on reducing annual energy consumption. In the case study, the thermal insulation of the external walls was installed on the inner face of the walls. And this is attributed to the designer's approach that aims to emphasize the massive, opaque concrete structure free of exterior finishing.

2.4. THERMAL COMFORT AND ENERGY EFFICIENCY IN MOSQUES

Mosque buildings have a special point of view among other buildings. The reason returns to the unique value of functional and operational use of this kind of buildings. In other words, mosque buildings have an intermittent occupancy during the five daily prayers Fajr (dawn), Dhuhr (after midday), Asr (afternoon), Maghrib (after sunset), and Isha (nighttime), and full occupancy during Friday day pray (Azmi et al., 2021; Azmi and Kandar, 2019). This gives the studies of mosques building energy performance a unique treat in the literature, especially in the mosques operated by active systems.

In a study conducted by Alhemiddi (2003) to determine strategies to reduce energy consumption in mosques in a hot and arid climate region, the researcher focused on studying the effect of outdoor temperature on energy consumption inside active and passive mosques, the study proved that when outdoor temperature raised the operation of AC system in active mosques also raised while the passive mosque which uses Malqaf did not affect (Alhemiddi, 2003).

Al-Homoud et al. (2009) conducted a study to assess monitored energy use and thermal comfort in mosques located in hot and humid climate regions. The study proved that thermal insulation significantly impacts energy consumption and thermal comfort. Despite the high use of air conditioning systems, a deterioration was observed in the level of thermal comfort in non-insulated mosques, proving that high-energy consumption does not necessarily mean an improvement in the level of indoor thermal comfort. On the contrary, the study showed that insulated mosques are less energy-consuming and provide better indoor thermal comfort (Al-Homoud et al., 2009).

In a study by Al-Homoud (2009), he examined two mosques, one in a hot, humid climate and the other in a hot, dry climate. The study proved that using thermal insulation, less glazing ratio, shading devices, and the air-tightened envelope has a positive effect on reducing energy consumption. In this study, energy-save was obtained up to 21% and 18.8%, respectively (Al-Homoud, 2009).

In their study, Al Anzi and Al-Shammeri (2010) concluded that improving the building envelope and the efficient operation of the HVAC systems can save energy consumption up to 72% in a mosque in a hot, dry climate. Furthermore, energy-save of up to 42% can be contributed by using thermal insulation in the roof (Al Anzi and Al-Shammeri, 2010).

A study by Budaiwi et al. (2012) aimed to evaluate a retrofit of a mosque building in a hot, dry climate. The study proved that using thermal insulation for walls and roofs and reducing air infiltration can reduce cooling loads by 26%. Moreover, the reduction can reach 48% by using retrofit strategies and air conditioning systems (Budaiwi et al., 2012).

Ibrahim et al. (2014) investigated thermal comfort conditions in a mosque located in a hot and humid climate. The results showed users' discomfort because of the high indoor temperature resulting from the absorption of the solar sun by the roof. Adding thermal insulation to the roof can fix this issue (Ibrahim et al., 2014). Moreover, Maarof (2014) conducted a study to assess the impact of the roof shape on the thermal comfort of worshippers in a mosque located in a hot, humid climate. The study proved that the pitched roof allows the best performance of the mosque in terms of thermal comfort due to the ability to circulate air inside the prayer hall, which provides the thermal balance of the indoor air, while the domed roof contributes to the stagnation of air and divides it into levels according to its temperature where cold air settles in the lower level (Maarof, 2014).

Another study conducted by Faghih and Bahadori (2011) aimed to evaluate the effect of the domed roof and the flat roof on the thermal comfort in mosques in a hot, dry climate. The study proved that the dome roof could provide thermal comfort to worshippers during hot days provided that the dome contains openings that allow airflow, while in the absence of openings, the flat roof is better (Faghih and Bahadori, 2011).

Alabdullatief et al. (2016) conducted a study to discover the effect of sustainable techniques on energy consumption in a mosque located in a hot and dry climate. The

study proved that cooling loads could be reduced up to 10% by establishing green roof and shading devices for windows (Alabdullatief et al., 2016). In the same context, Alabdullatief and Omer (2017) examined six different scenarios for a mosque roof in a hot arid climate. Non-insulated roof, insulated roof, insulated roof with chipped stones finishing, insulated roof with a green roof, shaded insulated roof with chipped stones finishing, and shaded insulated roof with a green roof. The results showed that the insulated roof with a green roof is the best performance in terms of reducing annual cooling loads (Alabdullatief and Omer, 2017).

Mushtaha and Helmy (2016) tested the effect of passive design strategies on thermal comfort in a mosque in a hot, humid climate. The tested strategies included thermal insulation, shading, and ventilation. The results showed that applying passive design strategies could improve the thermal performance of the building but could not improve the level of indoor thermal comfort to an acceptable level. Moreover, passive design strategies could reduce energy consumption by 10%. Furthermore, indoor thermal comfort can be obtained by supporting passive design strategies with an active system (Mushtaha and Helmy, 2016).

A study conducted by Sanusi et al. (2020) aimed to investigate the effectiveness of passive design strategies in three mosques in a hot, humid climate. These mosques were provided with five passive design techniques, oriented to the prevailing winds, periodic ventilation, placement of openings in different locations in the walls and roofs, openings equal to 50% of the wall, verandah surrounding the openings. The study proved that the most effective strategy in reducing indoor temperature was verandah. Moreover, the study verified that the shape and size of the dome has a great effect in cooling the indoor vacuum and can be included as an effective passive technique to cooling the vacuum (Sanusi et al., 2020).

Shohan and Gadi (2020) conducted a study to verify the thermal comfort and energy performance of mosque buildings in the semi-arid moderate/cold climate in Saudi Arabia. A number of small and large mosques were examined for this purpose. The study revealed that the poor quality of the envelopes of the mosque buildings that were examined caused the gain and loss of heat irregularly throughout the year,

where the heat loss in winter and the heat gain in summer led to the deterioration of the level of thermal comfort and thus negatively affected the annual heating and cooling loads (Shohan and Gadi, 2020).

In Turkey, most of the literature focused on the study of energy performance and thermal comfort in mosque buildings located in a moderately humid climate, and the Mediterranean climate.

Bughrara et al. (2017) conducted a study in a mosque in a Mediterranean climate to evaluate adaptive thermal comfort. The study showed most of the discomfort time is during the winter period. The researchers suggested adding an underfloor heating system to improve thermal comfort. By using this system, the discomfort time was reduced by 55% (Bughrara et al., 2017).

Yüksel et al. (2020) examined the level of thermal comfort and the concentration of carbon dioxide in the air using passive design systems in a mosque in a temperate climate. The techniques tested included using fans, turning on air conditioning systems, and opening windows. The study showed that although indoor air quality improved by opening windows, the relative humidity level increased. Moreover, the operation of the fans raised the rate of air quality and reduced the concentration of pollution. On the contrary, the operation of the air-conditioning system during the prayer led to discomfort and less indoor air quality (Yüksel et al., 2020).

Atmaca and Gedik (2020) conducted a study to determine thermal comfort in a temperate humid climate. The study aimed to evaluate the influence of active air conditioning systems on thermal comfort by studying two mosques, one of which contains an air-conditioning system and the other contains radiator-type split air conditioners. The study proved that the air-conditioning system is more efficient than the radiator-type split system in improving the level of thermal comfort. The researchers attributed this to the abuse of the radiator-type split system. Furthermore, the study proved that the thermal comfort levels stipulated in the standards are not appropriate for all buildings in a temperate humid climate (Atmaca and Gedik, 2020).

Diler et al. (2021) in their study examined a number of passive and active retrofit strategies to improve the level of indoor thermal comfort in a mosque building in a temperate climate. Examined passive retrofit strategies included replacing single glazing with double glazing with low-emissivity panels, night ventilation, and thermal insulation, while active retrofit strategies included implementing an underfloor heating system, an electric radiator, and a split air conditioner. The study proved that passive retrofit strategies have no effect on indoor thermal comfort, but the insulation of the walls negatively affected indoor thermal comfort. Whereas using active retrofit strategies led to the improvement of thermal comfort and reduced energy consumption (Diler et al., 2021).

By reviewing the literature, it seems clear the lack of studies of mosque buildings in terms of thermal comfort and energy consumption in cold climates. This study will be distinguished as one of the first studies that shed light on this field.

Like any other building, the design of the mosque is influenced by many factors, these factors include the components of the building envelope, building materials, orientation, geographical location, and climate. These factors are controlled to build buildings with high efficiency in terms of thermal comfort and energy consumption. Regardless of the rest of the factors, the orientation factor is not controllable in mosque buildings as the direction of the Qibla determines the orientation in mosques.

Qibla is the direction of Mecca, where the Kaaba is located that specifies the direction of prayer. The worshipers from any point on the Earth must direct to the Kaaba. According to the geographical location of Turkey, the Qibla direction is located in the Southeast. The direction of the Qibla in Ankara city deviates from the north by 160 degrees (Figure 2.15), which means that the Mihrab Wall must be located in the preferred direction to gain solar radiation (the main element of the passive solar system).



Figure 2.15. Qibla direction in Turkey (Ilçi et al., 2018).

The direction of the Qibla was the inspiration in the design of traditional mosques. The traditional philosophy of designing mosques is based on several factors, the most important of which is the holiness of the direction of the Qibla, where it must be free from any manifestations that would distract worshippers from their prayers (Ghouchani et al., 2019). This can be noticed through the opaque walls facing the Qibla.

The first appearance of the modern mosque in more than three decades, TBMM mosque was built in Ankara in 1989 as an abstract version of the traditional Ottoman mosque. The mosque is distinguished by the transparent wall facing the Qibla (Figure 2.16). “The mihrab on the south wall is made of glass. Designed as a transparent element, it brings a unique and successful interpretation of the traditional mihrab form and attracts attention with all the symbolic values loaded on it”. (Ürey, 2010). For the courage and boldness of the mosque's design, the Aga Khan Award was awarded in 1995.



Figure 2.16. Mihrab wall of TBMM mosque (URL9).

TBMM Mosque opened the door to the challenge for architects to free their ideas and imagination in designing more modern mosques. During the past few years, many mosques have been implemented with a modern character, where the use of large glazed surfaces is the most recognized feature of them. Appendix D contains photographs of examples of these mosques.

In a study conducted by Ürey (2010) to explore the use of the traditional Ottoman mosque elements, and the following can be retrieved:

1. Modern mosques are a re-exploration of traditional mosques as modern mosques in Turkey have preserved the basic elements of the traditional mosque.
2. Modernity is represented by building materials and modern technologies. For example, the appearance of reinforced concrete had an impact on the design of mosques, where its use led to the possibility of the appearance of large flat roofs and the possibility of dispensing with arches in addition to being utilized in the repositioning of the dome.
3. The modern approach of Architects is to build modern mosques based on an abstract basis of traditional mosque architecture taking into account the

prevailing factors affecting the formation of mosques. These factors may include construction techniques, building materials, and climate.

4. Daylight is an important element in modern mosques by using large glazing surfaces in mosque facades especially in the Qibla direction. The source of this approach may be the ideology of guiding worshippers to the sunlight during worship.

However, before designing mosques with south-facing glazed facades, we must determine the risks involved to avoid them. They are as follows:

1. Distracting the attention of worshipers.
2. High heat gain during summer.
3. High heat loss during winter.

The use of dark glass or covered with shading patterns can help solve the issue of distraction. Also, shading devices can be established to reduce heat gain during summer in hot climates. Moreover, using glass panels with high SHGC can decrease heat loss through the glazing surfaces.

PART 3

MATERIAL AND METHOD

This part provides detailed background about the materials and methods that were utilized in this research. The materials section includes details about Yaşamkent mosque located in Ankara, data loggers, data collection tools, simulation software, and weather data. The method section describes the procedures for data collection, data evaluation, and the description of retrofit scenarios in this research.

3.1. MATERIAL

The main purpose of this research is to verify the effect of passive solar design strategies on heating loads in cold semi-arid climate regions. For this purpose, the study was conducted in one of the mosques in Ankara city in Turkey. Yaşamkent Mosque was selected as a case study of this research. The mosque building was modeled by drawings obtained from the designer's website, and field measurements were taken using a laser meter. The RC-51H data logger was used to collect temperature measurements inside the mosque prayer hall. Rhino/Grasshopper program with Ladybug and Honeybee plugins were used to examine the proposed scenarios, and the data were collected to verify the hypotheses of the study.

3.1.1. Case Study

The case study was performed at the Yaşamkent Mosque, which is located in a newly developed residential area on the western axis of Çankaya district in Ankara (Figure 3.1). In order to determine the case study that is conformable with the objectives of the study, criteria have been set for selecting the case study, which are as follows:

1. Due to the pandemic situation, attendance to the mosque must be easy and available.
2. The mosque must have passive solar design elements.
3. The mosque should be simple and devoid of complexity in shape, which may negatively affect the measurement and modeling process.



Figure 3.1. Location of Yaşamkent mosque (Google Earth).

The mosque of design A Tasarım Mimarlık. The construction of the mosque began in 2009 and opened in 2016. In addition to being an icon in the modern architecture of mosques, the designer has included passive solar design strategies within the building, and this is evident through the concrete walls of 40 cm thickness, in addition to the exploitation of the Qibla wall facing almost to the south by using it as an element to collect direct solar sun, which is the most important technique of passive solar design systems.

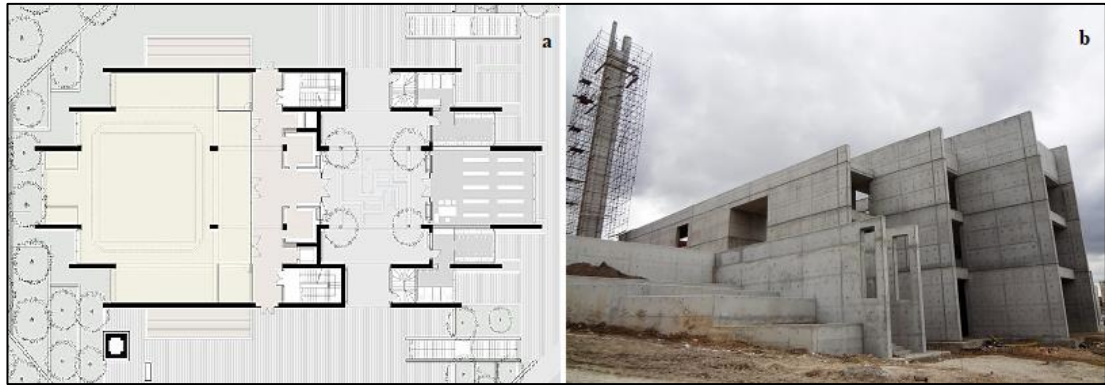


Figure 3.2. (a) The ground floor of the mosque, (b) The mosque during construction (URL10).

The field measurements of the mosque were done using SNDWAY SW-T60 Laser distance meter, and then the mosque was modeled by Revit 2020.

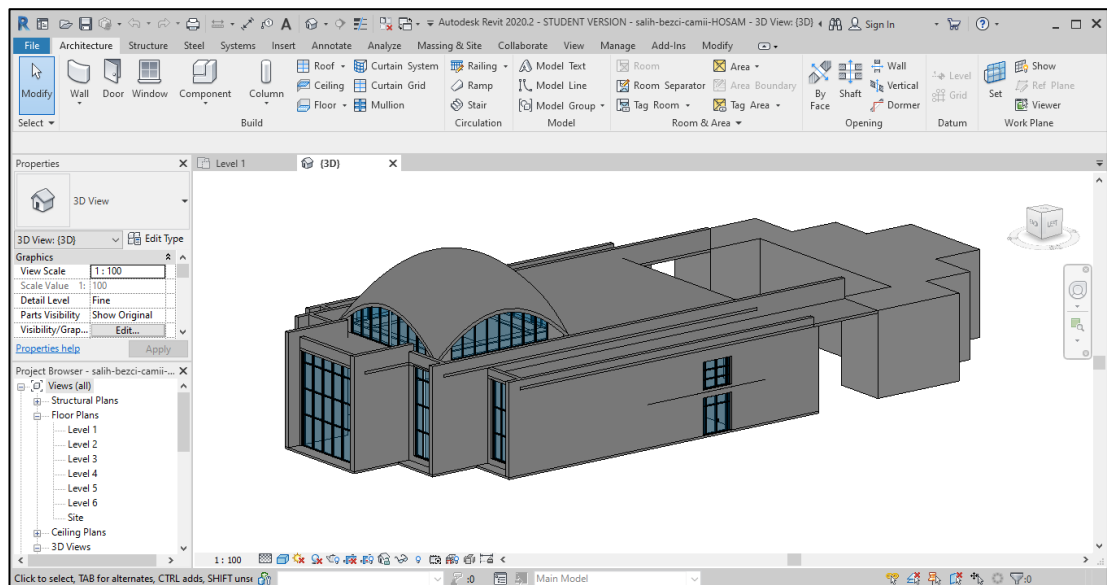


Figure 3.3. The mosque model through Revit 2020.

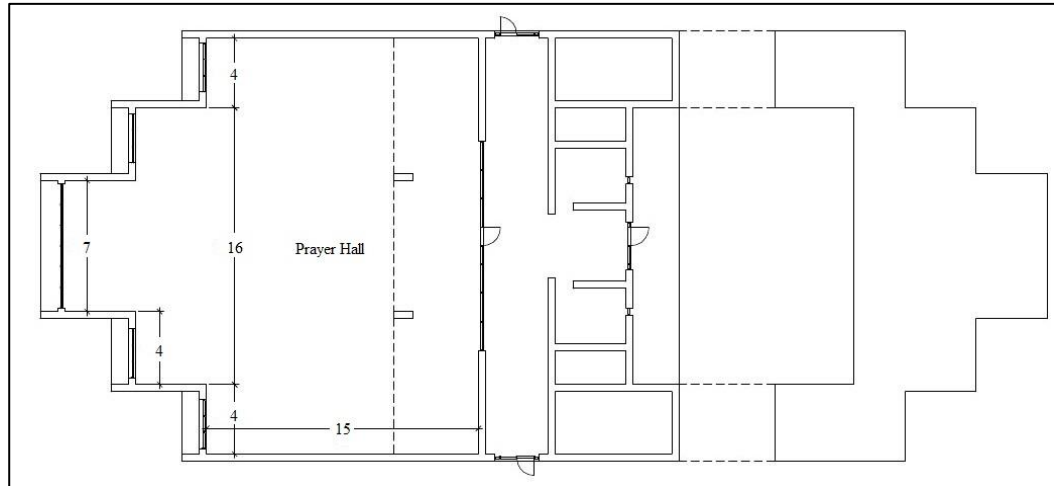


Figure 3.4. The ground floor of the mosque.



Figure 3.5. SNDWAY SW-T60 Laser distance meter.

The data about the building materials of the case study building was collected through communication with the designer. The designer's approach to employing passive solar design techniques in the building is evident. This can be recognized by the thick concrete walls (thermal mass) and the southern facade with a glazing ratio of 95% (solar collector). Table 3.1 and Figure 3.6 show layers of external walls.

Table 3.1. External walls materials and their properties (Revit library).

Material	Thickness (mm)	Density (kg/m ³)	Specific Heat (J/kg.K)	Thermal Conductivity (W/m.K)
Precast concrete	400	2300	657	1,046
Thermal insulation	50	23	1470	0,035
Plaster	20	1120	960	0,51

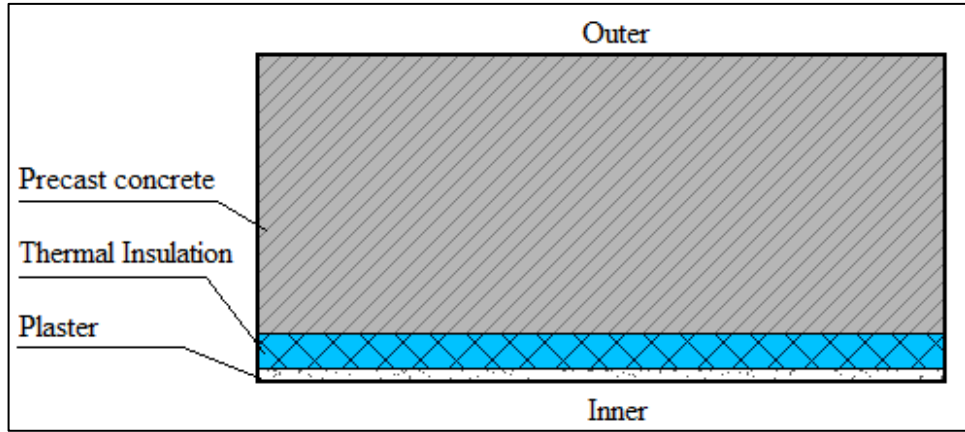


Figure 3.6. External walls layers.

The construction materials of the external walls were established according to their physical and thermal properties by using HoneyBee tools (Figure 3.7).

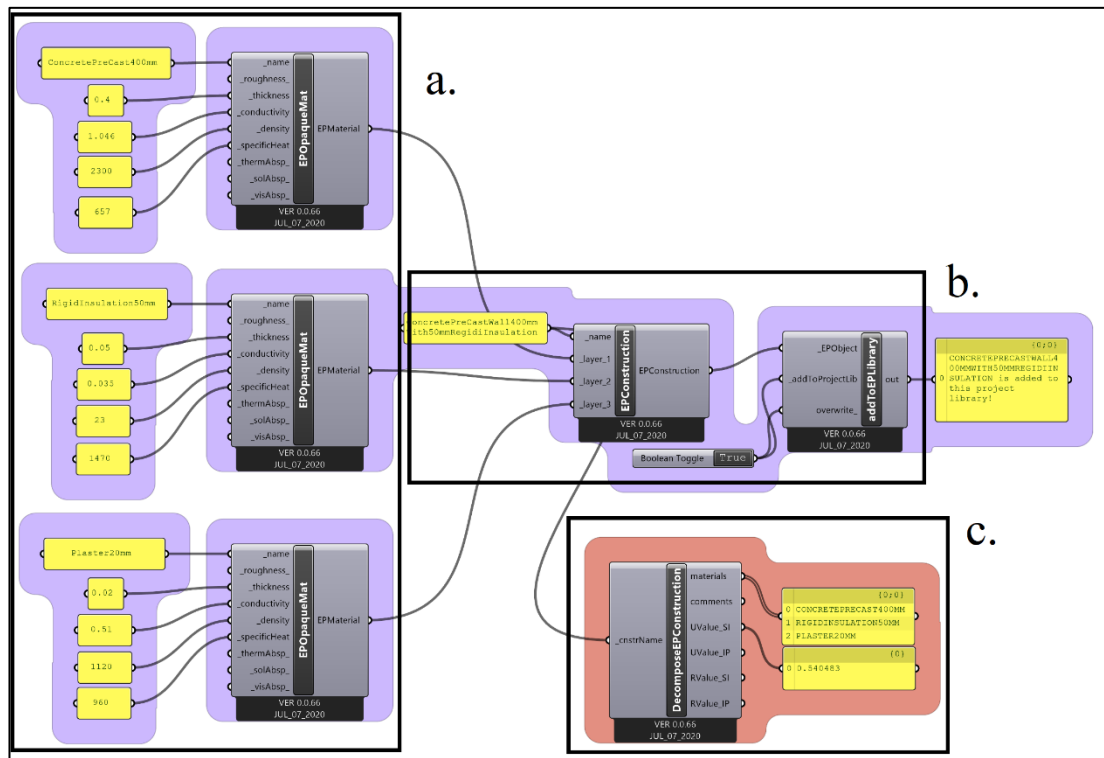


Figure 3.7. Workflow for preparing external walls, a. Construction materials, b. Establishing the wall, c. Properties of the wall.

Table 3.2. Roof materials and their properties (Revit library).

Material	Thickness (mm)	Density (kg/m ³)	Specific Heat (J/kg.K)	Thermal Conductivity (W/m.K)
Gravel	30	1840	840	0,36
Thermal insulation	35	23	1470	0,035
Precast concrete	120	2300	657	1,046
Plaster	20	1120	960	0,51

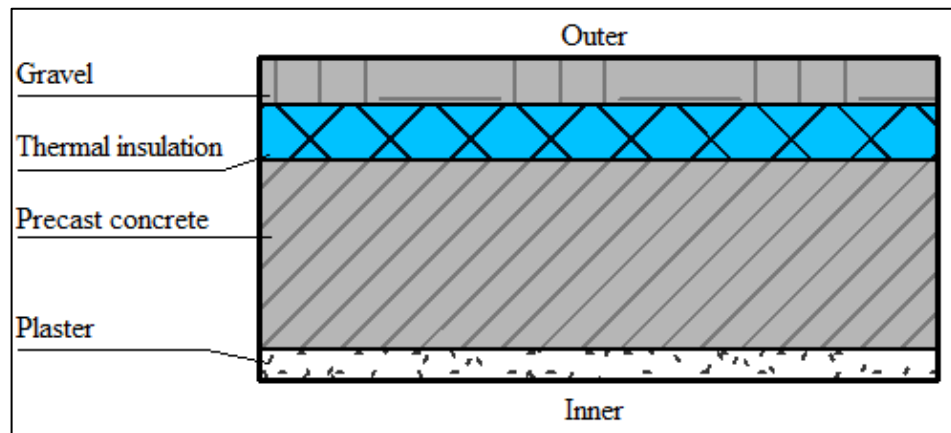


Figure 3.8. Roof layers.

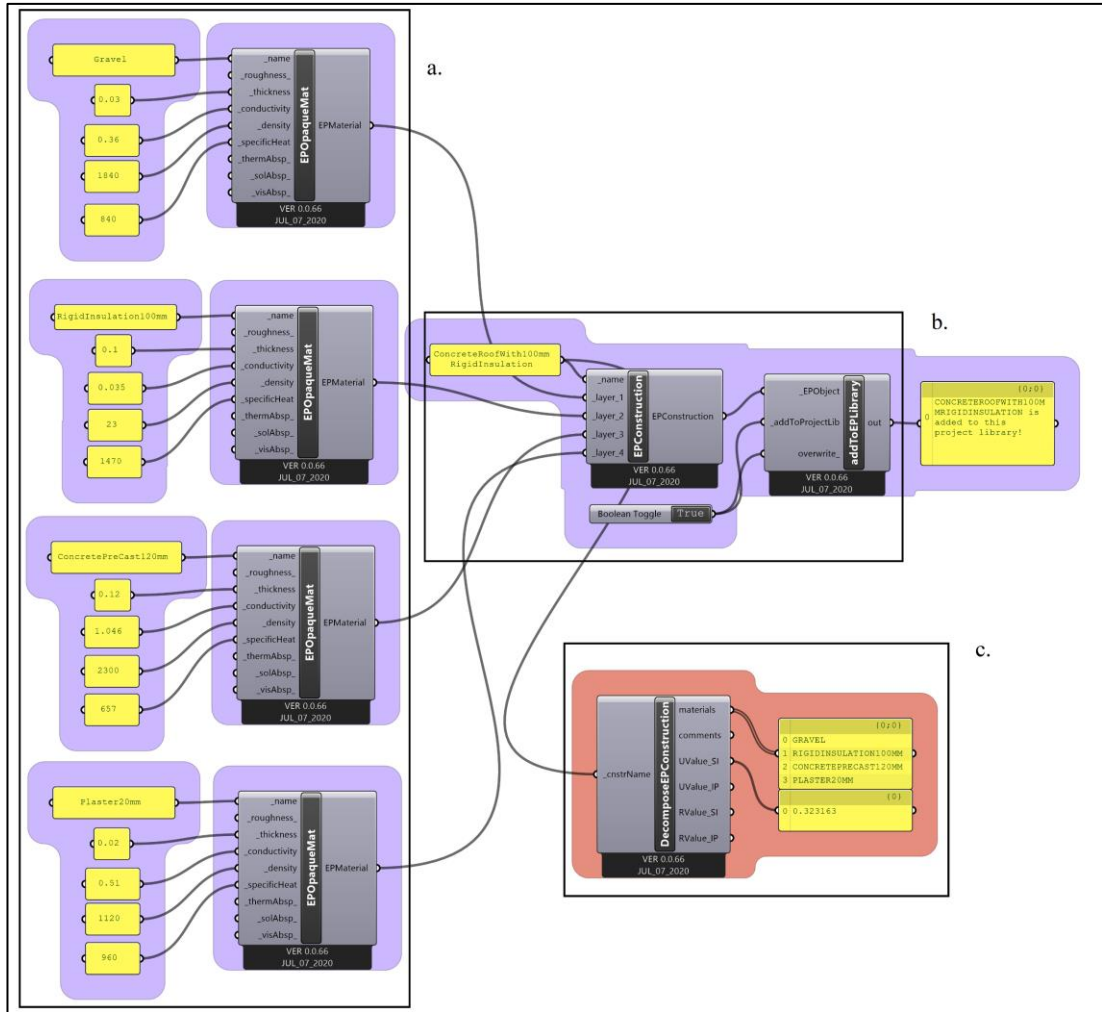


Figure 3.9. Workflow for preparing the roof, a. Construction materials, b. Establishing the roof, c. Properties of the roof.

Table 3.3. Floor materials and their properties (Revit library).

Material	Thickness (mm)	Density (kg/m ³)	Specific Heat (J/kg.K)	Thermal Conductivity (W/m.K)
Porcelain	5	2000	850	1,20
Mortar	20	1120	960	0,51
Thermal insulation	50	23	1470	0,035
Precast concrete	120	2300	657	1,046

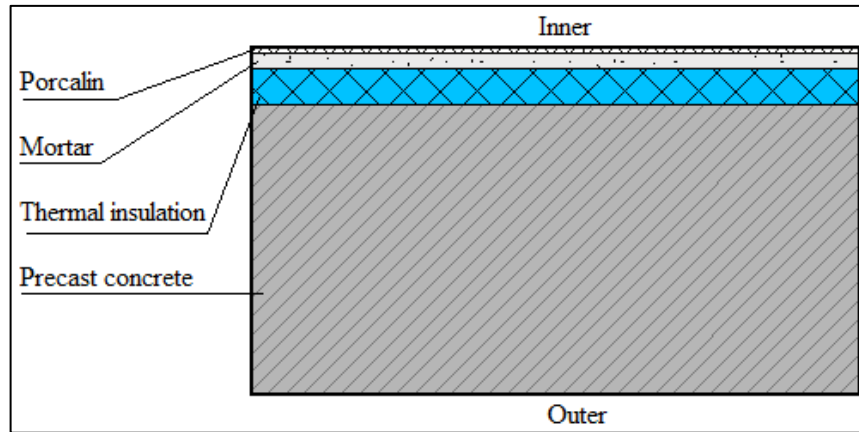


Figure 3.10. Floor layers.

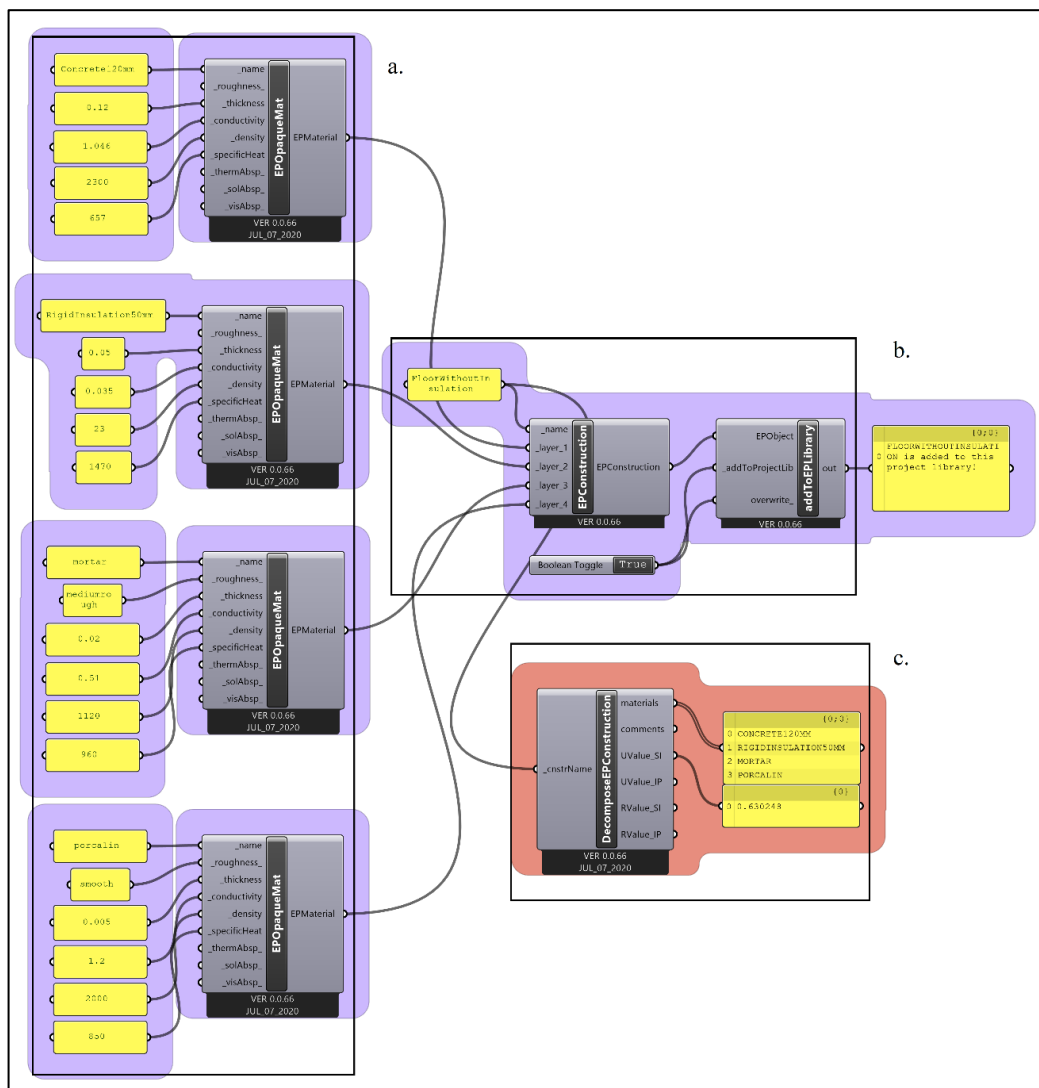


Figure 3.11. Workflow for preparing the floor, a. Construction materials, b. Establishing the floor, c. Properties of the floor.

The use of passive solar design techniques is evident through the glazing, where the designer glazed the southern facade by 90% of the facade surface. On the other hand, there is no glazing used on the eastern and western facades, as well as the northern facade, which is separated from the prayer hall by the entrance hall, and the service zone. Double-glazing windows have been used in the southern facade. The thickness of each panel is 6 mm, divided by a 12 mm thick air gap.



Figure 3.12. A view inside the prayer hall showing the glazing façade.

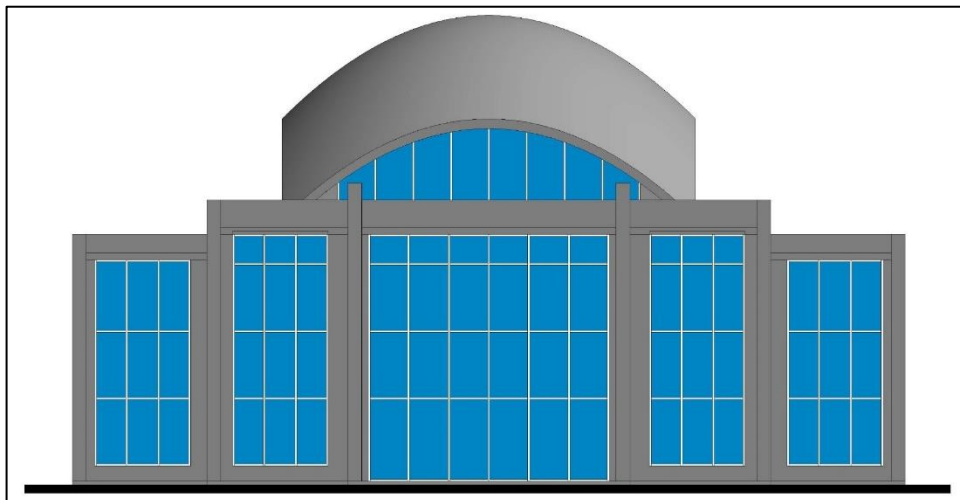


Figure 3.13. South façade of Yaşamkent mosque.



Figure 3.14. Double glazing window.

Table 3.4. Properties of the glass material (Revit library).

Material	Thickness	Solar Transmittance	Solar Reflectance	Visible Transmittance	Visible Reflectance	Front Emissivity	Back Emissivity	Conductivity
Glass	6 mm	0,75	0,14	0,80	0,14	0,95	0,50	2,7

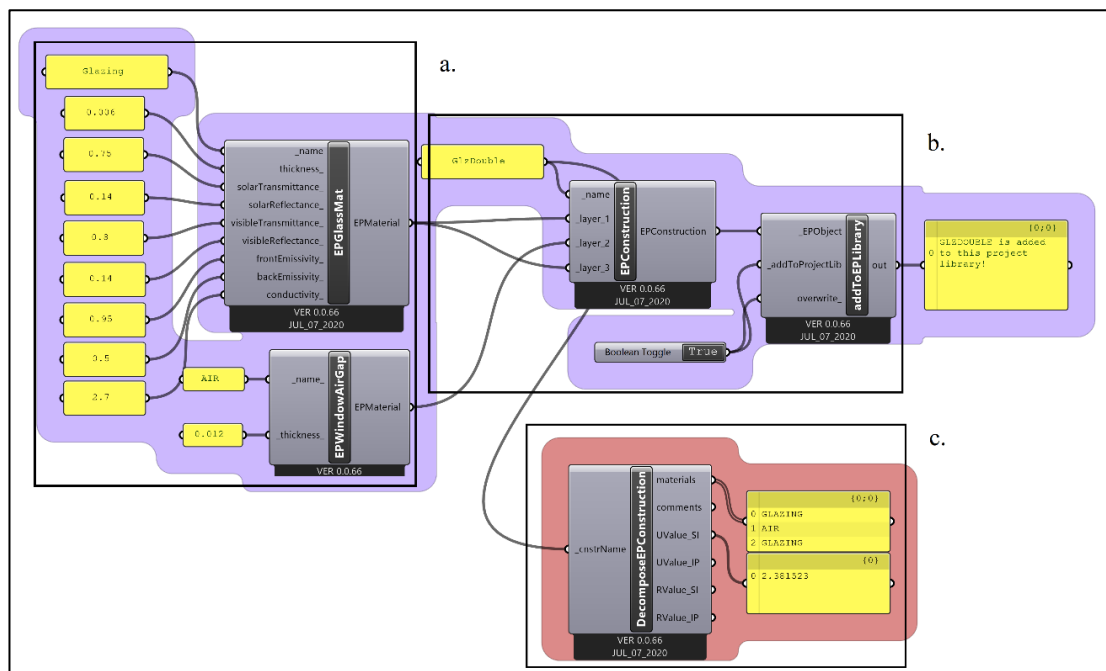


Figure 3.15. Workflow for preparing the window, a. Material properties, b. Establishing the window, c. Properties of the window.

Table 3.5 contains U-values of the building envelope according to the construction materials that the mosque is built from, which are explained in detail in this section.

Table 3.5. Thermal properties of the building constructions (By author).

	Wall	Roof	Floor	Window
U-value	0,540	0,323	0,630	2,38

3.1.2. Climate Analysis of Ankara

Climate has a substantial influence on energy usage in buildings, so the climate is considered an influencing factor in the building industry sector. There are four climate zones in Turkey according to the method suggested by the IEA. This climate classification was used for calculating required energy for heating in The Turkish Standards Manual for Thermal Insulation for Buildings TS 825 (Pusat & Ekmekci, 2015).

The International Energy Agency (IEA) proposes a model consisting of six climate zones and uses the heating and cooling degree-days method. The suggested base temperature in this model is 18°C (Table 3.6).

Table 3.6. Heating and cooling degree-day limits (IEA, 2008).

Climatic Zones	Heating Cooling	Cooling
Cold Climate	$2000 \leq \text{HDD } 18^\circ\text{C}$	$\text{CDD } 18^\circ\text{C} < 500$
Heating Based Climate	$2000 \leq \text{HDD } 18^\circ\text{C}$	$500 \leq \text{CDD } 18^\circ\text{C} < 1000$
Combined Climate	$2000 \leq \text{HDD } 18^\circ\text{C}$	$1000 \leq \text{CDD } 18^\circ\text{C}$
Moderate Climate	$\text{HDD } 18^\circ\text{C} < 2000$	$\text{CDD } 18^\circ\text{C} < 1000$
Cooling Based Climate	$1000 \leq \text{HDD } 18^\circ\text{C} < 2000$	$1000 \leq \text{CDD } 18^\circ\text{C}$
Hot climate	$\text{HDD } 18^\circ\text{C} < 1000$	$1000 \leq \text{CDD } 18^\circ\text{C}$

Ankara is the capital of Turkey and is located at the center of the Anatolian plateau in 39,57 latitudes, 32,53 longitudes, at an altitude of 894 m above sea level. Ankara has a cold semi-arid climate according to the Köppen classification (BSk).

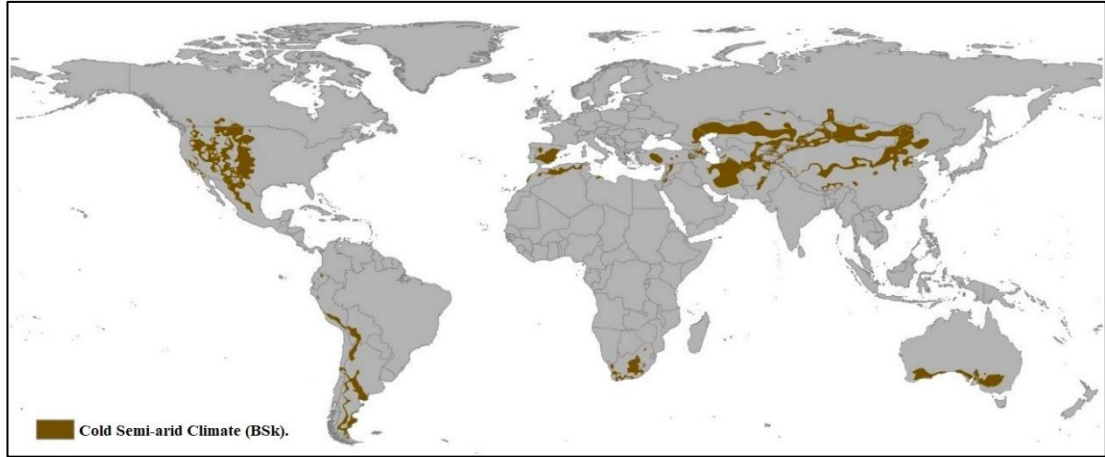


Figure 3.16. Cold semi-arid climate regions according to Köppen World Map (Köppen, W).

Büyükalaca et al. (2001) in their study determined the heating and cooling degree-days for Turkey by utilizing long-term observed data with variable base temperatures (Büyükalaca et al. 2001). Table 3.7 and Table 3.8 show the values of heating and cooling degree-days for Ankara.

Table 3.7. Heating degree-day for Ankara (Büyükalaca et al. 2001).

Location	Base temperature (C°)					Period
	14	16	18	20	22	
Ankara	1773	2199	2677	3214	3811	1981-1995

Table 3.8. Cooling degree-day for Ankara (Büyükalaca et al. 2001).

Location	Base temperature (C°)						Period
	18	20	22	24	26	28	
Ankara	433	240	109	37	8	1	1981-1995

Weather data for Ankara was obtained through weather maps provided by the Epwmap server in “<https://www.ladybug.tools/epwmap/>.” The weather file data was obtained from Typical Meteorological Year (TMY) data is used during the period 2004 to 2018. Weather data was observed and collected through Etimesgut Air Base station 15 km west of Ankara and can be downloaded from:(URL1).

The hourly temperature in Ankara ranges between -14 and 37 °C during the year. January is the coldest month, with a temperature range of -14 to 13 °C. July is the hottest month of the year, with an average temperature of 10,6 to 37 °C.

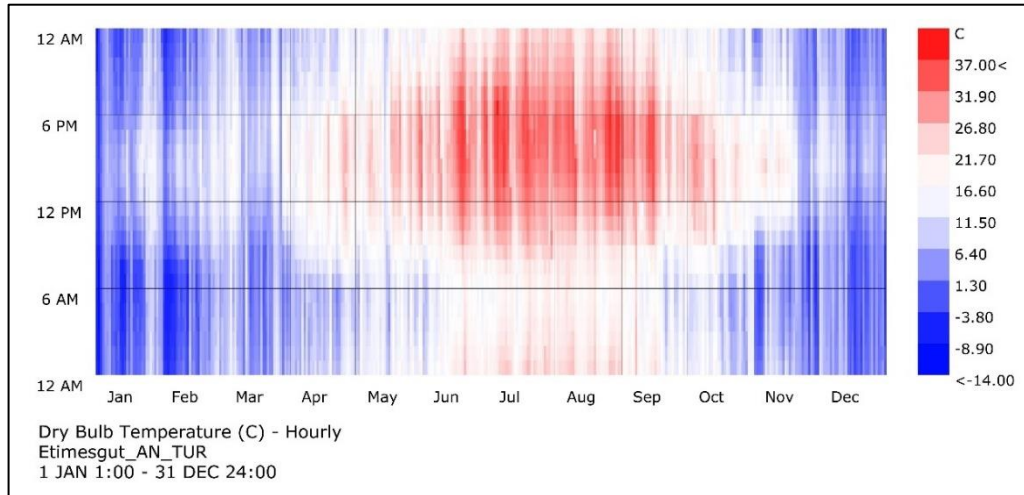


Figure 3.17. Annual air temperature in Ankara by LadyBug Tools

Hourly relative humidity range between 13% to 100% during the year. The highest relative humidity was in December with an average of 84,4%, and the lowest relative humidity was in August, where the average relative humidity was 48,9%.

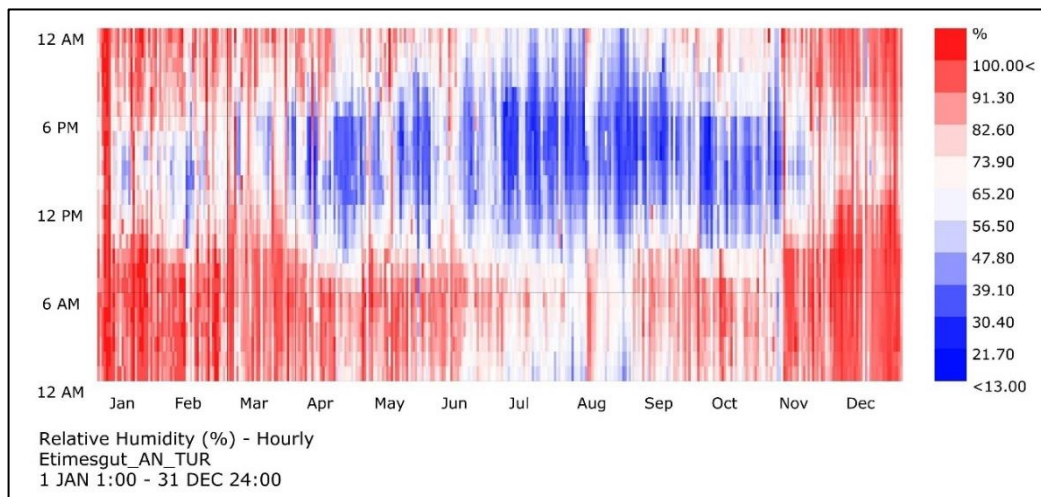


Figure 3.18. Annual relative humidity in Ankara by LadyBug Tool.

The prevailing wind throughout the year in Ankara is the west wind. According to the hourly wind speed data during the year, the wind speed ranges between 0 and 16,4 m/s.

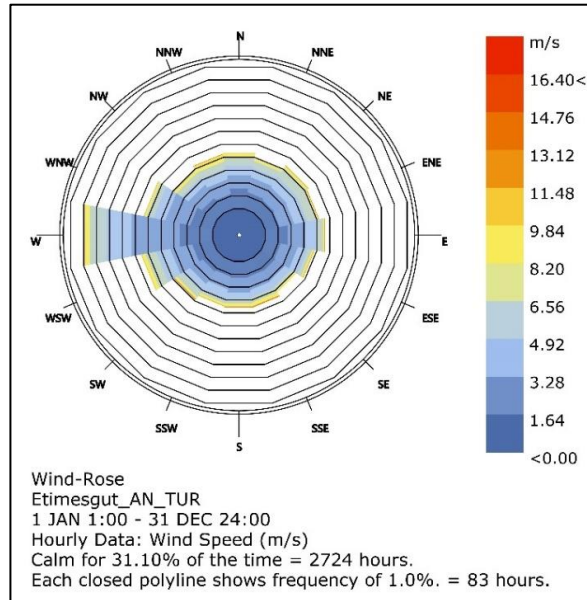


Figure 3.19. The wind rose for Ankara by LadyBug Tools.

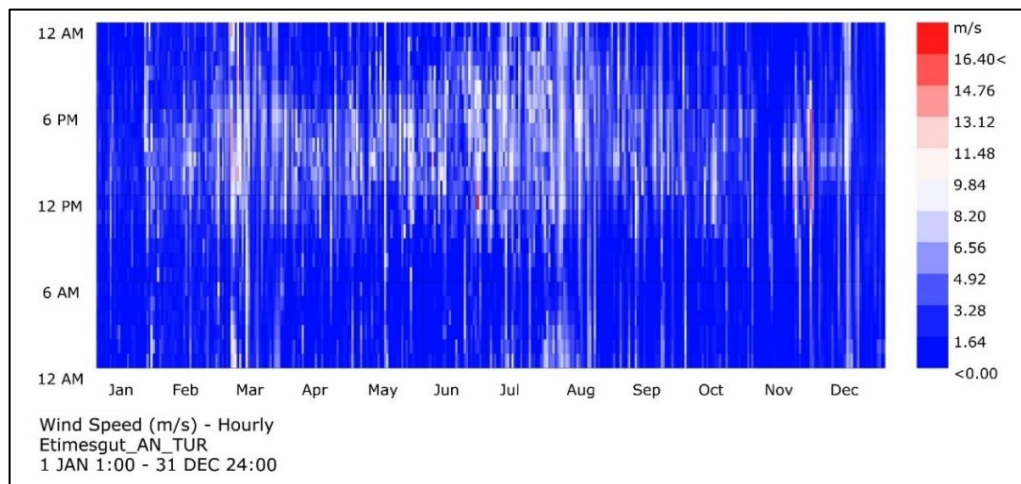


Figure 3.20. Hourly wind speed for Ankara by LadyBug Tools.

The comfort zone was calculated during the cold months through the psychrometric chart, and it was found that the comfort zone was equivalent to only 1,7% of the entire period. On the other hand, by using a passive solar heating system, the comfort zone can be increased by 30%.

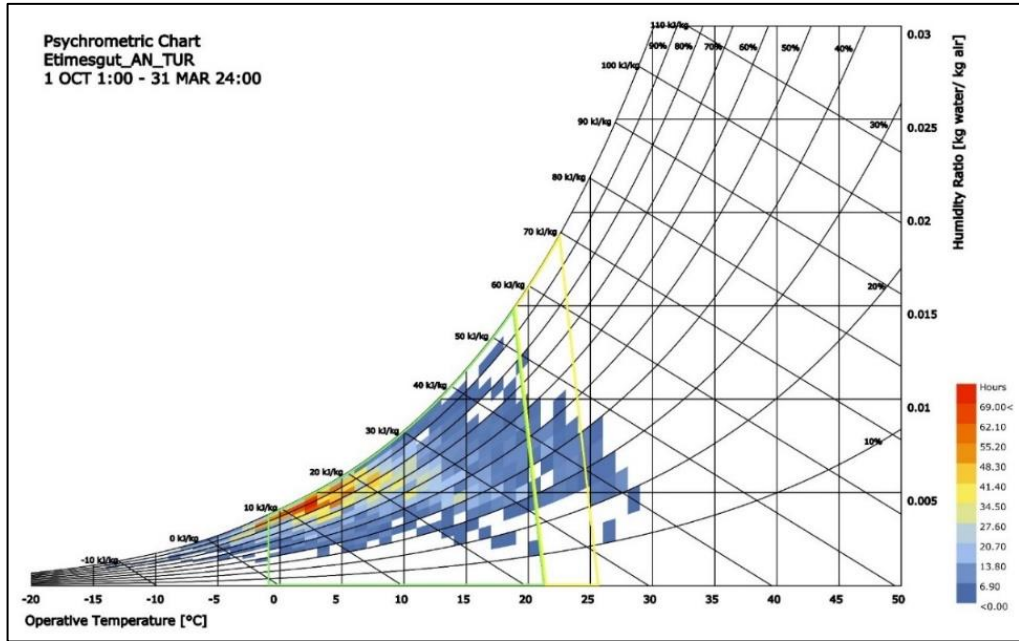


Figure 3.21. Psychrometric Chart for Ankara during cold months. The yellow polygon is the comfort zone without any passive or active systems, and the green polygon is the comfort zone with the passive solar heating system.

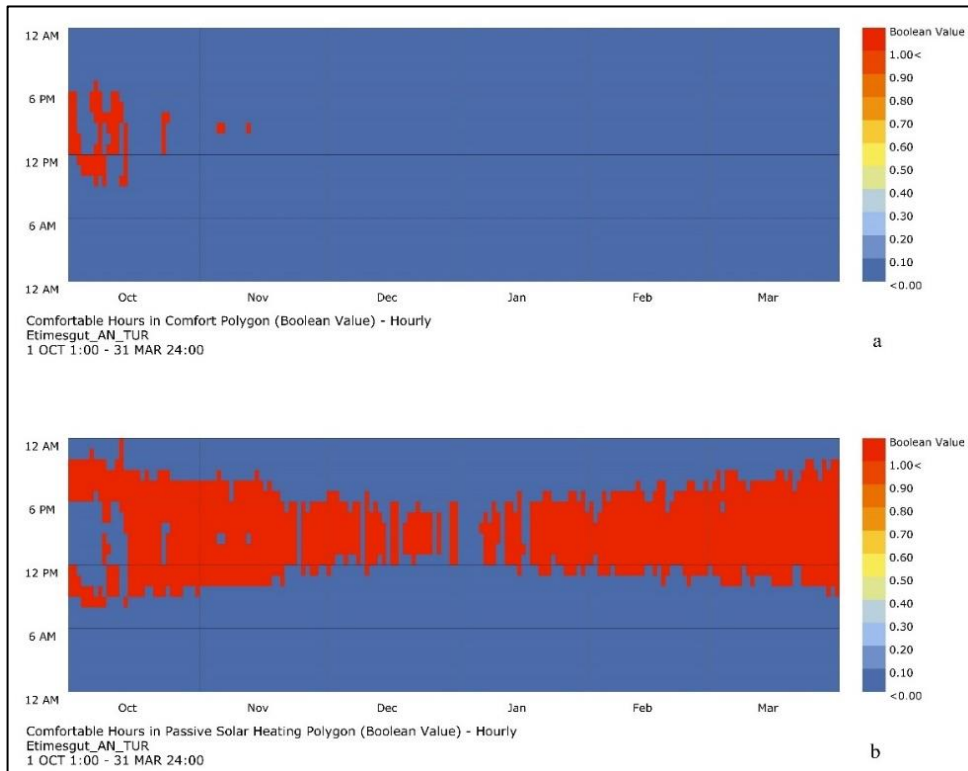


Figure 3.22. Comfortable hours of comfort zone for Ankara. (a) for comfort zone without any passive or active systems, (b) for comfort zone with the passive solar heating system by LadyBug Tools.

According to Figure 3.22, the red area shows the comfort zone. As might well be observed in Figure 3.22 (a), the comfort zone is in the daytime during October, while it is barely noticed in November. By establishing passive solar heating system parameters provided by Ladybug tools, the space becomes more comfortable, as shown in Figure 3.22 (b).

By analyzing weather data, it is obvious that the heating loads are the largest throughout the year. The highest heating load is in January at 522,55 degree days.

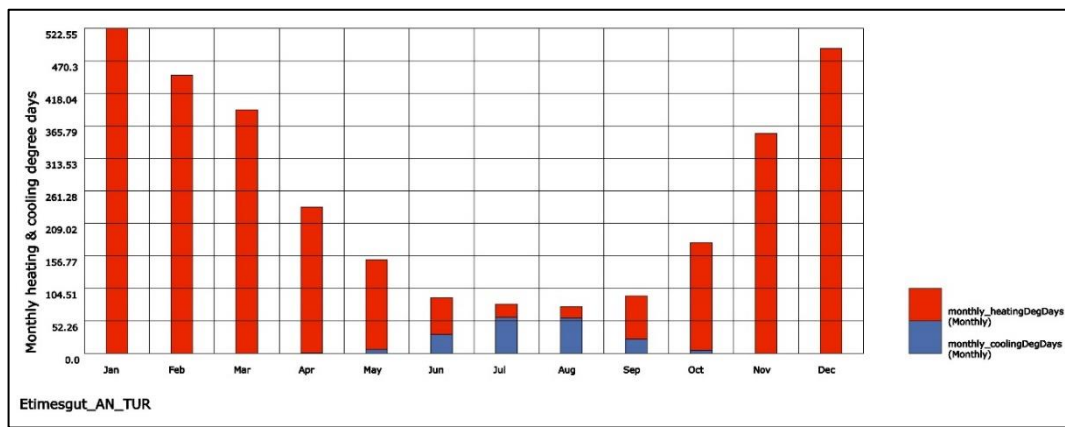


Figure 3.23. Monthly heating and cooling loads (HDD&CDD) for Ankara by LadyBug Tools.

3.1.3. Simulation Program

Computer simulation software is an essential tool for verifying the performance of buildings. With this software, the possibilities for further development are limitless. Building performance simulation has great benefits for many building stakeholders as well as the environment (Djunaedy et al. 2006). The benefits of computer simulation software are that they allow the effective improvement and development of the building form, user needs, mechanical equipment and systems, environmental elements, and the dynamic interactions of the building with its components and the surrounding environment. Hence, simulation software has become an important tool in supporting decision-making in the early design stages to determine the impacts on building performance (Bazafkan, 2017).

In this study, the Grasshopper plugin was employed to prepare the mosque 3D model for the simulation process. Grasshopper is an open-source tool and works only within the Rhino environment. Ladybug (LB) is a plugin that works inside Grasshopper. This tool imports weather data in EPW format and analyzes it to understand the site and its climatic conditions. Honeybee (HB) is another important plugin. It is used to create the energy model and connects it to EnergyPlus and OpenStudio engines to analyze the building performance.

3.1.3.1. Grasshopper

Grasshopper is a visual programming language and environment that runs inside the Rhinoceros 3D software. It was produced by David Rutten at Robert McNeel & Associates. Grasshopper is essentially used to create generative algorithms such as creative art, parametric modeling for architecture and structure engineering, digital fabrication, optimization and automation, jewelry design, evolutionary design, and biomimicry (Mode Lab, 2015). Grasshopper is an open-source plugin and functions within a development community, where many users and developers create and develop their own components for use by others (Baker, 2017). Visual Programming like Grasshopper can be handled by the user through programming languages where the logical elements are dealt with graphically instead of text. In Grasshopper, Python language is used to enter and modify data.

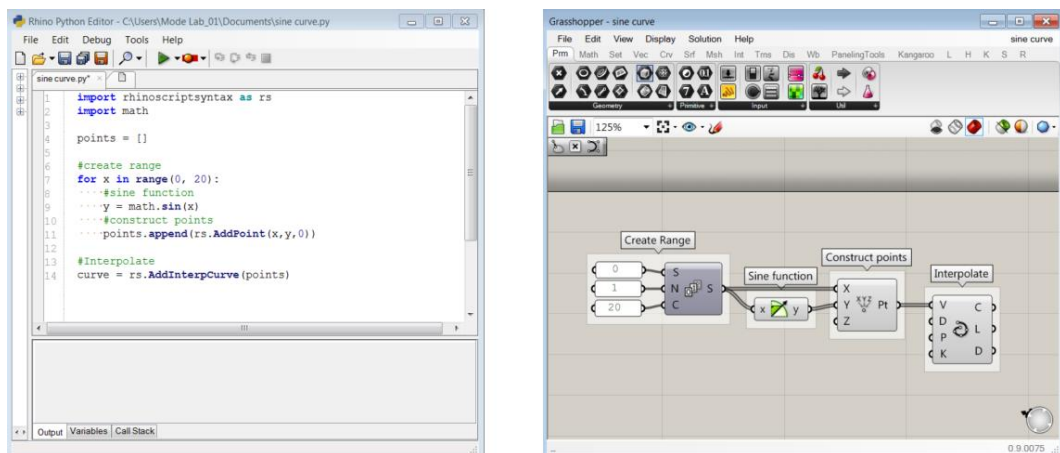


Figure 3.24. The process for drawing a sine curve within python and in Grasshopper (Mode Lab, 2015).

3.1.3.2. Building Performance Simulation in Grasshopper

Recently, Grasshopper has been considered one of the most significant building performance simulation (BPS) software. Several open-source plugins are available for Grasshopper that deal with BPS. They can run a large range of simulation and optimization operations. These plugins are interfaces for preparing the energy model of the building and then performing simulations using external simulation engines such as Energyplus, OpenStudio, Radiance, etc. (Bazafkan, 2017).

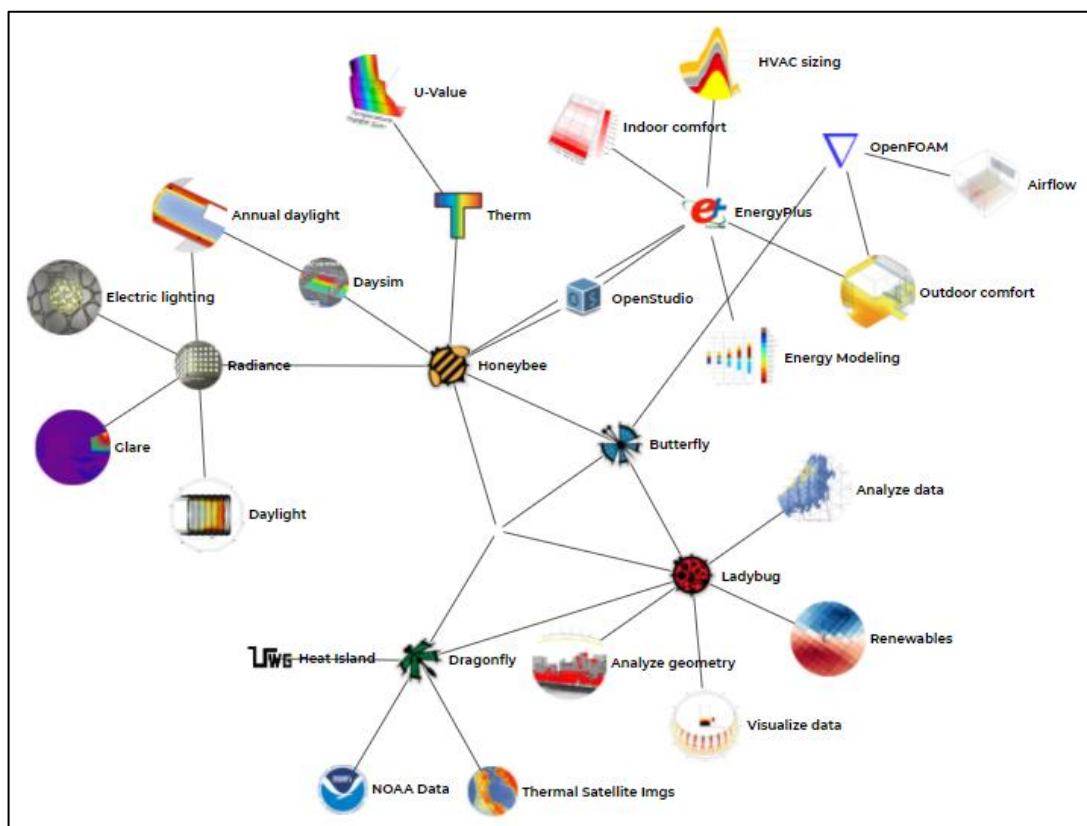


Figure 3.25. Building Performance Simulation tools in Grasshopper (URL2).

It is a complex process that is done within Grasshopper through BPS tools and needs to understand how it works in preparing the energy model to avoid any errors that lead to the model not working properly. The following figure shows the complexity and precision of building the energy model for the case study and that any error in the workflow will lead to the failure of the simulation process.

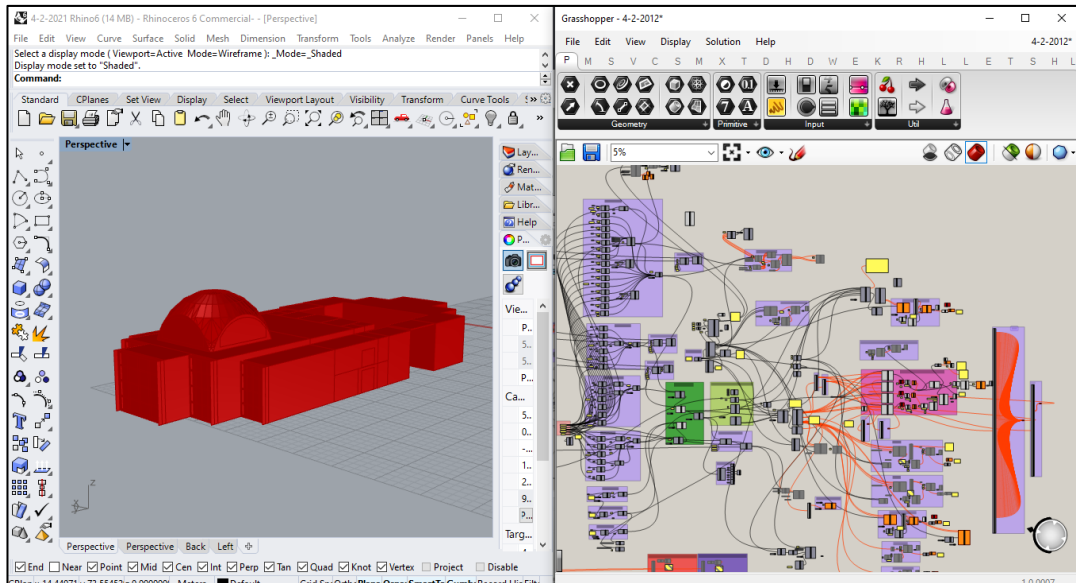


Figure 3.26. Complexity of preparing energy model for the case study.

Ladybug tools and Honeybee tools are the most popular and most widely used BPS tools in Grasshopper. Ladybug and honeybee tools are characterized by the ability to exchange data with the most distinguished simulation engine EnergyPlus in addition to other well-known and validated engines such as OpenStudio and Radiance.

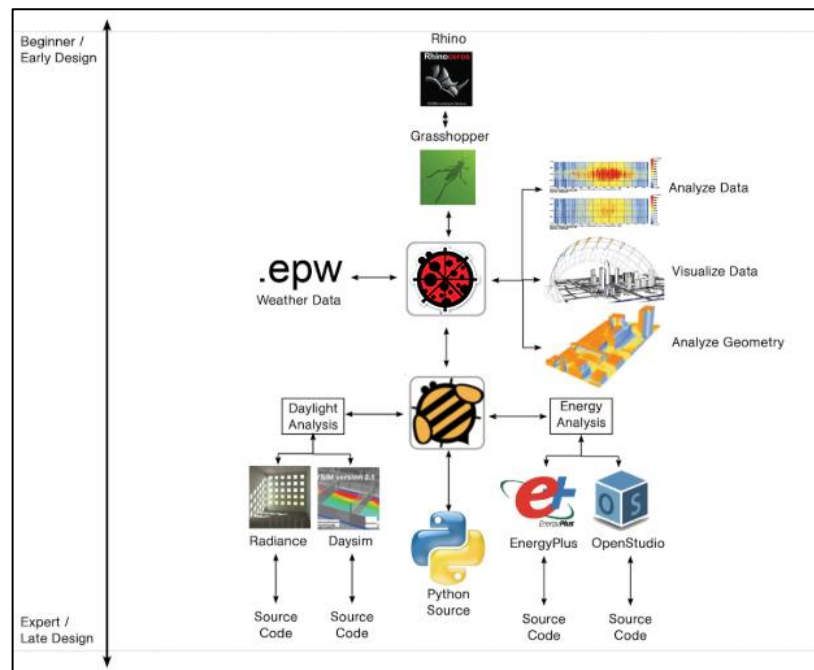


Figure 3.27. The relationship between Rhino, Grasshopper, Ladybug, Honeybee, and the simulation engines (URL3).

3.1.3.3. LadyBug Tools

Ladybug is an open-source environmental tool that is compatible with Grasshopper developed by Mostapha Sadeghipour Roudsari and others. This plugin contains more than 100 components and is responsible for obtaining and analyzing EnergyPlus weather files (EPW) as well as analyzing the site and using this data in the simulation process of the energy model. Ladybug allows to build charts such as sun-path, wind-rose, radiation-rose, etc., configure charts in diverse ways, conduct radiation analysis, shadow studies, and visualize the analysis in 2D and 3D forms (Roudsari and Pak, 2013).

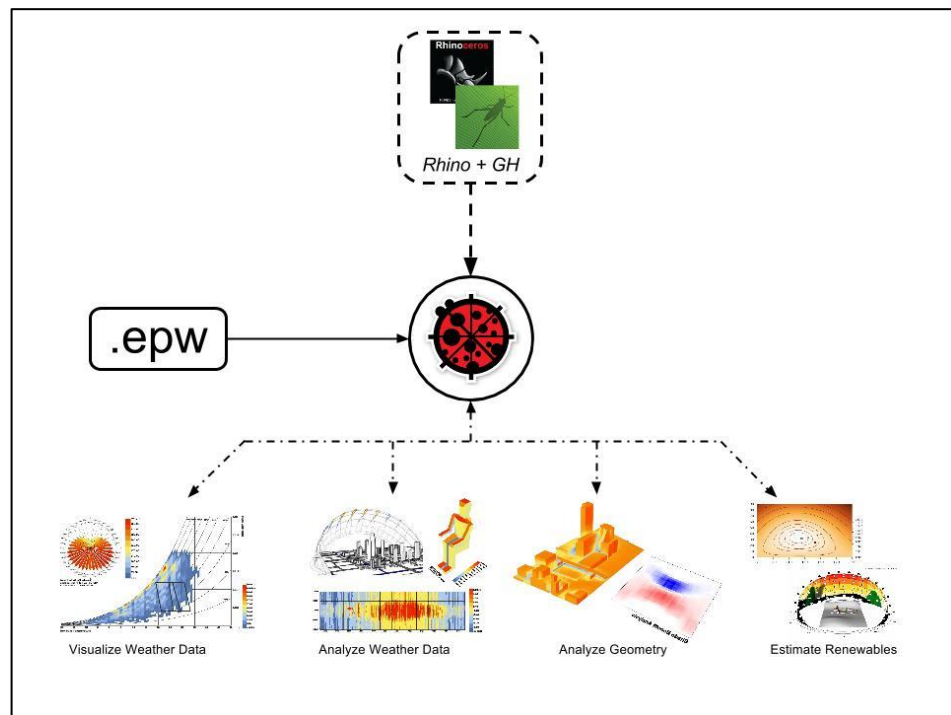


Figure 3.28. Outputs of Ladybug tools (URL4).

For example, a simple Ladybug workflow to explain sun-path for the case study in this research is described as follows:

1. Run Ladybug mother component by dragging and dropping it into Grasshopper workspace. It is the main component that all ladybug classes will not work without running it.

2. Call up the EPW weather file directly from Epwmap in the Ladybug tools website.
3. Open the EWP file by importing it from the hard drive or the website by copying the URL link of the weather file.
4. Use Ladybug SunPath components to draw a 3D sun path in the Rhino scene.

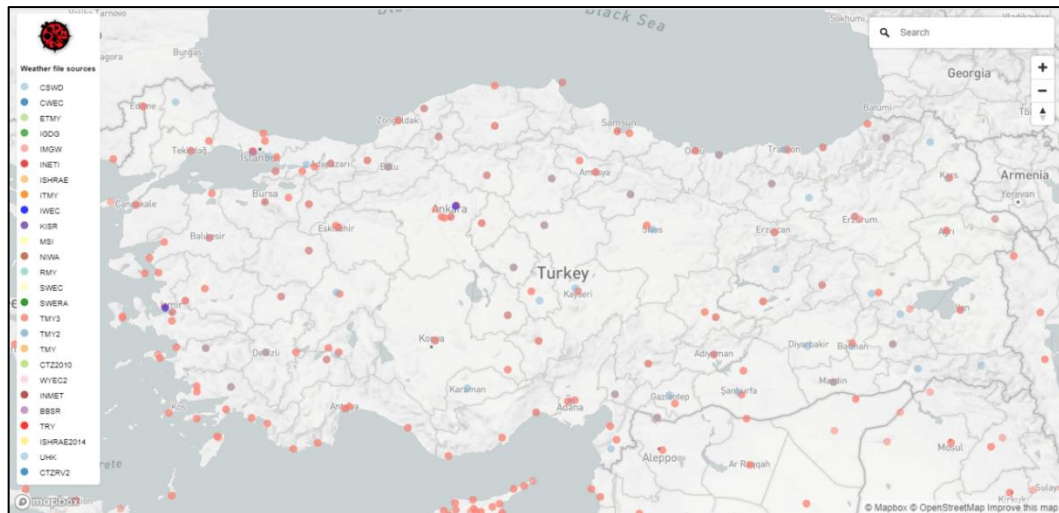


Figure 3.29. The Ewpmap for Turkey (URL5).

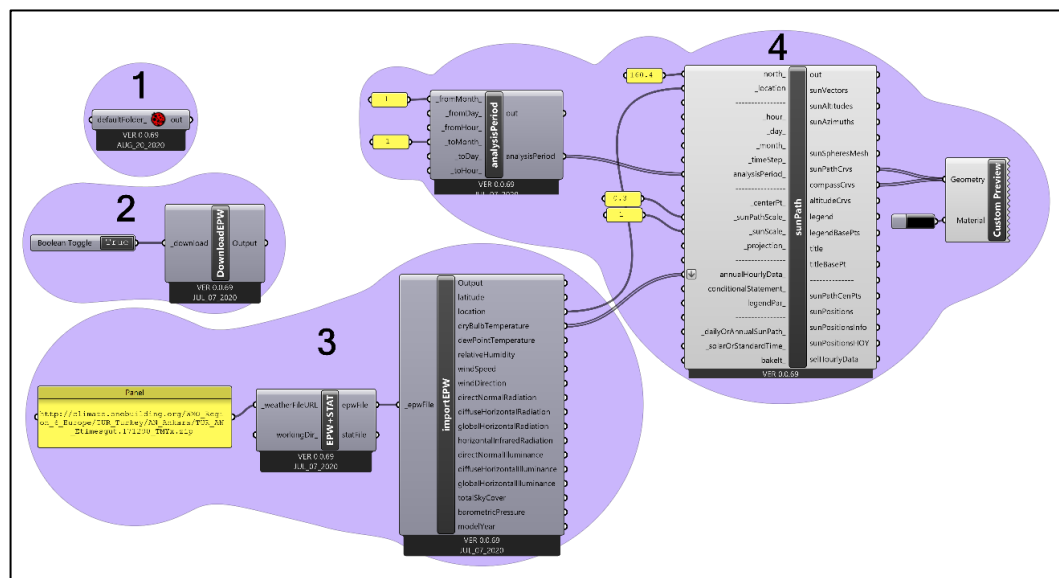


Figure 3.30. Steps to analyze sun-path for the case study by Ladybug tools.

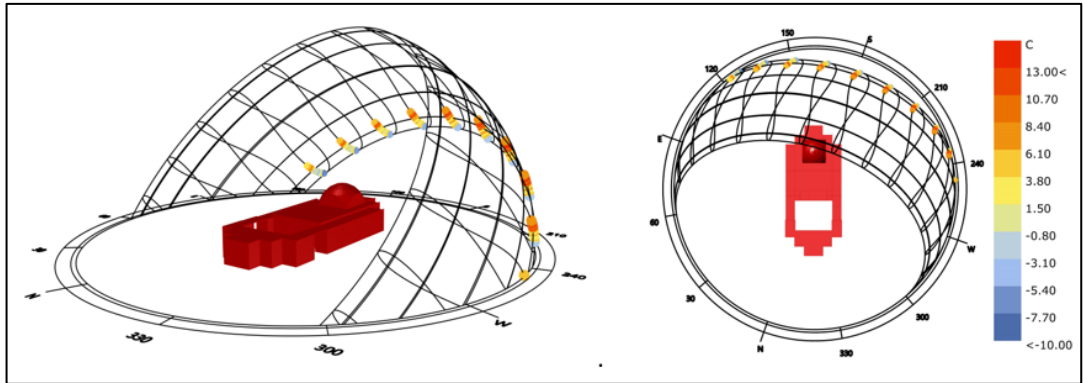


Figure 3.31. 3D diagram of sun-path visualizations for the case study.

3.1.3.4. HoneyBee Tools

Honeybee is an open-source plugin for Grasshopper developed by Mostapha Sadeghipour Roudsari and others to work at the building level to manage the analysis of building performance. HoneyBee performs simulation processes through validated external engines like EnergyPlus, Radiance, Daysim, and OpenStudio.

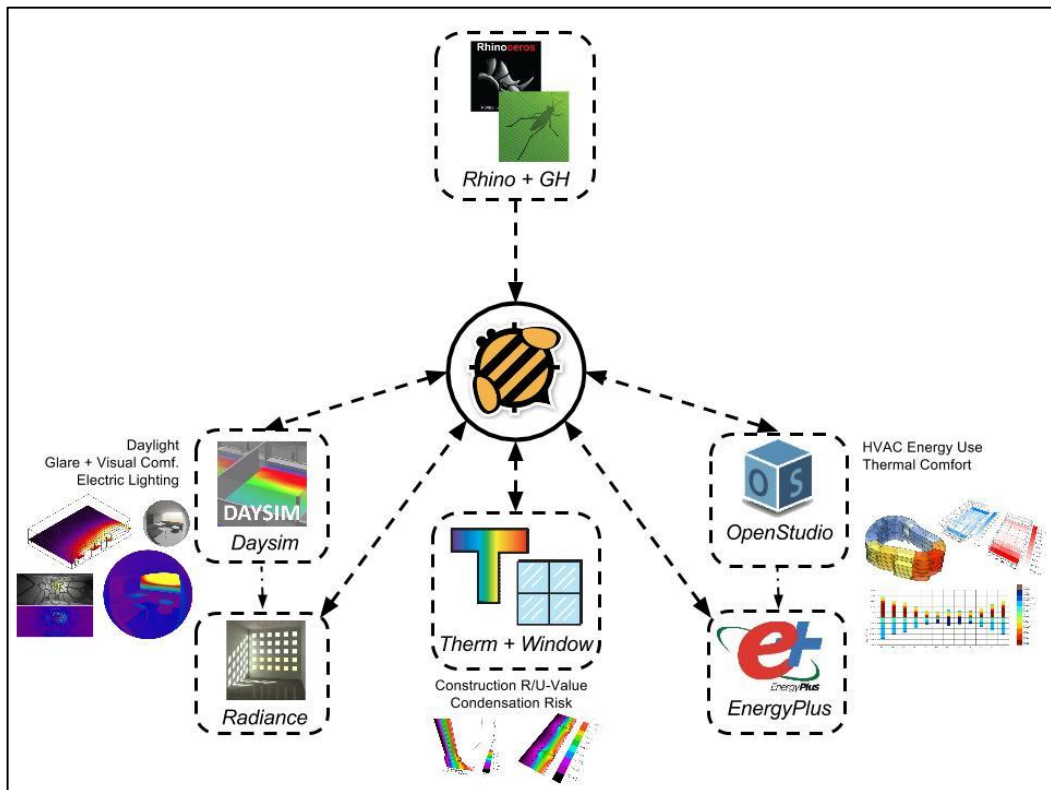


Figure 3.32. HoneyBee working methodology (URL6).

HoneyBee works seamlessly with LadyBug tools and takes advantage of the weather data and environmental analyzes performed by LadyBug. There are four main steps to conduct analysis in Honeybee (Roudsari and Pak, 2013):

1. Preparing energy model (simulation geometry).
2. Checking the input data and files.
3. Running the simulation.
4. Visualizing the results.

Many studies used the simulation tools utilized in this research. For example, Konis et al. (2016) used them to assess the impact of passive design strategies during the early stages of design; Toutou et al. (2018) used them to assess energy performance in a hot, dry climate; and Ardabili (2020) employed Ladybug tools to analyze smart facades.

3.1.4. Data Logger

The RC-51H data logger was employed in this study to collect and measure the data. The RC-51H data logger was located inside the mosque in the prayer hall in which is close to the south facade. RC-51H data logger works with ElitechLogWin software. By this software, the settings of the data logger can be edited, such as choosing the method of measuring the temperature and determining the time interval between each measurement process and another. Also, data can be obtained and exported as Excel or PDF files by ElitechLogWin software (Appendix A).



Figure 3.33. RC-51H data logger.

3.2. METHOD

The methodology of this research is based on two main steps. Firstly, the indoor temperatures of the case study were measured by using a Datalogger. The data has been collected over six continuous days. Secondly, a simulation process of the case study was conducted to extract the data and match it with the field data, and then the retrofitting was made on the case study and tested to verify the hypotheses of the study.

Six steps have been taken to conduct this research. Firstly, the case study was visited to take real measurements with the help of architectural maps obtained from the designer's website. Secondly, Temperature data were collected for six consecutive days. Thirdly, the mosque model was created by Revit 2020 Rhinocross 7. Fourthly, analysis steps were done by Ladybug and Honeybee Tools through Grasshopper environment. Fifthly, simulated data were validated. Finally, the proposed retrofitting scenarios were examined.

3.2.1. Data Collection and Calibration

The main purpose of this research is to examine indoor thermal comfort in a cold semi-arid climate. So the data was collected during the winter for six continuous days from the 28th of November until the 3rd of December 2020. The indoor temperature data was collected by placing one data logger inside the mosque prayer hall. Elitech RC-51H data logger was used to record the data. The temperature data were recorded with an interval of one minute. In order to exclude external influences and obtain real data, the mosque officials were asked not to operate the HVAC system during the days of data collection.

The mosque was modeled using Revit 2020. Then the model was exported to Rhino 7 for the simulation process using LadyBug and HoneyBee Tools through the Grasshopper plugin, which is developed for just working with Rhino software. The data for indoor temperatures were collected during the same period as the real data

collected by Datalogger. The simulation results were contrasted with the observed data to validate the accuracy of the study.

Appendix A contains tables that present the observed and simulated temperature data during the period of field measurements, including hourly temperatures for 144 continuous hours.

The simulation process was carried out through Grasshopper by LadyBug and HoneyBee tools according to the following steps:

1. In the first step, Honeybee surfaces were created. Note that each zone must be created individually, then joined together later to set the building mass.
2. In the second step, all the zones of the building were collected to form the energy model. This step is important in terms of focusing on merging adjacent surfaces in order to avoid any barrier that prevents the model from being properly adjusted.
3. In the third step, building materials were added to the energy model, where building materials are created according to their properties through Honeybee tools. Then the simulation parameters were set, which included the analysis period, the surroundings, and the simulation outputs. In order to carry out the simulation process correctly and realistically, weather data must be used, which can be obtained through Ladybug tools.
4. The final step, the simulation process was conducted by Energyplus engine through Honeybee tool Run Energy Simulation.

Appendix B presents figures describing the workflow for creating the energy model inside Grasshopper environments.

3.2.2. Data Evaluation

Day by day, the interest in using smart technologies to measure the performance of the built environment is increasing. Many devices and computer programs have been developed in order to assess and expect the performance of buildings and their

impact on energy efficiency (Ruiz and Bandera, 2017). Verifying the accuracy of the data collected from these techniques is the most significant task. Once the data is validated by calibrating the measured and simulated data, it can be used in the implementation of any relevant studies.

In this regard, several agencies have developed methodologies for measuring data accuracy. The calibration models developed by ASHRAE Guideline 14-2014, the International Performance Measurement and Verification Protocol (IPMVP), and the Federal Energy Management Program (FEMP) are the most known. Simulation programs and tools have gained great importance due to the ability to simulate reality and the ability to predict. Simulation tools are considered reliable when the results are within the margins of error allowed by the criteria set by the agencies mentioned before (Güçyeter, 2018).

The first appearance of these three protocols was in North America, when there was a need to reduce energy and water consumption by analyzing the effectiveness of energy-saving measures and their impact on energy saving. For this purpose, the North American Energy Measurement and Verification Protocol (NEMVP) was published in 1996 (Ruiz and Bandera, 2017). With the growing interest in this field internationally, Efficiency Valuation Organization (EVO), with a coalition of international organizations, developed the International Performance Measurement and Verification Protocol (IPMVP) in 1997. This protocol suggests the best practices to determine the benefits of energy efficiency investments and expand investment in energy and water management, demand management, and renewable energy applications. Because of the US Department of Energy's approach to reducing energy consumption in federal buildings, the Federal Energy Management Program (FEMP) was developed (CanmetENERGY). In 2002, Guideline 14 was published by the American Society of Heating, Refrigeration, and Air-Conditioning Engineers (ASHRAE), which is the most widely used model. This protocol offers information on measurement tools, uncertainty estimates, regression analysis methodologies, and samples of different systems approaches. In 2014, ASHRAE updated Guideline 14 (Ruiz and Bandera, 2017).

In this research, two indicators were used to measure uncertainty which compatible with the three protocols: 1) Normalized Mean Bias Error (NMBE). It is the normalization of the MBE indicator that is used to extend the range of the MBE indicator results to make them comparable. It can be calculated by equation 3.1.

$$NMBE = \frac{1}{\bar{m}} \frac{\sum_{i=1}^n (m_i - s_i)}{n-p} \times 100 (\%) \quad (3.1)$$

Where: (\bar{m}) is the mean of observed values, (m_i) is the observed data, (s_i) is the simulated data, (n) is the number of observed points, and (p) is the number of adjustable model parameters that are recommended to be zero.

2) Coefficient of Variation of the Root Mean Square Error CV(RMSE). It calculates the variation of errors among observed and simulated data. Also, it demonstrates the capacity of the model to determine the shape of the total load that is reflected in the data. CV(RMSE) can be calculated by equation.3.2.

$$CV(RMSE) = \frac{1}{\bar{m}} \sqrt{\frac{\sum_{i=1}^n (m_i - s_i)^2}{n-p}} \times 100 (\%) \quad (3.2)$$

In this equation, (p) is recommended to be one.

Table 3.9. Calibration criteria of IPMVP, FEMP, and ASHRAE Guideline 14 (Ruiz and Bandera, 2017).

Calibration Type	Index	Acceptable Value		
		IPMVP	FEMP	ASHRAE Guideline 14
Hourly data	NMBE	± 5%	± 10%	± 10%
	CV(RMSE)	20%	30%	30%
Monthly data	NMBE	± 20%	± 5%	± 5%
	CV(RMSE)	-	15%	15%

In general, the calibration results showed an increase in the value of NMBE on the first day, where reaching -21,17 %. And on the sixth day, it amounted to 16.69%. While it was within the tolerances regulated according to the three protocols on the second, third, fourth, and fifth days, the average value of NMBE over the entire period was 9%. All CV(RMSE) values were within the permissible limits under the three protocols IPMVP, FEMP, and ASHRAE.

Table 3.10. Calibration data of the case study.

Index (Hourly)	Time					
	28/11/20	29/11/20	30/11/20	01/12/20	02/12/20	03/12/20
NMBE	-21,17%	-3,85%	-2,11%	-9,98%	0,266%	16,69%
CV(RMSE)	22%	14%	13%	16%	7%	17%

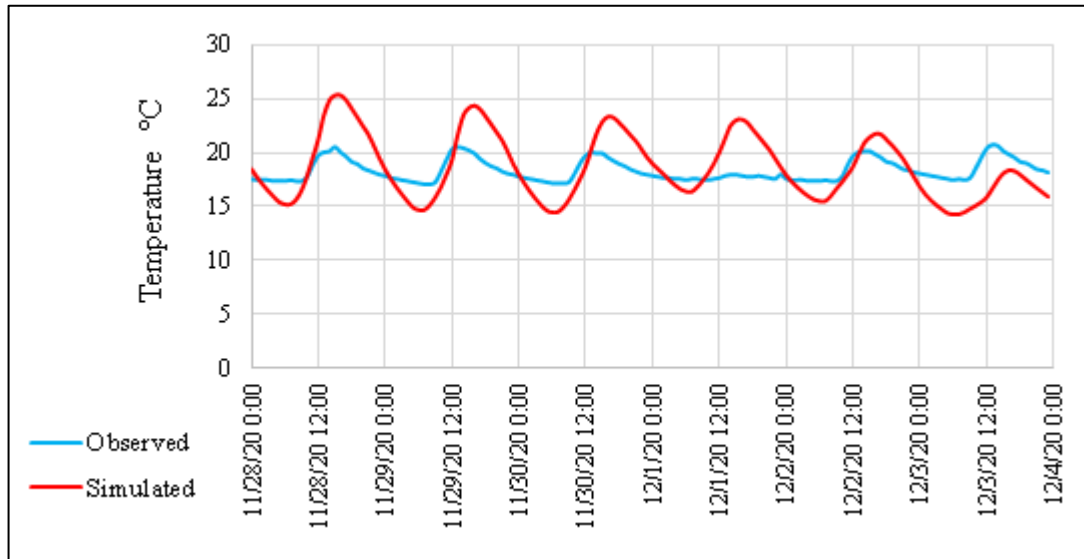


Figure 3.34. Hourly observed and simulated temperature data.

Appendix A contains charts comparing observed and simulated hourly temperature data for every single day of field measurements.

3.2.3. Determination of the Retrofitting Scenarios

Since the main objective of this study is to evaluate the performance of passive solar design systems in the comfort of users in cold climates, so the main criterion for evaluating the efficiency of the model is how effective it is in reducing heating loads through the model. In this study, the efficiency of the existing model was examined, then five retrofitting scenarios have been examined: In the first scenario, different thicknesses of thermal insulation were examined. In the second scenario, different rates of the glazing ratio of the south facade were examined. In the third scenario, different types of glazing were examined. In the fourth scenario, the efficiency of using the green roof was examined, and in the fifth scenario, the best variables in each previous scenario have been established and examined.

3.2.3.1. Scenario 1

In this scenario, thermal insulation thicknesses have been examined for external walls, ground floor, and roof. In this research, four different values of the thickness of the thermal insulation in the external walls were examined, as shown in Table 3.11. With keeping the wall thickness as it is without any modification.

Table 3.11. U-value of the wall with different thermal insulation thicknesses.

Sub scenario	Wall thickness (mm)	Insulation thickness (mm)	U-value (w/m ² -k)
S1.a	400	80	0,36
S1.b		100	0,30
S1.c		150	0,21
S1.d		200	0,16

Also, a retrofit was made to the floor thermal insulation. For this purpose, floor thermal insulation with 75 mm thickness and with 100 mm thickness was examined to assess the effect of increasing thermal insulation for the floor on indoor thermal comfort and energy consumption. Moreover, the floor without insulation was examined to understand the thermal behavior of the floor.

Table 3.12. U-value of the floor with different thermal insulation thicknesses.

Sub scenario	Insulation thickness (mm)	U-value (w/m ² -k)
S1.e	75	0,43
S1.f	100	0,33

The roof is one of the most vulnerable components of the building to climatic conditions. It is a significant source of heat infiltration, whether inside the building or outside. Therefore, the thermal insulation of the roof is very important, particularly in cold climates. In this study, roof thermal insulation with 150 mm thickness was examined.

Table 3.13. U-value of the roof with different thermal insulation thicknesses.

Sub scenario	Insulation thickness (mm)	U-value (w/m2-k)
S1.g	100	0,32
S1.h	150	0,22

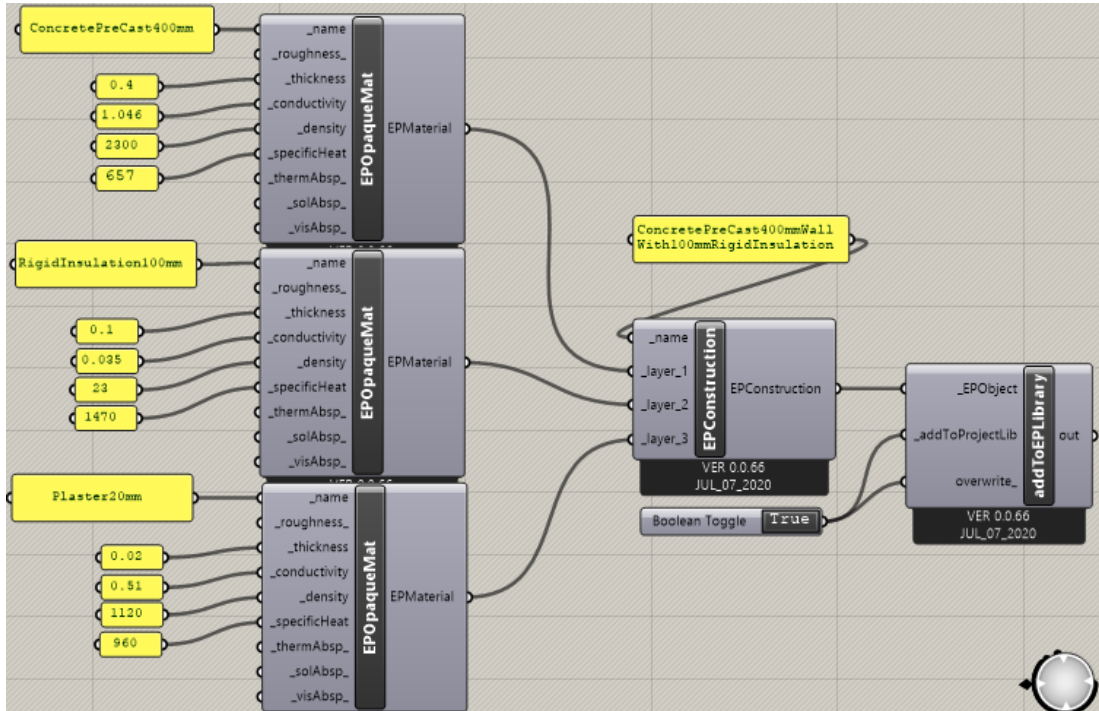


Figure 3.35. Creating opaque materials by HoneyBee components.

3.2.3.2. Scenario 2

Glazing is the most significant element in passive solar design systems, as it is a collecting element for direct sunlight and transmits it inside the building. To ensure the efficient performance of passive solar systems, it is very crucial to identify the location and size of the glazing in the building. To verify this purpose, Three different values of the glazing ratio were examined in this study WWR 75%, WWR 50%, and WWR 30%. HoneyBee tools allow high flexibility in generating the glazing ratio within the energy model.

Table 3.14. Glazing ratio scenario.

Sub scenario	WWR%
S2.a	75
S2.b	50
S2.c	30

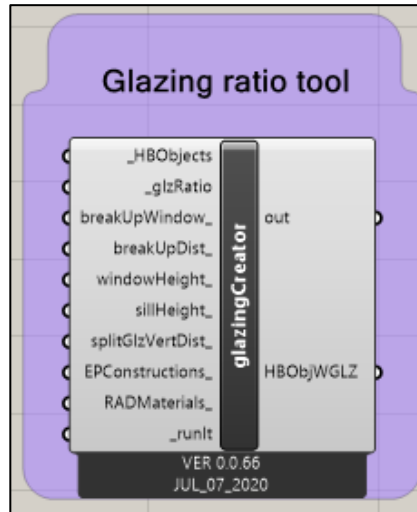


Figure 3.36. HoneyBee Glazing based on ratio component.

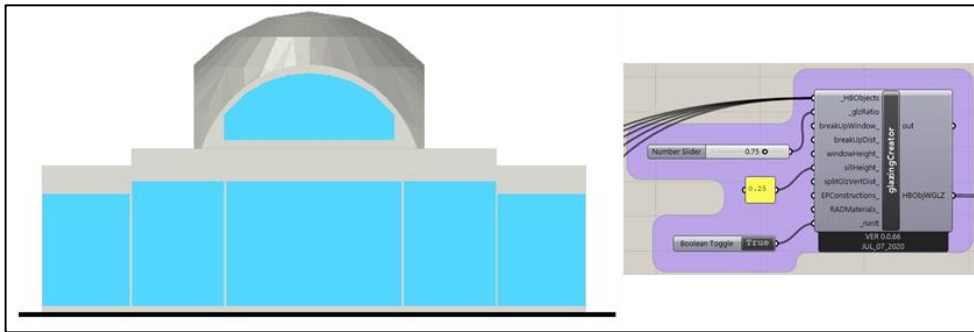


Figure 3.37. The building with 75% glazing ratio (WWR=0,75).

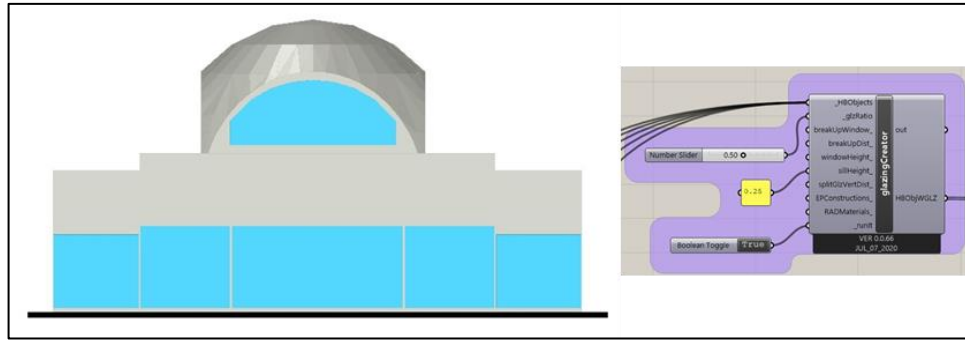


Figure 3.38. The building with 50% glazing ratio (WWR-0,50).

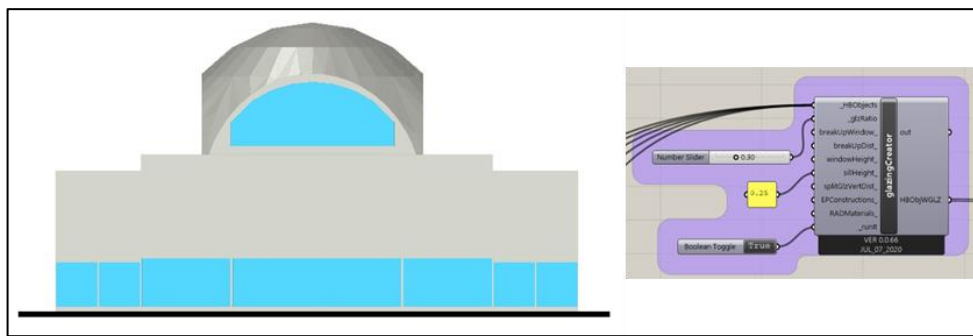


Figure 3.39. The building with 30% glazing ratio (WWE-0,30).

3.2.3.3. Scenario 3

Determining the appropriate type of glazing is a crucial issue that influences the performance of buildings in cold climates. In this research, different types of glazing were taken into account.

Table 3.15. Properties of glazing types in the study (By author).

Sub scenario	Glazing type	Thickness (mm)	Air thickness (mm)	U-value (w/m ² -k)
S3.a	Triple glazing	6	6	1,19
S3.b	Triple glazing	6	10	1,19
S3.c	Double glazing low-E	6	12	0,70

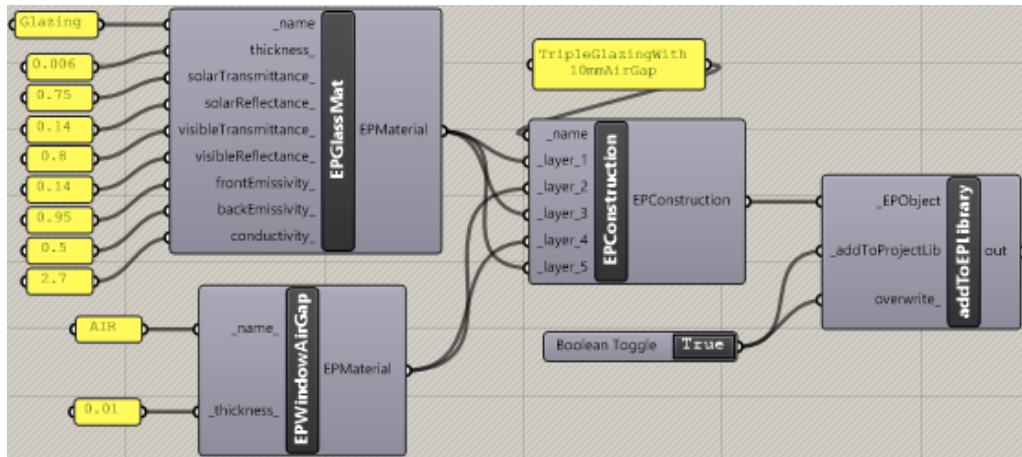


Figure 3.40. Creating windows by HoneyBee components.

3.2.3.4. Scenario 4

The green roof is a specialized roofing system that meets the requirements of sustainable architecture. The use of green roofs has positive effects on the environment. The green roof can reduce energy consumption, minimize the effect of heat islands on the urban environment, in addition to the possibility of benefiting from rainwater or recycled wastewater.

In this study, the use of the green roof, in general, was discussed. The extensive Green roof was examined as a replacement for the thermal insulation layer. Also was examined as a supporting layer for the thermal insulation layer. The example provided by EnergyPlus was used in order to prepare the layers of the green roof. The example file can be obtained through this link: (URL7)

```

Material:RoofVegetation,
GreenRoof,                !- Name
0.2,                      !- Height of Plants (m)
1,                        !- Leaf Area Index (dimensionless)
0.22,                    !- Leaf Reflectivity (dimensionless)
0.95,                    !- Leaf Emissivity
180,                     !- Minimum Stomatal Resistance (s/m)
Green Roof Soil,         !- Soil Layer Name
MediumRough,            !- Roughness
0.1,                    !- Thickness (m)
0.35,                   !- Conductivity of Dry Soil (W/m-K)
1100,                   !- Density of Dry Soil (kg/m3)
1200,                   !- Specific Heat of Dry Soil (J/kg-K)
0.9,                    !- Thermal Absorptance
0.7,                    !- Solar Absorptance
0.75,                   !- Visible Absorptance
0.3,                    !- Saturation Volumetric Moisture Content of the Soil Layer
0.01,                   !- Residual Volumetric Moisture Content of the Soil Layer
0.1,                    !- Initial Volumetric Moisture Content of the Soil Layer
Advanced;               !- Moisture Diffusion Calculation Method

```

Figure 3.41. Green roof layers were used in the study (URL7).

Table 3.16. U-value of green roofs examined in the study.

Sub scenario	Roof system	U-value (w/m ² -k)
S4.a	Roof with green roof	1,68
S4.b	Roof with a green roof and 100mm thermal insulation	0,28
S4.c	Roof with a green roof and 150mm thermal insulation	0,20

3.2.3.5. Scenario 5

In the previous scenarios, each variable was tested separately. For example, in the first scenario, the thickness of the thermal insulation of the external walls was examined individually, while maintaining the other components of the building envelope as it is, and so on in all previous scenarios.

In this scenario, a modification to the entire envelope of the building was proposed. The best variable in each of the previous four scenarios was examined according to the building's performance in terms of reducing heating and cooling loads and improving the thermal comfort level of the indoor environment in the previous scenarios. The best was selected based on the U-values that are compatible with the Turkish standard (TS 825).

Table 3.17. U-value of building envelope in the retrofitted model (By author).

Scenario 5	U-value (w/m ² -k)	TS825 U-value
Wall with 150 mm insulation	0,21	0,50
Floor with 75 mm insulation	0.43	0,45
Roof with a green roof and 150 mm thermal insulation	0,20	0,30
Double glazing low-E	0,70	2,40

PART 4

RESULTS AND DISCUSSION

This part covers the results of the case study simulation process in addition to the simulation processes of the proposed retrofitting scenarios to the case study. These processes were done through the EnergyPlus engine by LadyBug and HoneyBee tools. The results of the performance analysis of the case study and the proposed retrofit scenarios will be presented and discussed.

4.1. CASE STUDY ANALYSIS

The energy model was prepared according to collected information by Ladybug and Honeybee tools and analyzed through the EnergyPlus engine as explained in detail in part3.

As shown in Table 4.1 and Figure 4.1, the heating load is 76,20 kilowatt-hours per square meter. Despite the high thermal mass of the building envelope, the thermal insulation layer with a thickness of 5 cm for the external walls was not sufficient to reach the acceptable value in the Turkish standard (TS 825), also for the roof with 10 cm of insulation and the floor with 5 cm of insulation. Furthermore, although Ankara is characterized by a temperate summer, the cooling loads amounted to 65,75 kilowatt-hours per square meter. The main factor in increasing the indoor temperature of the building during the summer is the glazing facade facing the south with a glazing ratio of 90%. With this transparent surface, the solar gains will especially increase during the summer because of the increased daylight hours and the period of sunlight.

Table 4.1. Annual heating and cooling loads for the existing model by floor area (Kwh/m²).

Loads	Energy use intensive (EUI) kWh/m ²	Total
Heating	76,20	141,95
Cooling	65,75	

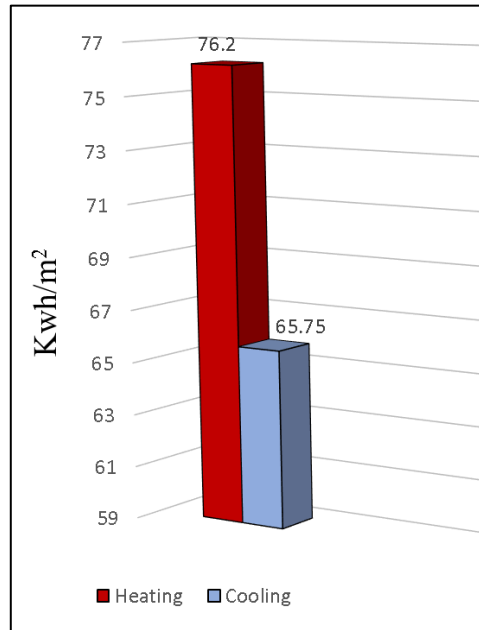


Figure 4.1. Annual heating and cooling loads for the existing model by floor area (Kwh/m²).

The thermal comfort of the existing envelope was studied during the field measurements period according to the ASHRAE 55 standard. The results showed that the users were within the range of dissatisfaction most of the time.

As it is shown in Figure 4.2, The results of calculating the monthly average of the predicted mean votes (PMV) and percentage of people dissatisfied (PPD) according to Fanger's model show that the percentage of dissatisfaction rises significantly during the cold months (winter) and the hot months (summer), while it witnesses a significant decrease during the temperate months (spring and autumn).

Appendix C contains tables showing the monthly average values of the predicted mean votes and the percentage of people dissatisfied calculated by HoneyBee tools.

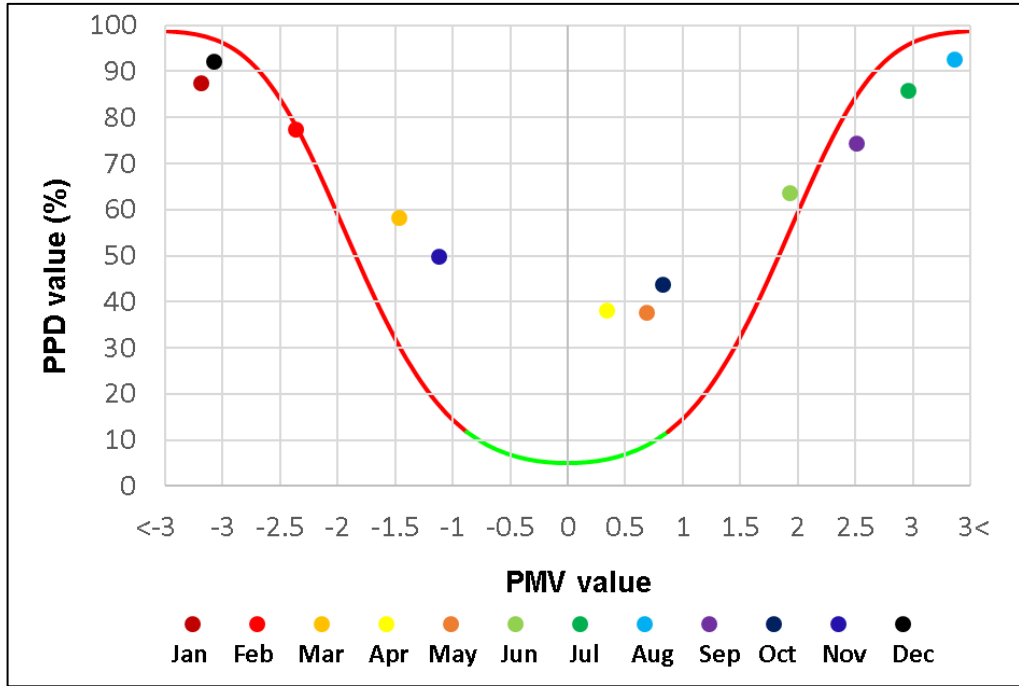


Figure 4.2. PMV and PPD values for the existing building.

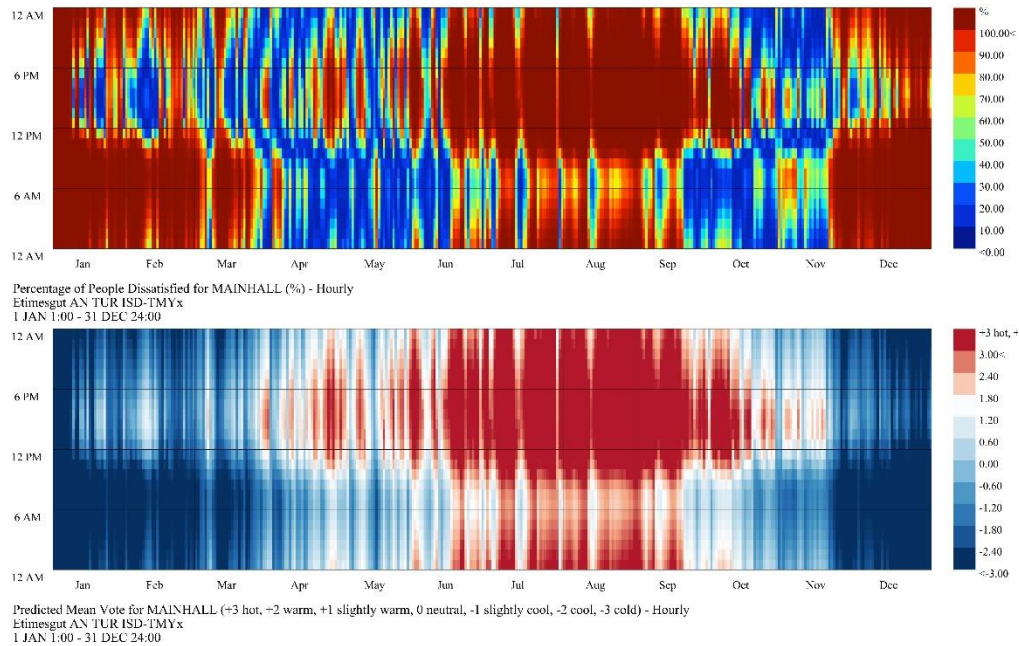


Figure 4.3. Annual PMV and PPD chart for the existing building.

4.2. THE RESULT OF SCENARIO 1

All studies conducted to examine the effect of thermal insulation on the performance of buildings have proven that the use of insulation has a positive impact on

decreasing the rate of energy consumption inside buildings. In this study, different values of thermal insulation thickness were tested for external walls, floor, and roof, and the results were as the following:

Table 4.2. Annual heating and cooling loads for each thickness of external walls by floor area (Kwh/m²).

Sub scenario	Thermal insulation thickness (mm)	Energy use intensive (EUI) kWh/m ²		Total
		Heating	Cooling	
S1. a	80	73,84	65,96	139,80
S1. b	100	72,91	66	138,91
S1. c	150	71,50	66,12	137,62
S1. d	200	70,71	66,14	136,85

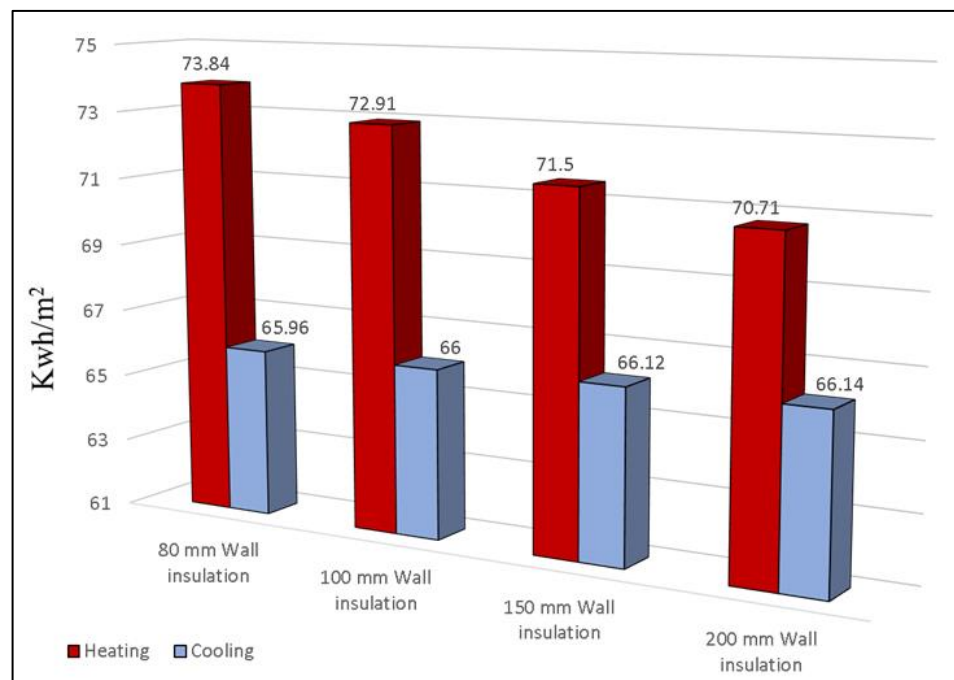


Figure 4.4. Heating and cooling loads for wall insulation by floor area (Kwh/m²).

Table 4.2 and Figure 4.4 show that increasing the thickness of the thermal insulation of the external walls had a positive effect on reducing heating loads while it led to a slight increase in cooling loads. Scenario (S1.a) examined increasing the thickness of the thermal insulation of the external walls to 80 mm. The results showed an

improvement in reducing heating loads by 3%. On the other hand, it led to a slight increase in the cooling loads by 0,30%. Increasing the thickness of the thermal insulation to 80 mm reduced the total energy consumption by 1,5%.

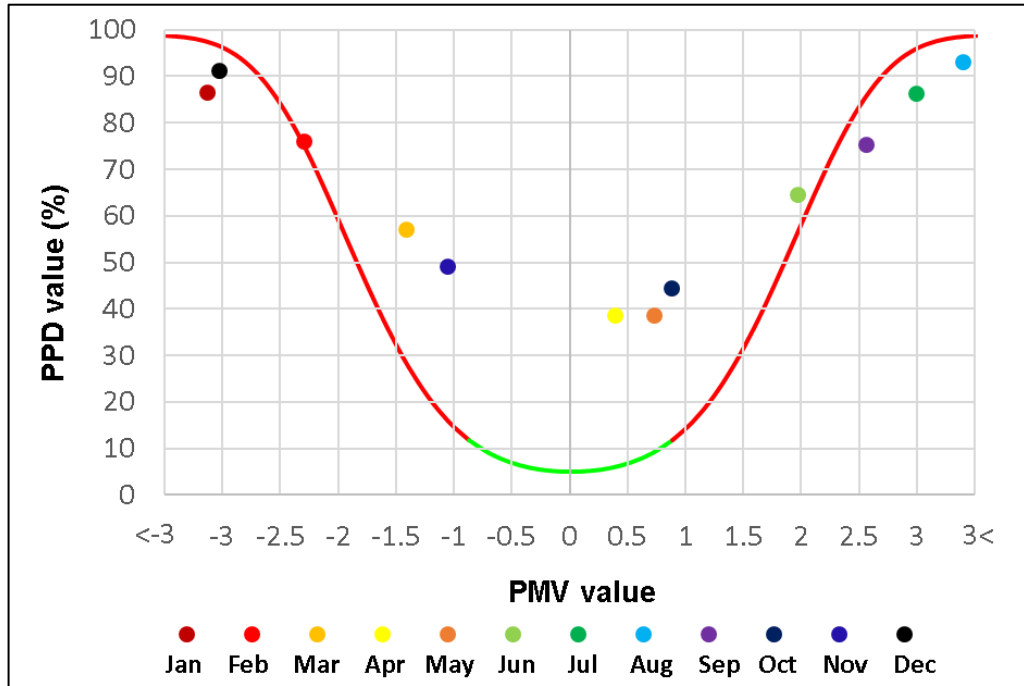


Figure 4.5. PMV and PPD values for the wall with 80 mm insulation.

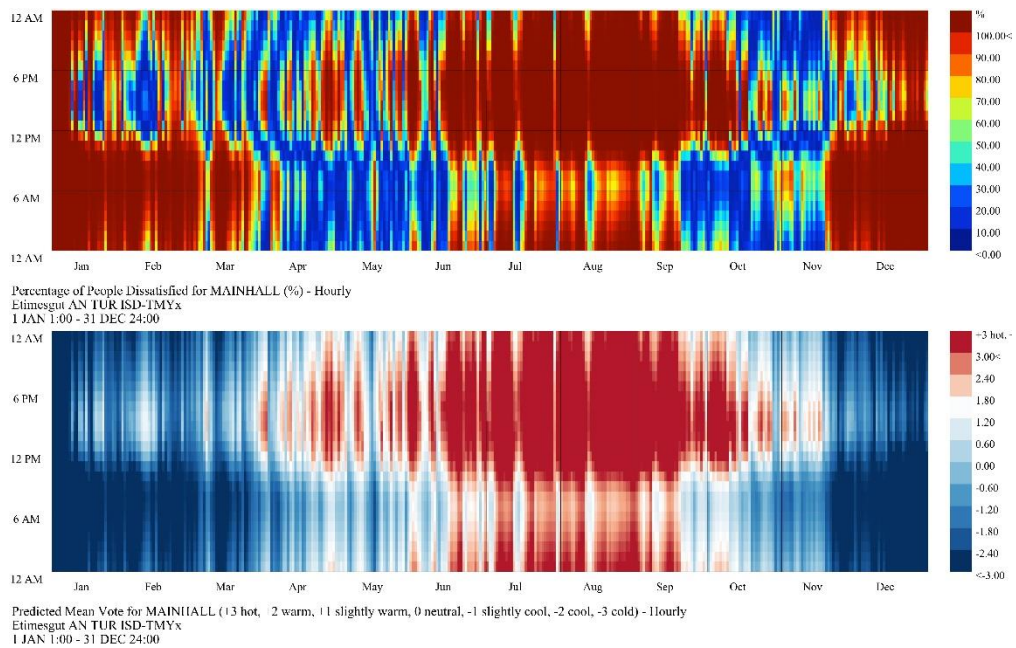


Figure 4.6. Annual PMV and PPD chart for the wall with 80 mm insulation.

Scenario (S1.b) examined increasing the thickness of the thermal insulation of the external walls to 100 mm. The results indicated a reduction in heating loads of 4%. As in the previous scenario (S1.a), this scenario raised the cooling loads by 0,40%. Increasing the thickness of the thermal insulation to 100 mm reduced the total energy consumption by 2%.

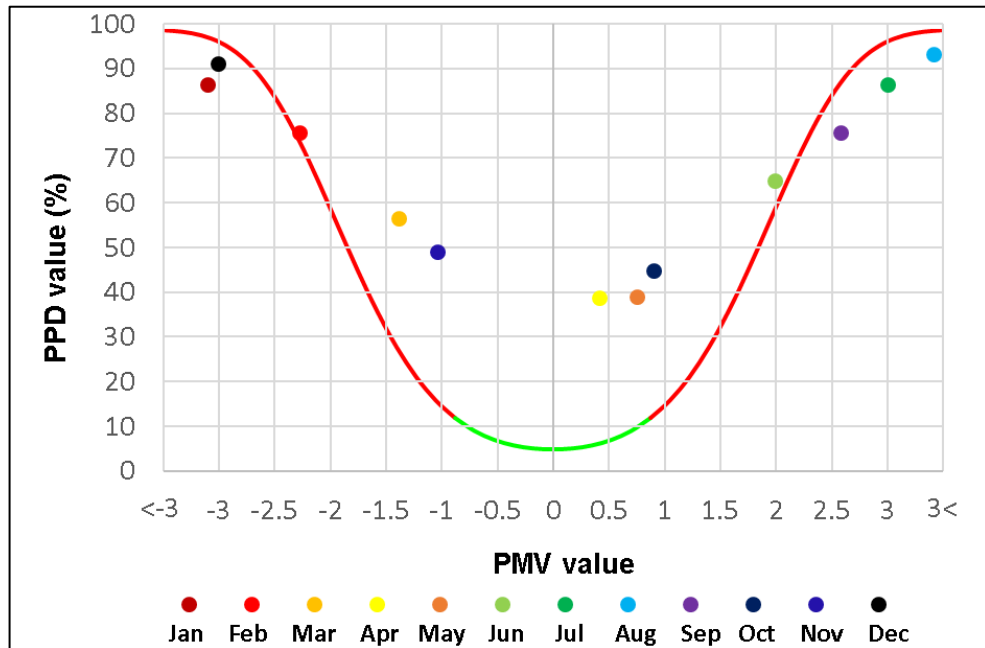


Figure 4.7. PMV and PPD values for the wall with 100 mm insulation.

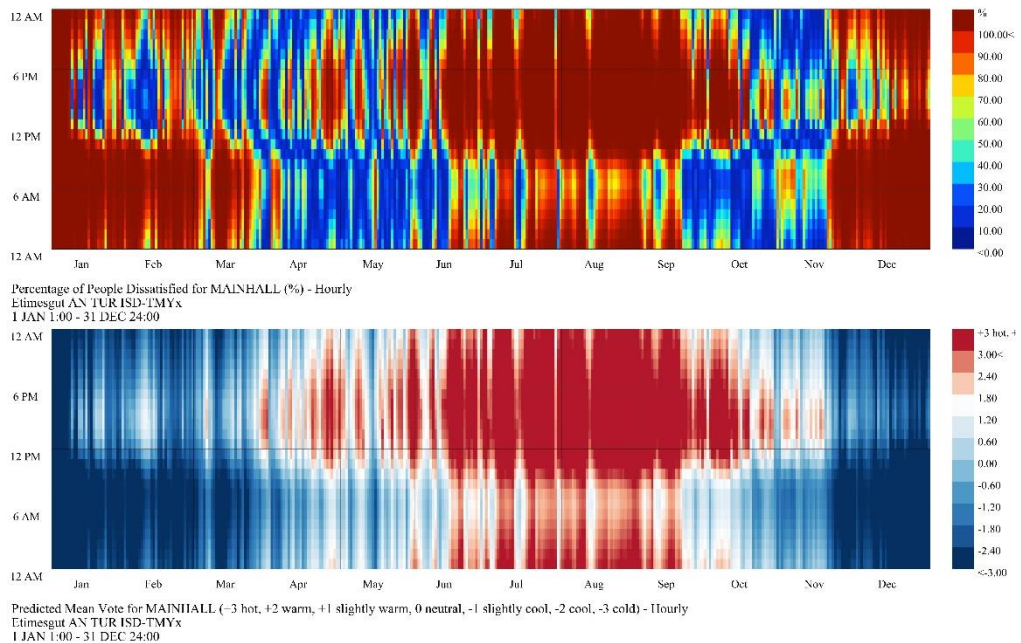


Figure 4.8. Annual PMV and PPD chart for the wall with 100 mm insulation.

Scenario (S1.c) investigated raising the thickness of the exterior wall thermal insulation to 150 mm. The results revealed a 6% improvement in decreasing heating loads. However, it resulted in a 0,55% increase in cooling loads. By increasing the thickness of the thermal insulation to 150 mm, the total energy consumption was decreased by 3%.

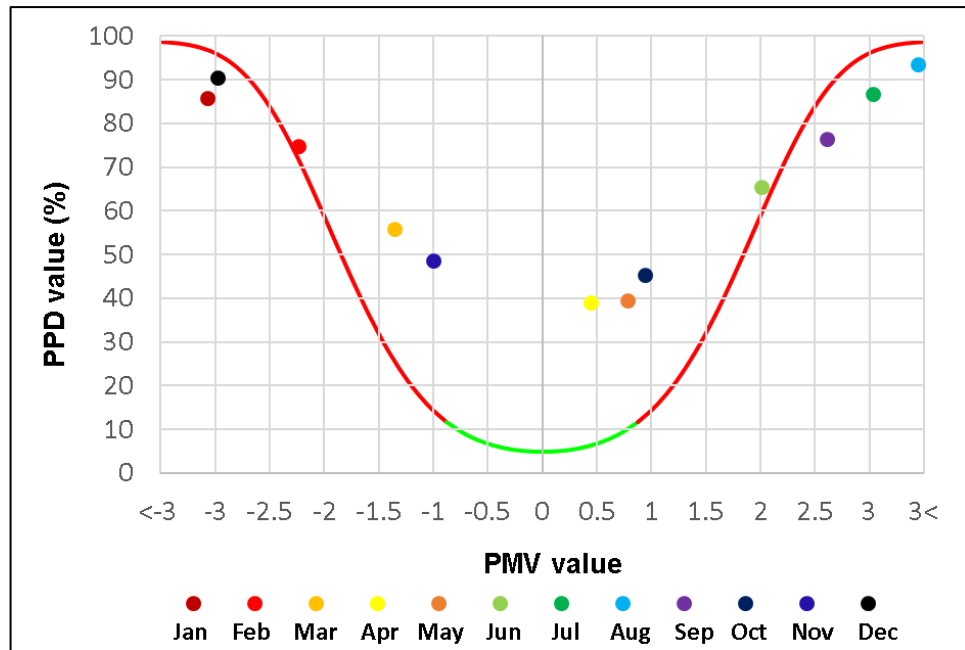


Figure 4.9. PMV and PPD values for the wall with 150 mm insulation.

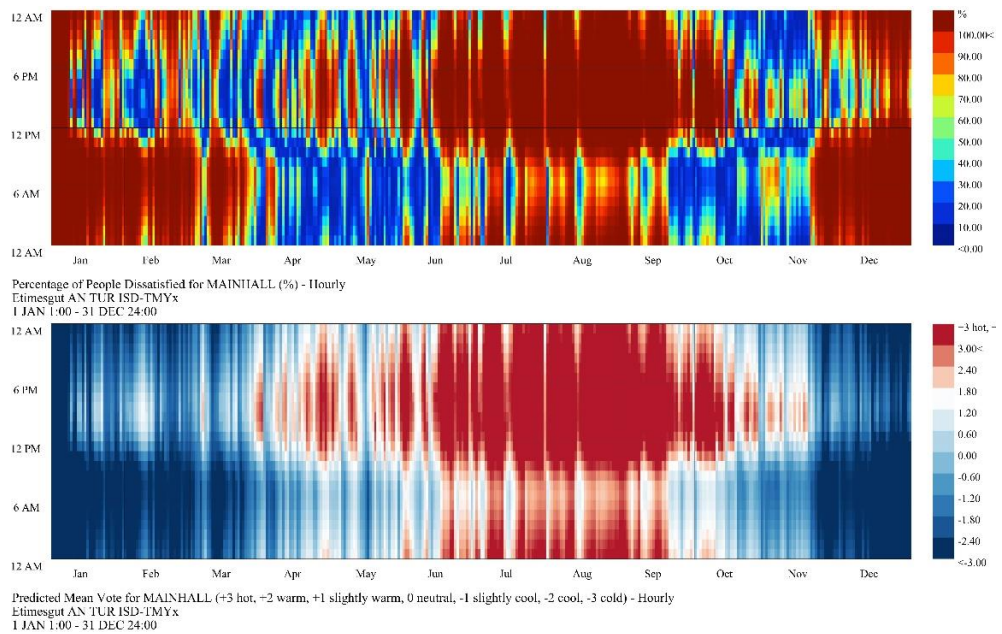


Figure 4.10. Annual PMV and PPD chart for the wall with 150 mm insulation.

In scenario (S1.d), the thickness of the exterior wall thermal insulation was increased to 200 mm. The results showed a 7% reduction in heating loads. However, this causes a 0,60% increase in cooling loads. The total energy usage was reduced by around 3% by raising the thickness of the thermal insulation to 200 mm.

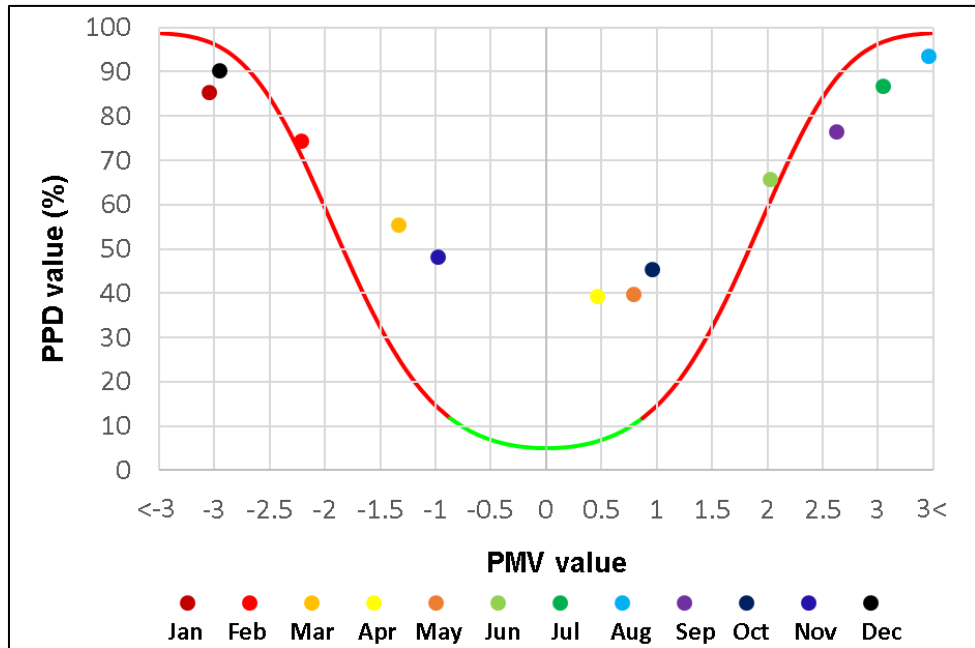


Figure 4.11. PMV and PPD values for the wall with 200 mm insulation

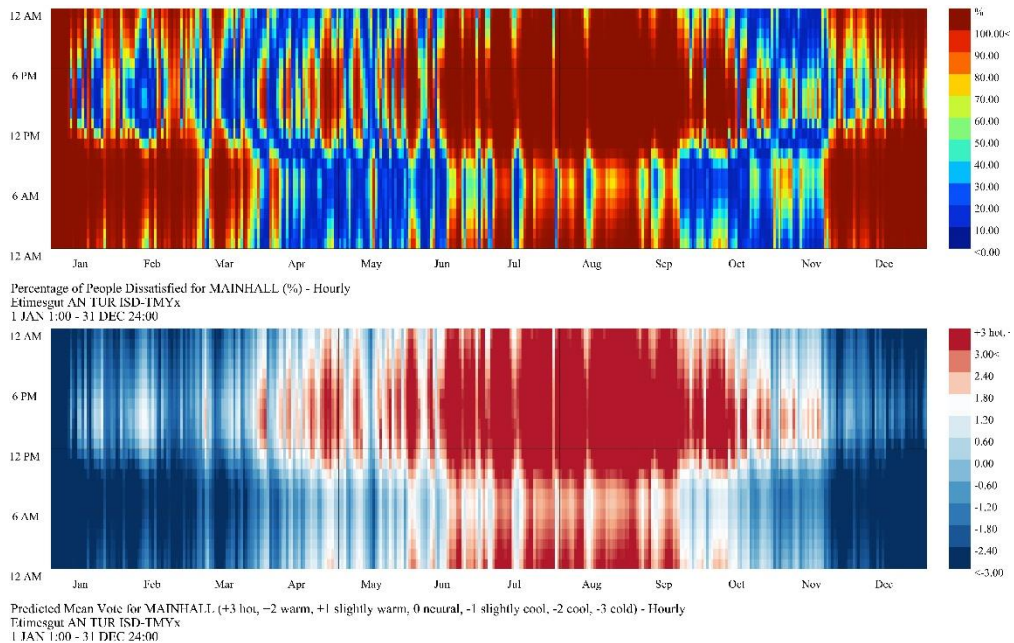


Figure 4.12. Annual PMV and PPD chart for the wall with 200 mm insulation.

The results of thermal comfort showed that increasing the thickness of the thermal insulation of the exterior walls had no significant effect on the indoor environment. The results show that the increase in insulation for the external walls contributes to improving indoor thermal comfort during the heating season, but not to the required extent. On the contrary, the increase in insulation contributed to a further deterioration in the level of thermal comfort during the cooling season.

In conclusion, increasing the thickness of the thermal insulation of the external walls has a positive role in reducing energy consumption, which is consistent with the literature conclusions in this respect. In this study, increasing external wall insulation reduced the annual energy consumption by 3%.

In this scenario, increasing the thickness of the thermal insulation of the floor was also examined, which did not lead to significant results in reducing energy consumption. On the contrary, increasing the insulation thickness of the floor raised cooling. Besides, increasing the thermal insulation thickness for the floor raised the total energy consumption as it appears in Table 4.3 and Figure 4.13.

Table 4.3. Annual heating and cooling loads for the ground floor by floor area (Kwh/m²).

Sub scenario	Thermal insulation thickness (mm)	Energy use intensive (EUI) kWh/m ²		Total
		Heating	Cooling	
S1. e	75	76	67,13	143.13
S1. f	100	75,95	68,51	144,46

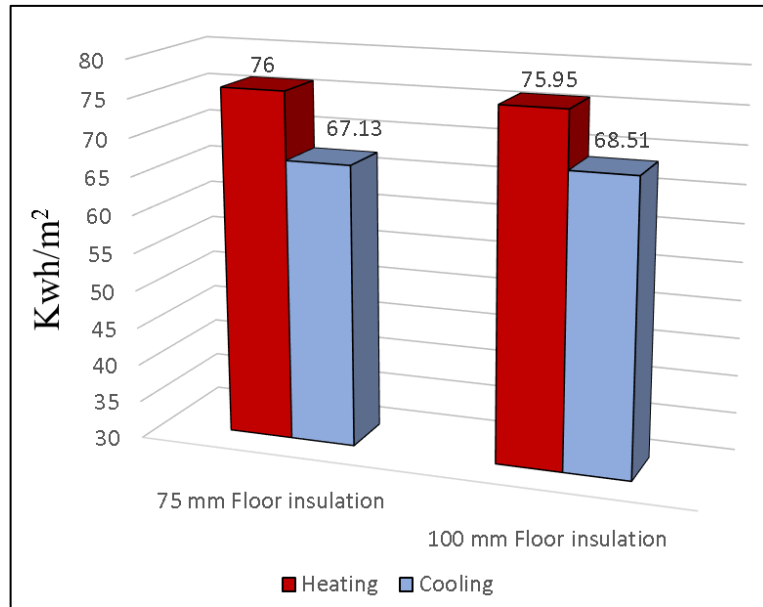


Figure 4.13. Heating and cooling loads for the floor by floor area (Kwh/m²).

The thickness of the floor thermal insulation was raised to 75 mm in the scenario (S1.e). Heating demands were reduced by 0,25 percent as a result of the findings. However, this results in a 2% increase in cooling demand. The total energy consumption was increased by approximately 0,80 percent by increasing the thickness of the thermal insulation to 75 mm.

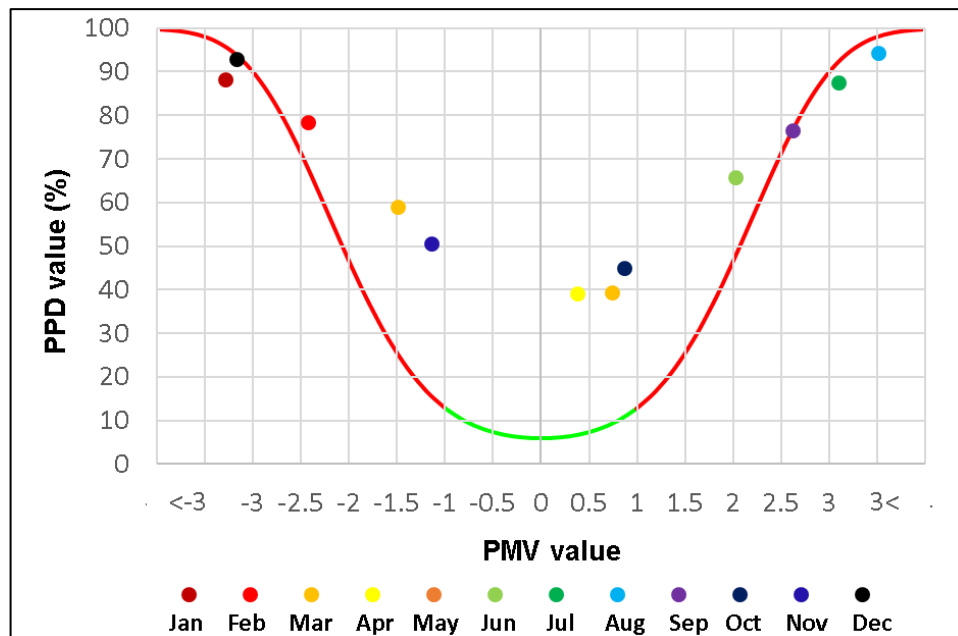


Figure 4.14. PMV and PPD values for the floor with 75 mm insulation.

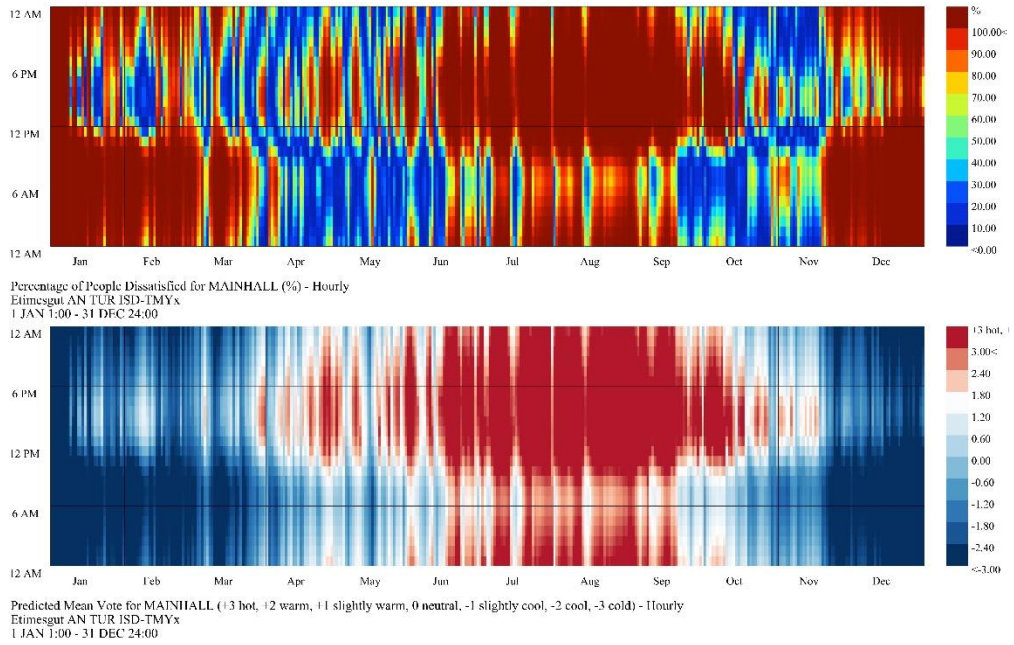


Figure 4.15. Annual PMV and PPD chart for the floor with 75 mm insulation.

In the scenario (S1.f), the thickness of the floor thermal insulation was increased to 100 mm. As a result of the findings, heating demands were decreased by 0,30%. However, it led to a 4% rise in cooling demand. By raising the thickness of the thermal insulation to 100 mm, the total energy consumption was increased by 1,70%.

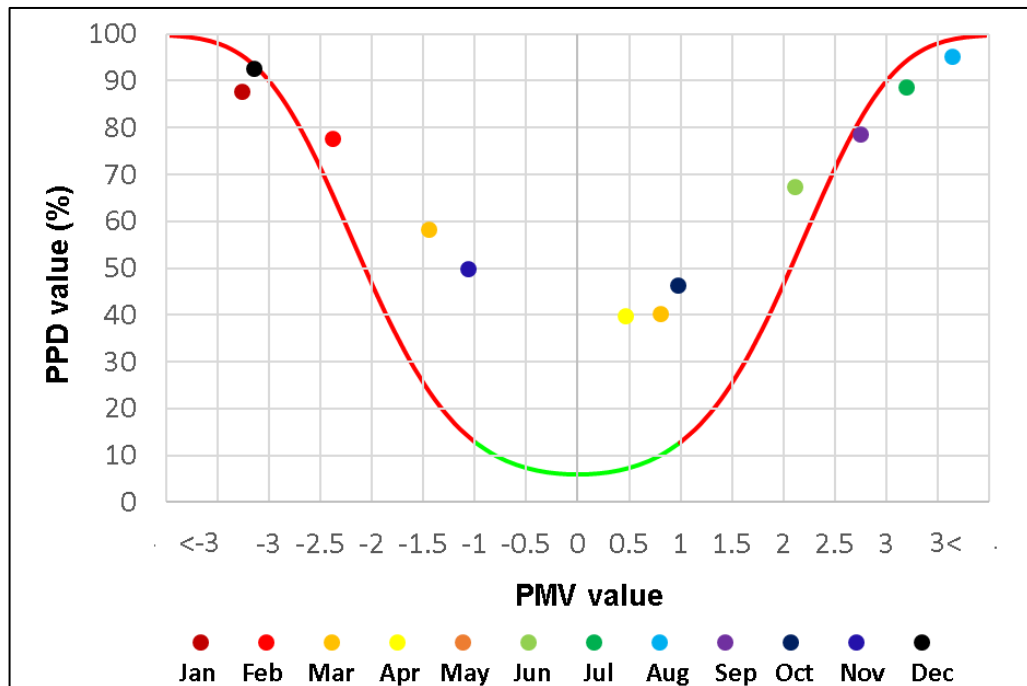


Figure 4.16. PMV and PPD values for the floor with 100 mm insulation.

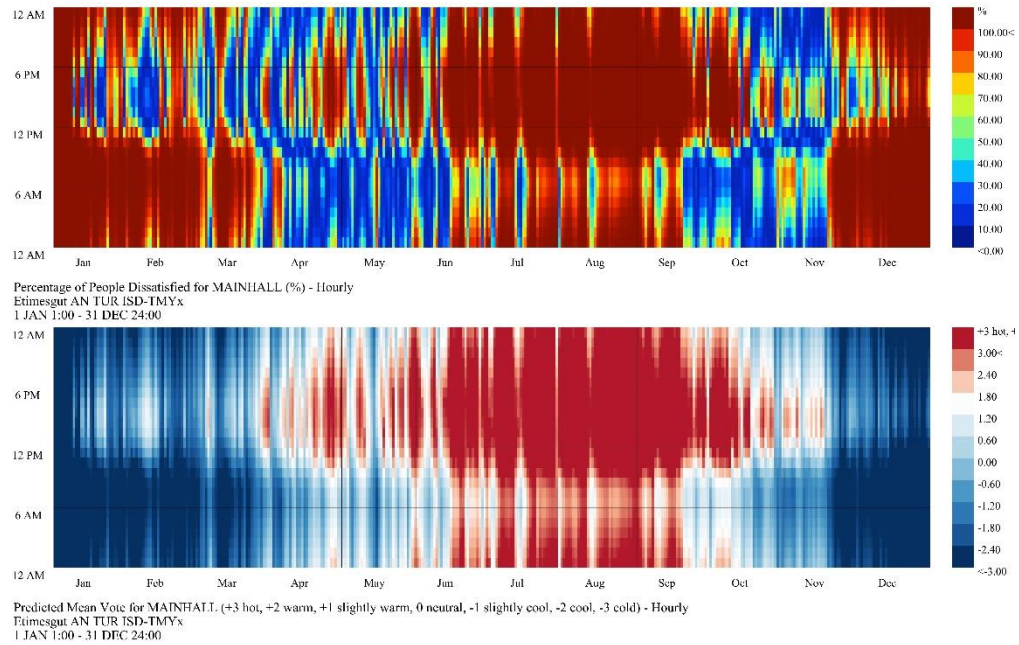


Figure 4.17. Annual PMV and PPD chart for the floor with 100 mm insulation.

The thermal comfort results revealed that increasing the thickness of the floor's thermal insulation had no influence on the indoor environment. The results suggest that increasing the thickness of the floor's thermal insulation correlates to a decrease in indoor thermal comfort during the cooling season.

The effect of increasing the thickness of the thermal insulation on the roof was also examined. In the scenario (S1.g), the thermal insulation thickness of the roof was increased to 150 mm. The results showed that increasing the thermal insulation of the roof reduced heating loads by 3% and cooling loads by 0,40%. Moreover, increasing the thickness of roof thermal insulation reduced total energy use by 2% (Table 4.4).

Table 4.4. Annual heating and cooling loads for the roof by floor area (Kwh/m²).

Sub scenario	Thermal insulation thickness (mm)	Energy use intensive (EUI) kWh/m ²		Total
		Heating	Cooling	
S1. g	150	73,83	65,46	139,29

However, there is no noticeable effect on indoor thermal comfort by increasing the thickness of the roof thermal insulation as is shown in Figure 4.18 and Figure 4.19.

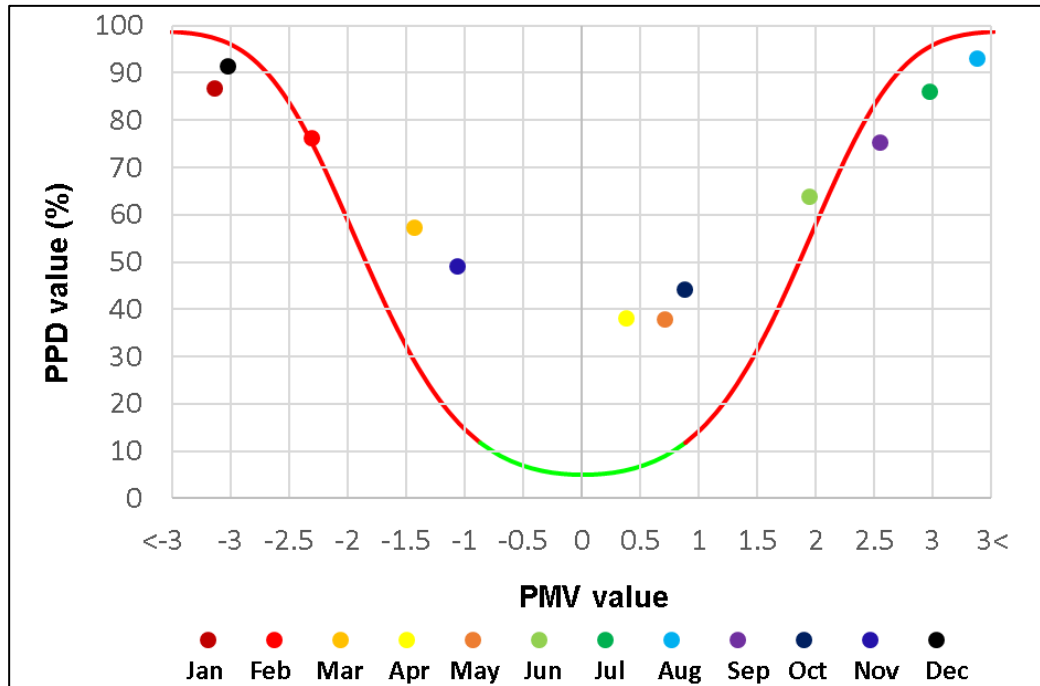


Figure 4.18. PMV and PPD values for the roof with 150 mm insulation.

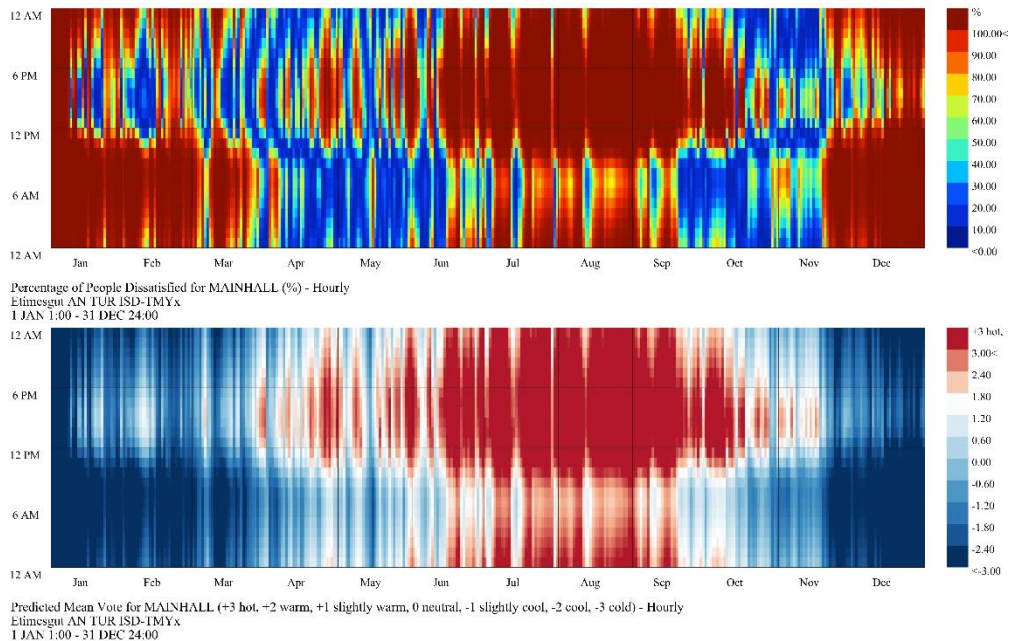


Figure 4.19. Annual PMV and PPD chart for the roof with 150 mm insulation.

According to the results, it is clearly noticeable that increasing the thickness of the thermal insulation is directly proportional to the savings in energy consumption for heating.

4.3. THE RESULT OF SCENARIO 2

The results of examining three different rates of glazing ratio on the south facade showed that the higher the glazing ratio relative to the wall area, the lower the heating loads inside the building. On the contrary, when the glazing ratio decreases, the heating loads increase. As shown in Table 4.5 and Figure 4.22, reducing the glazing ratio of the south facade has a positive influence on the annual total energy use. According to the results, the reduction in the glazing ratio achieved an energy saving of 7%.

Table 4.5. Annual heating and cooling loads for each supposed glazing ratio by floor area (Kwh/m²).

Sub scenario	Glazing ratio (%)	Energy use intensive (EUI) kWh/m ²		Total
		Heating	Cooling	
S2. a	75	76,75	61,84	138,59
S2. b	50	79,51	55,34	134,85
S2. c	30	82,76	49,89	132,65

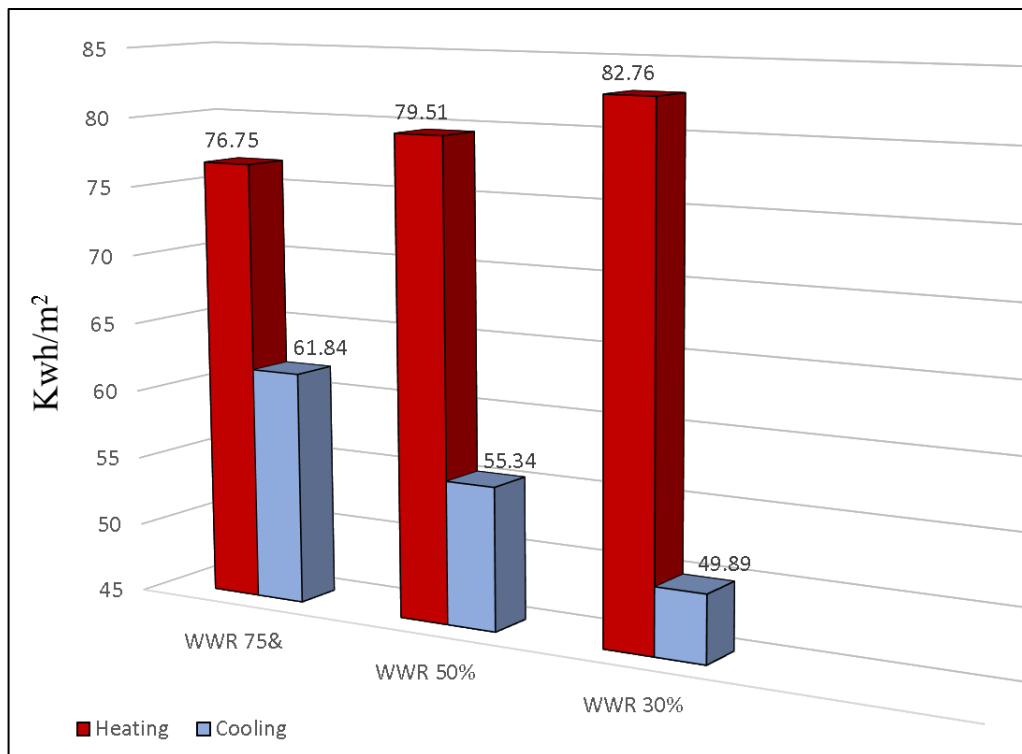


Figure 4.20. Heating and cooling loads for WWR values by floor area (Kwh/m²).

Scenario (S2.a) examined the window-to-wall ratio (WWR) of 75%. The results indicated an increase in heating loads of 0.70%. On the contrary, it led to a decrease in the cooling loads of 6%. The glazing ratio of 75% reduced the total energy consumption by 2%. In addition, the indoor thermal comfort was improved slightly in summer.

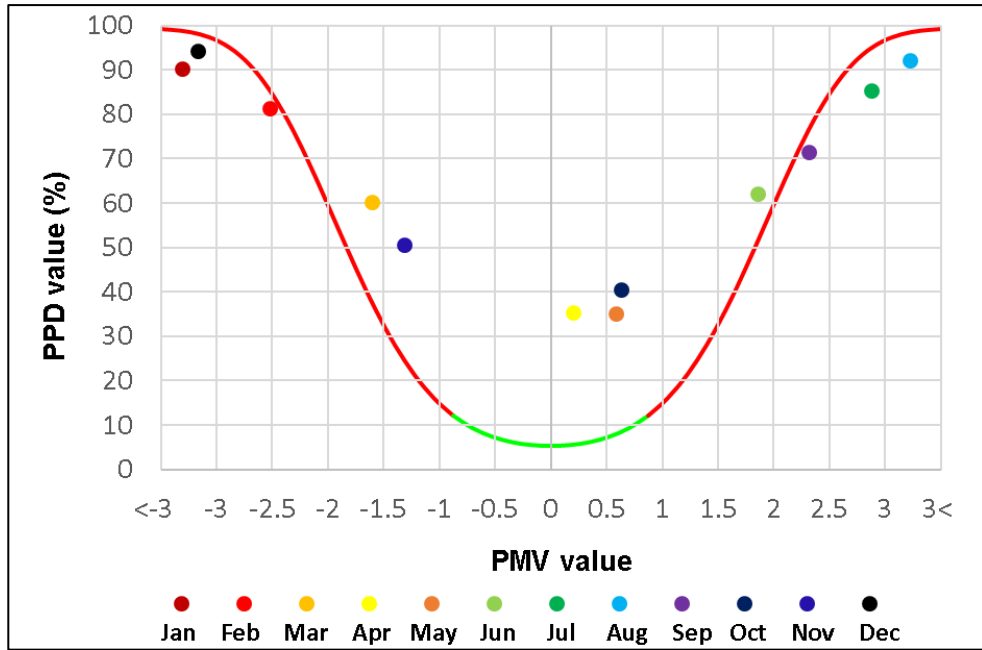


Figure 4.21. PMV and PPD values for WWR 75%.

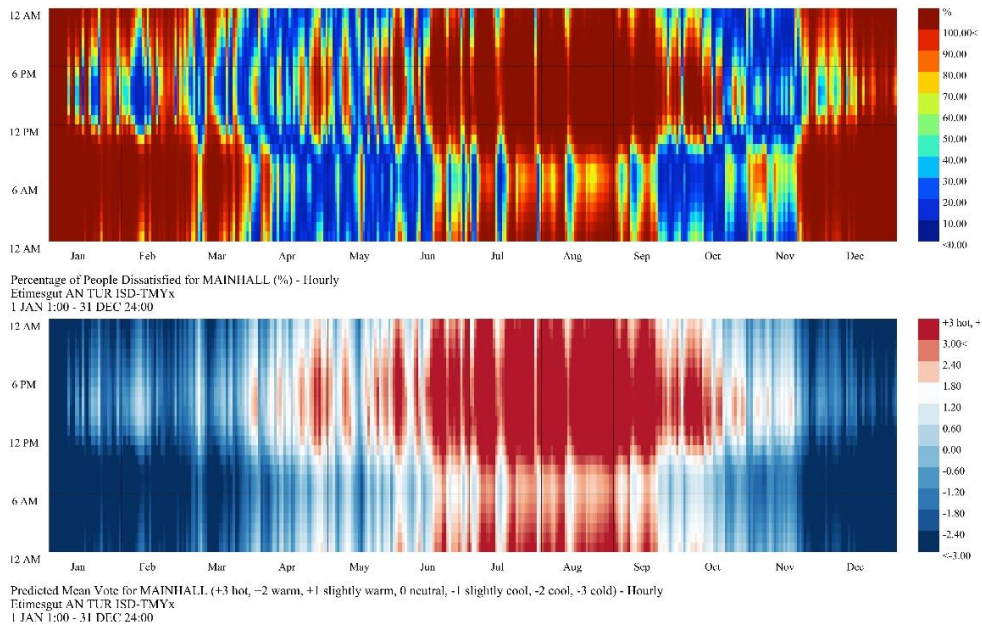


Figure 4.22. Annual PMV and PPD chart for WWR 75%.

Scenario (S2.b) examined a window-to-wall ratio (WWR) of 50%. According to the findings, heating demand increased by 4%. On the contrary, it resulted in a 16% decrease in cooling loads. The 50% glazing ratio reduced total energy use by 5%. Furthermore, in the summer, indoor thermal comfort has further improved compared to scenario S2.a.

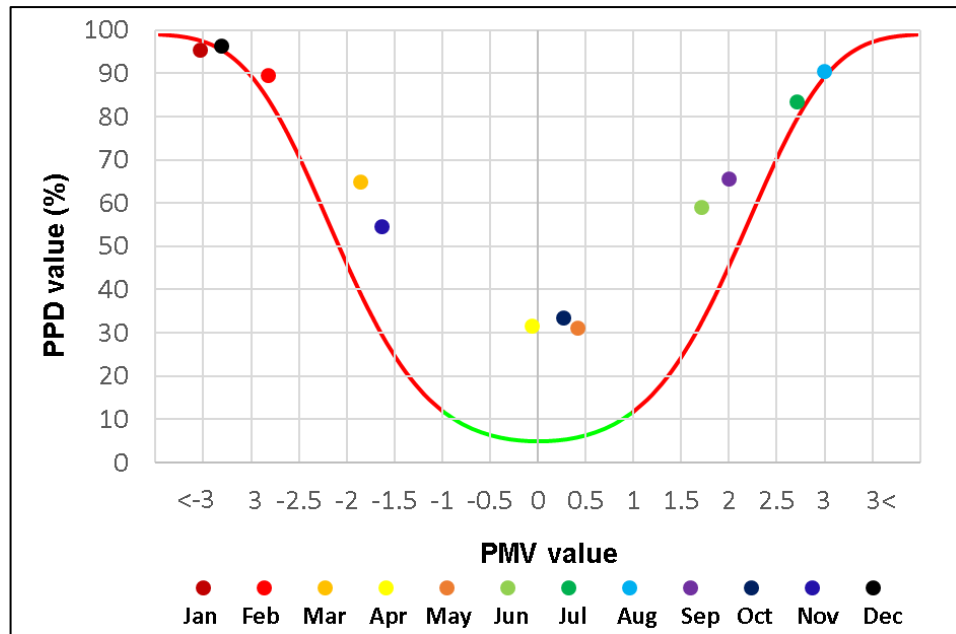


Figure 4.23. PMV and PPD values for WWR 50%.

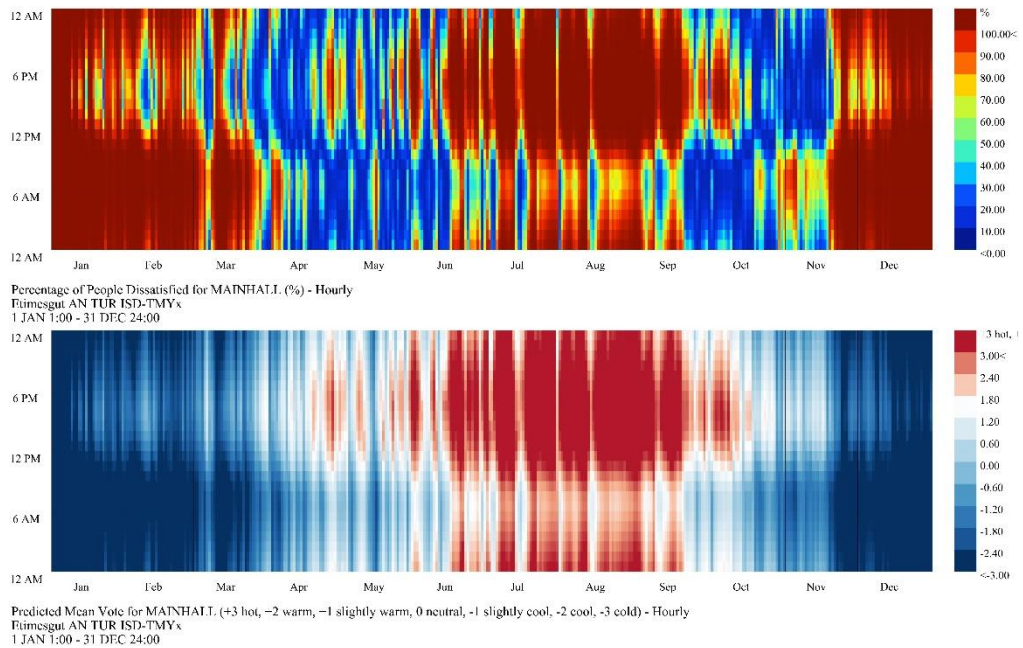


Figure 4.24. Annual PMV and PPD chart for WWR 50%.

Scenario (S2.c) evaluated a window-to-wall ratio (WWR) of 30%. According to the findings, heating demand climbed by 8%. On the contrary, it resulted in a 24% decrease in cooling loads. Therefore, indoor thermal comfort has increased in the summer compared to scenarios (S2.a) and (S2.b), whereas it has decreased significantly in the winter. The 30% glazing ratio saved total energy use by 7%.

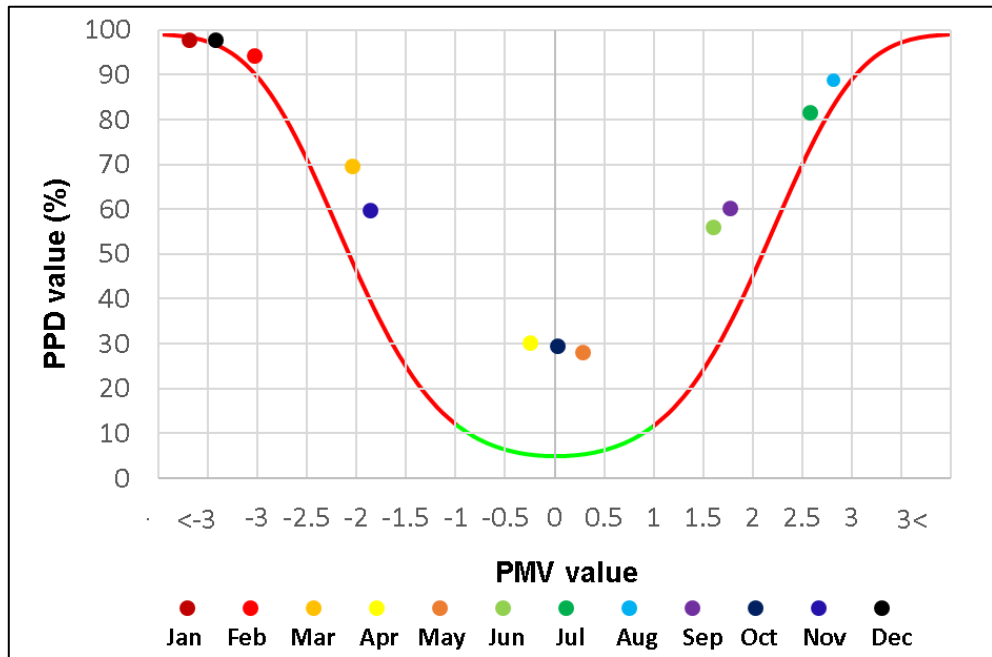


Figure 4.25. PMV and PPD values for WWR 30%.

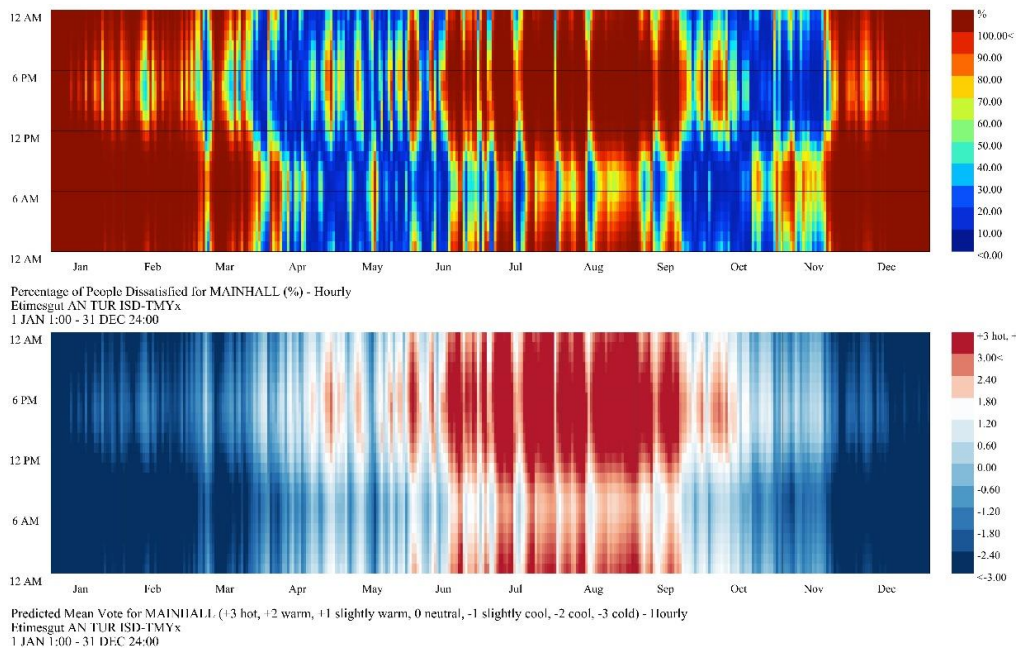


Figure 4.26. Annual PMV and PPD chart for WWR 30%.

The results of this scenario are very logical and explained as follows: increasing the glazing ratio in the south facade leads to absorbing a lot of solar radiation during the day. In the winter, increasing the gains from solar radiation has a significant impact on reducing heating loads with the largest glazing ratio, while reducing the glazing ratio will reduce the amount of solar radiation gained and thus increase the heating loads. In the summer, the exact contrary occurs, as increasing the size of the glazing leads to an increase in the gain of solar radiation and thus increase the cooling loads, while reducing the glazing ratio will reduce the gains from solar radiation and reduce the cooling loads.

In conclusion, the findings of examining different values of glazing ratio proved that the decrease in the glazing ratio of the south facade has a positive effect on reducing cooling loads by up to 24%. On the other hand, reducing the glazing ratio contributes to raising heating loads by up to 8%. The study proved that a low glazing ratio is more effective in reducing total energy consumption. The glazing ratio of 30% decreased energy consumption by 7% compared to the existing building with a glazing ratio of 90%.

4.4. THE RESULT OF SCENARIO 3

In this research, three types of glazing systems have been examined. Through the simulation process, it was observed that increasing the thickness of the air gap between the glass panels in the triple glazing system has no consequence on energy consumption. Moreover, the research confirmed that using low emissivity glass panels (low-E) can save 16% of energy consumption as is shown in Table 4.6 and Figure 4.27.

Table 4.6. Annual heating and cooling loads for each glazing type (Kwh/m²).

Sub scenario	Glazing type	Energy use intensive (EUI) kWh/m ²		Total
		Heating	Cooling	
S3. a	Triple glazing with 6 mm cavity	71,05	60,19	131,24
S3. b	Triple glazing with 10 mm cavity	71,05	60,19	131,24
S3. c	Double glazing with low-E panels	55,33	63,73	119,06

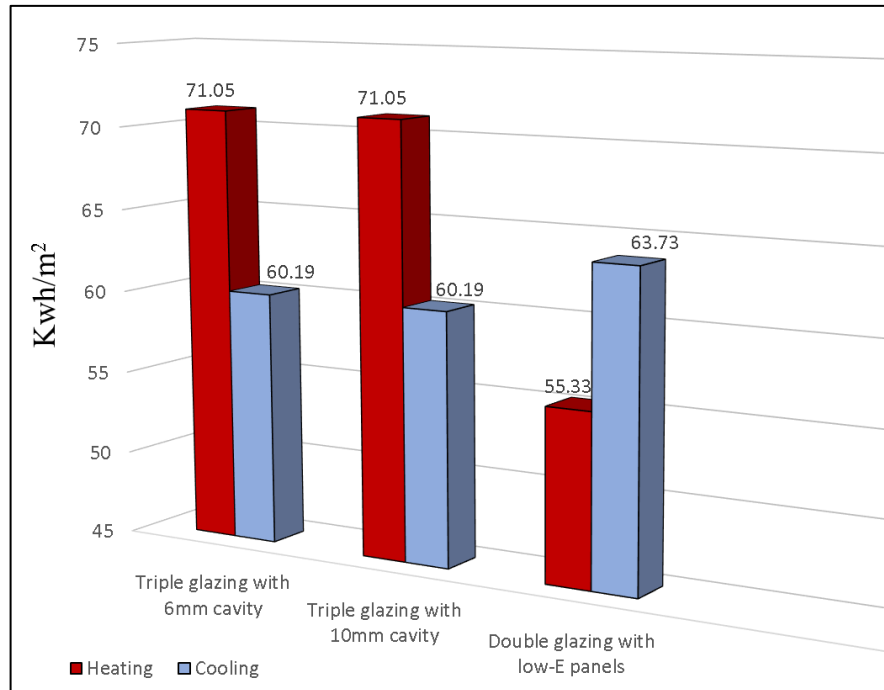


Figure 4.27. Heating and cooling loads for WWR values by floor area (Kwh/m²).

Scenario (S3.a) evaluated the use of a triple glazing system with an air cavity that has a 6 mm thickness. The results revealed a 7% improvement in decreasing heating loads. Moreover, it resulted in an 8% decrease in cooling loads. By using this glazing system, the total energy consumption was decreased by 8%. In the aspect of indoor thermal comfort, there was no noticeable effect.

Scenario (S3.b) examined the installation of a triple glazing system with a 10 mm thick air cavity. The results were the same as in scenario (S3.a), indicating that increasing the thickness of the air cavity in the triple glazing system had no influence on its performance.

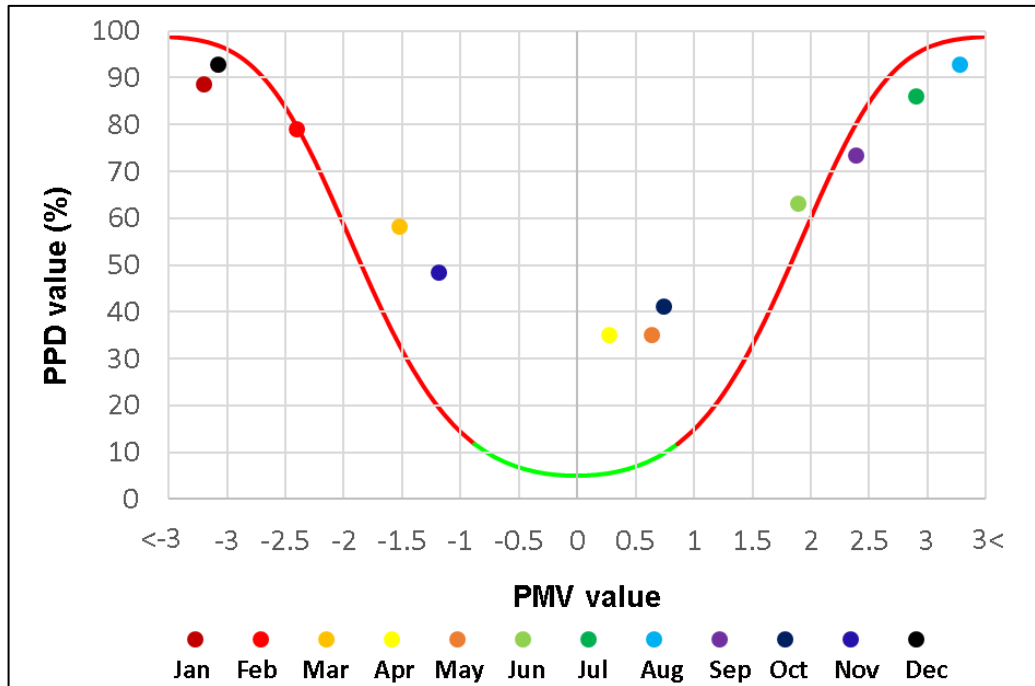


Figure 4.28. PMV and PPD values for triple glazing system.

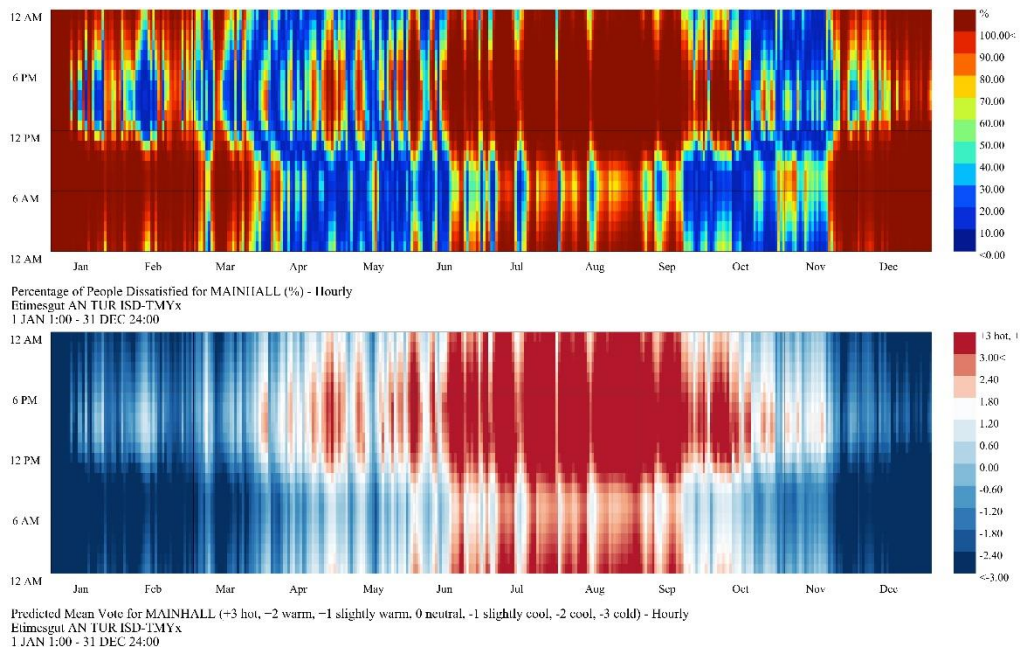


Figure 4.29. Annual PMV and PPD chart for triple glazing system.

Scenario (S3.c) examined the use of a double glazing system with low-E panels and a 12 mm thick air cavity. The results showed a 27% reduction in heating loads. Furthermore, it resulted in a 3% reduction in cooling loads. The total energy usage

was reduced by 16% by employing this glazing system. In terms of indoor thermal comfort, there was a slight reduction in winter as it appears in Figure 4.30.

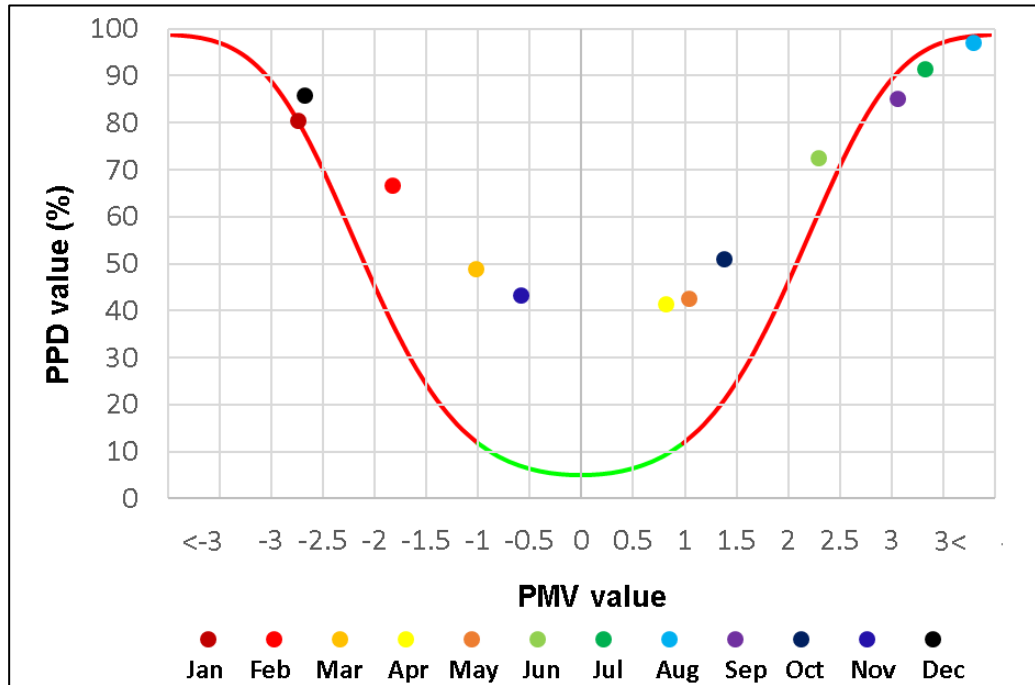


Figure 4.30. PMV and PPD values for double glazing system with low-E panels.

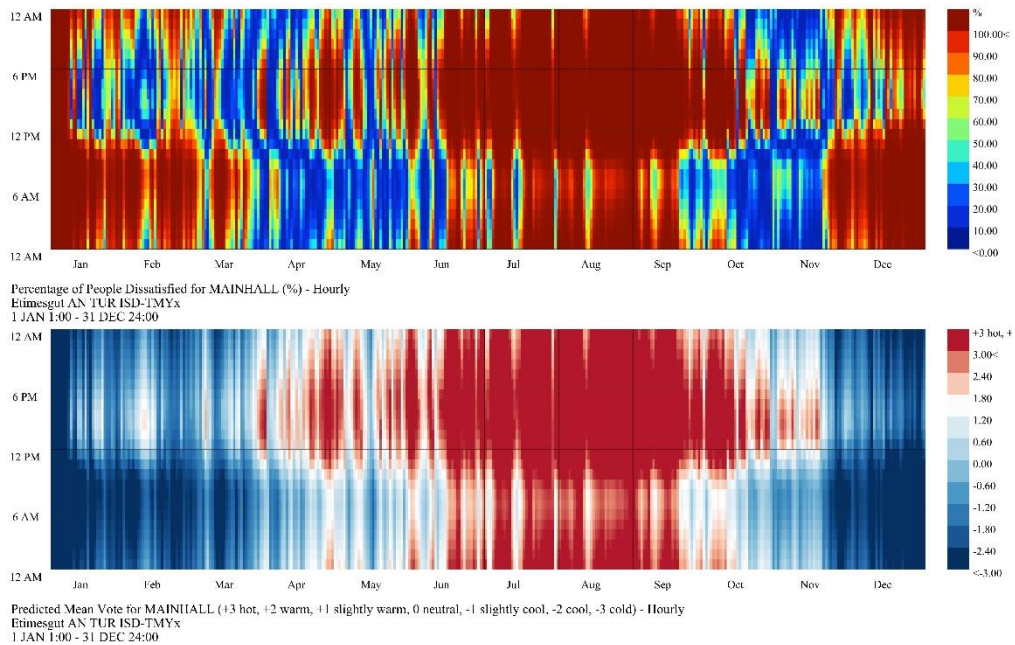


Figure 4.31. Annual PMV and PPD chart for double glazing system with low-E panels.

In conclusion, the use of the triple glazing system could achieve a reduction in heating loads of approximately 7%. At the same time, the most interesting finding in this scenario is that the utilization of a double glazing system with low-E panels reduced heating loads by 27%. On the other hand, the triple glazing system could reduce cooling loads by 8%. In comparison, the double glazing system with low-E reduced cooling loads by 3%. The indoor thermal comfort condition showed that the triple glazing system could slightly improve the indoor environment during summer, while in winter, the double glazing system with low-E panels is better.

4.5. THE RESULT OF SCENARIO 4

In order to assess the effect of using the green roof in the cold climate, three scenarios were conducted: the roof was examined with an extensive green roof and thermal insulating of 100 mm thickness, the roof with an extensive green roof and thermal insulating of 150 mm thickness, and the roof with an extensive green roof without thermal insulation. The findings appear in Table 4.7 and Figure 4.32.

Table 4.7. Annual heating and cooling loads for the green roof (Kwh/m²).

Sub scenario	Green roof	Energy use intensive (EUI) kWh/m ²		Total
		Heating	Cooling	
S4. a	Green roof with 100 mm insulation	73,28	66,79	140,07
S4. b	Green roof with 150 mm insulation	71,95	66,31	138,26
S4. c	Green roof without insulation	88,96	71,25	160,21

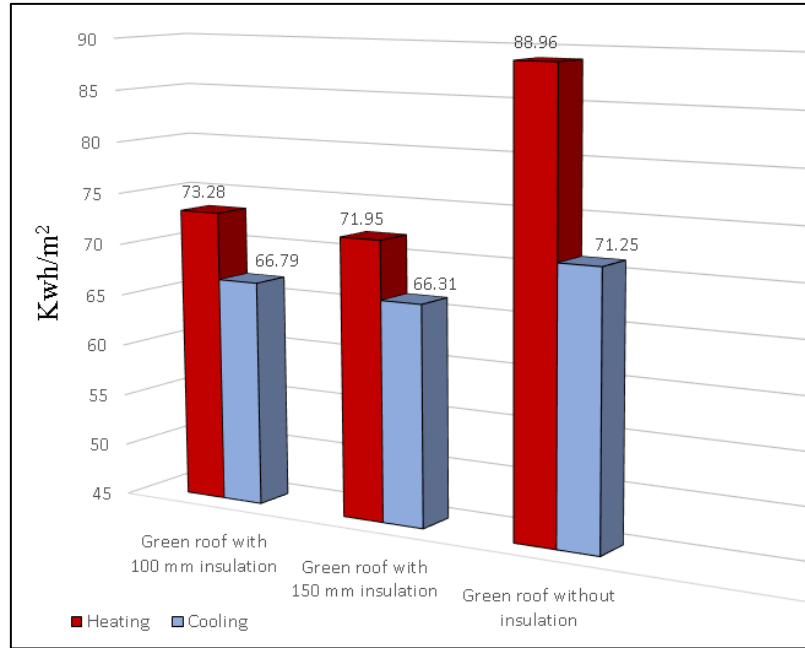


Figure 4.32. Heating and cooling loads for the green roof by floor area (Kwh/m²).

Scenario (S4.a) examined the performance of the roof with a green roof and a thermal insulation layer of 100 mm in thickness. The results showed a 4% reduction in heating loads. However, it resulted in a 1.5% increase in cooling loads. The total energy usage was slightly reduced by 1%. In terms of indoor thermal comfort, there was no noticeable effect, as it appears in Figure 4.33.

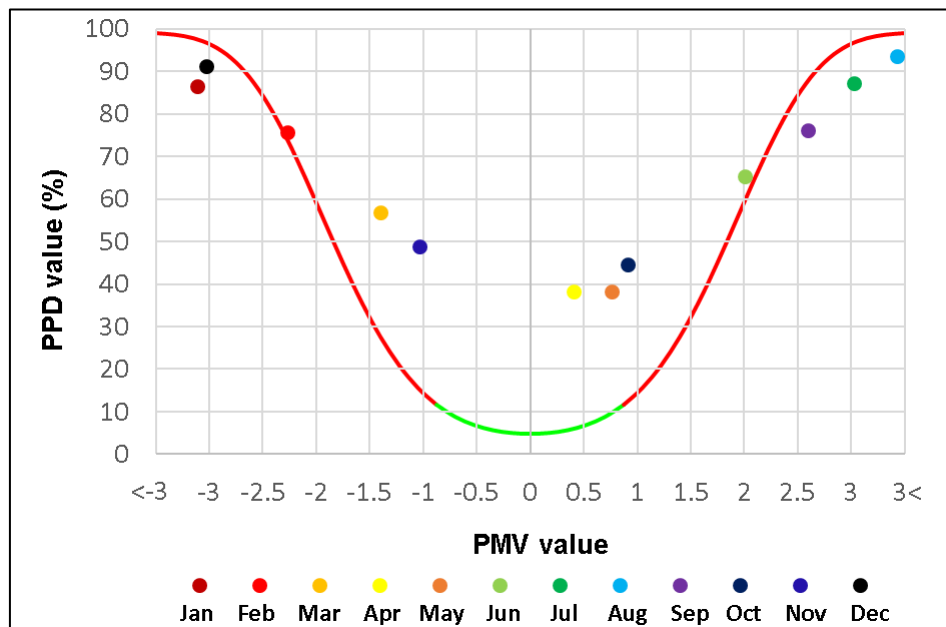


Figure 4.33. PMV and PPD values for the green roof with 100 mm insulation.

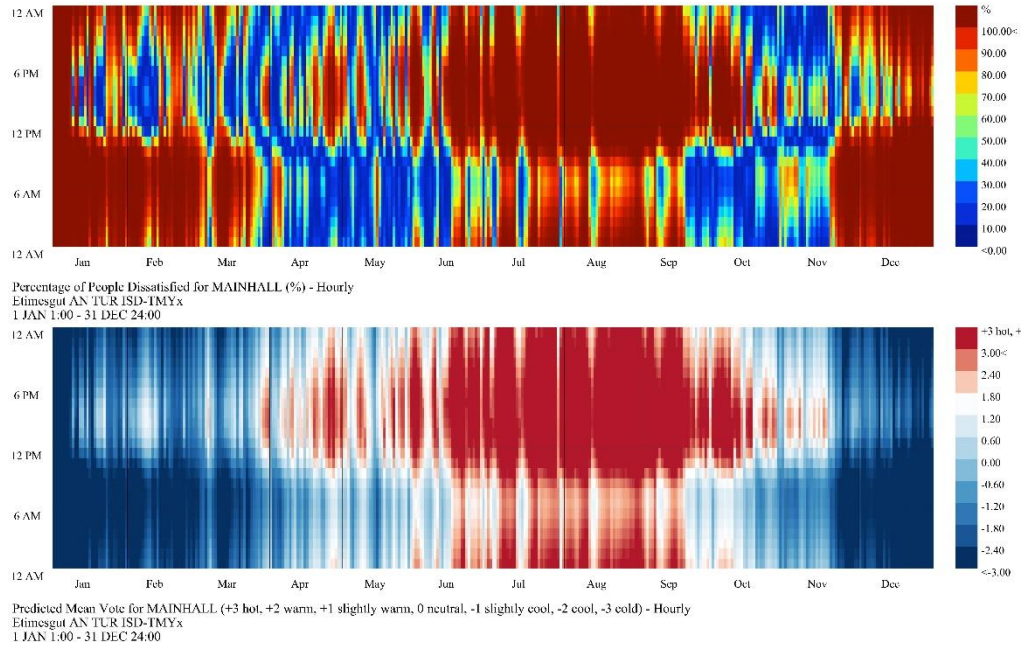


Figure 4.34. Annual PMV and PPD chart for the green roof with 100 mm insulation.

Scenario (S4.b) evaluated the influence of the roof with a green roof and a 150-mm-thick thermal insulation layer. Heating loads were reduced by 6% as a result of the findings. It did, however, result in about a 1% rise in cooling loads. The total energy consumption was reduced by 2%. As seen in Figure 4.35, there was no obvious influence on indoor thermal comfort.

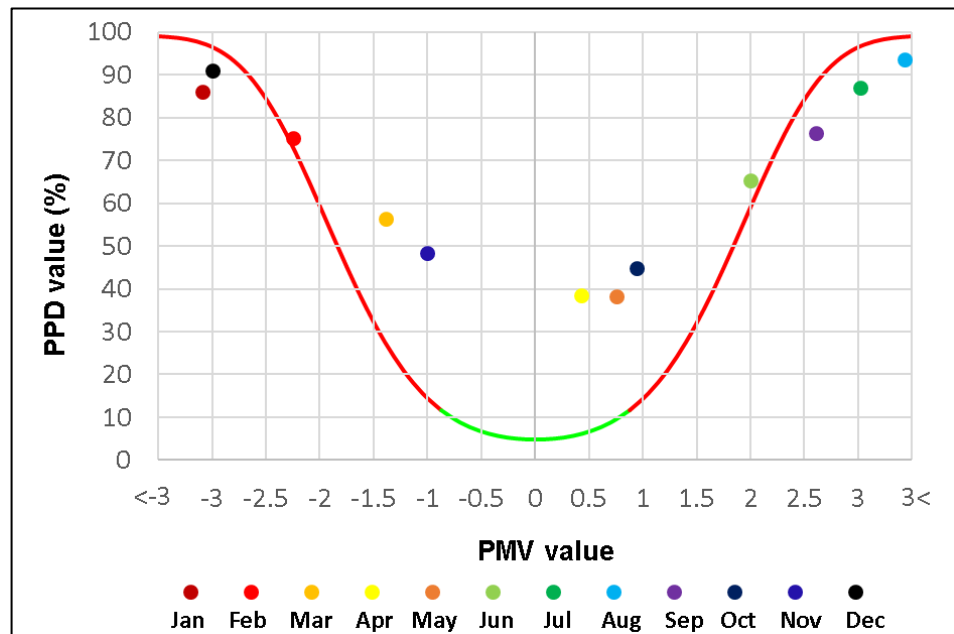


Figure 4.35. PMV and PPD values for the green roof with 150 mm insulation.

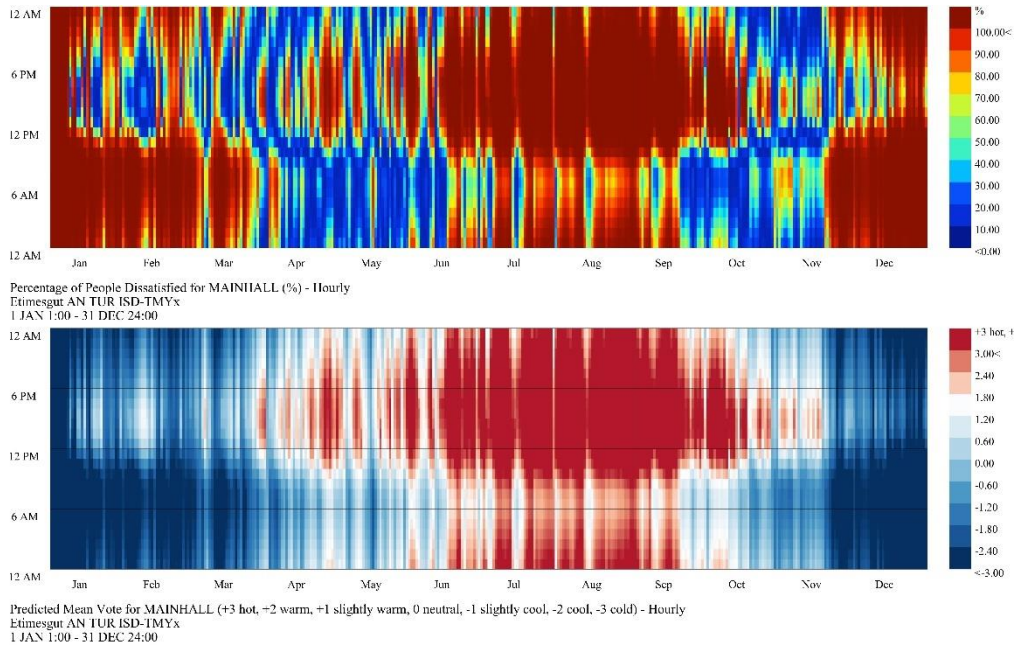


Figure 4.36. Annual PMV and PPD chart for the green roof with 150 mm insulation.

Scenario (S4.c) assessed the impact of a green roof without a thermal insulating layer on the roof. The thermal loads increased significantly in this scenario, with the heating demands increasing by 14%. Furthermore, cooling loads increased by 8%. The total amount of energy consumed has grown by 11%. As seen in Figure 4.37, indoor thermal comfort deteriorated.

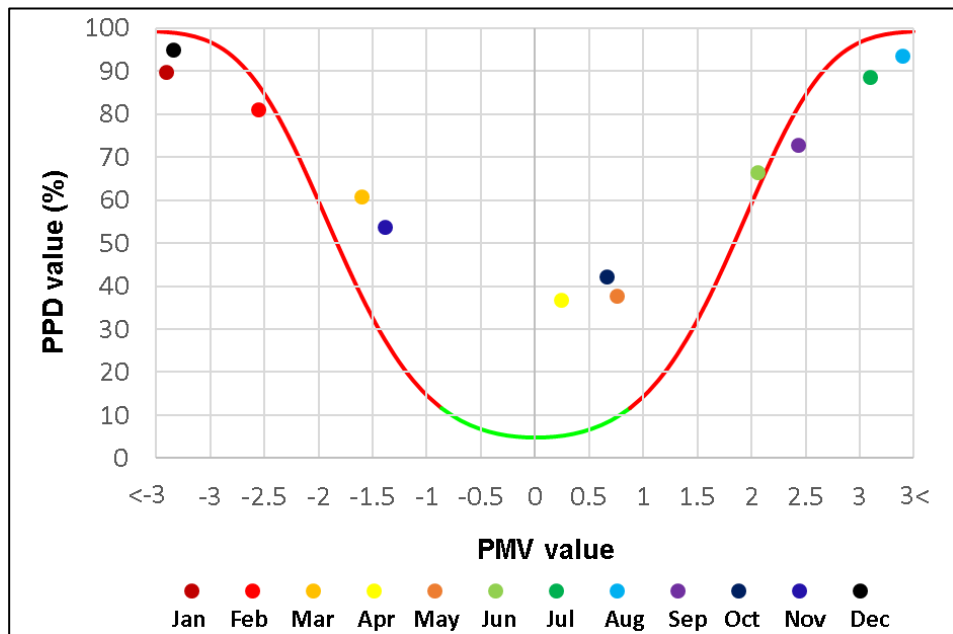


Figure 4.37. PMV and PPD values for the green roof without insulation.

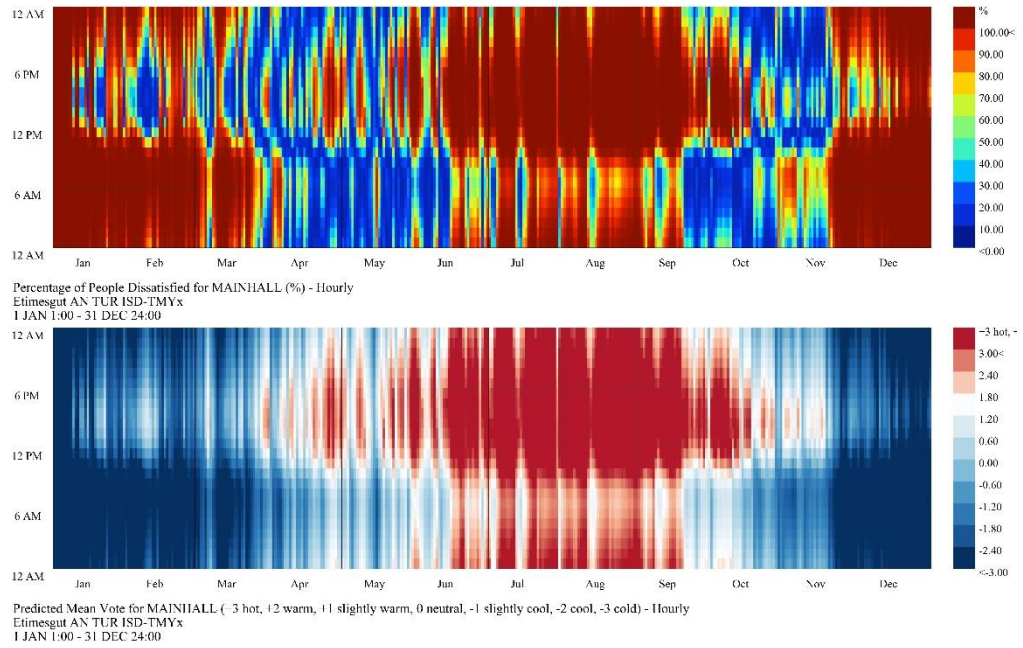


Figure 4.38. Annual PMV and PPD chart for the green roof without insulation.

In conclusion, scenario 4 showed that using the green roof in a cold semi-arid climate had a positive effect on reducing heating loads by up to 8%, provided that a thermal insulation layer is used within it. On the other hand, the use of the green roof in this climate has a slight negative effect in the summer. It could increase the cooling loads by 1.5%. Using the green roof without a thermal insulation layer in this climate had a significant negative impact on the thermal loads, raising heating loads by 14% and cooling loads by 8%. Otherwise, the green roof has many ecological benefits, such as the absorption of carbon dioxide, in addition to the great potential that the green roof has for reusing the water consumed in the process of ablution in mosques. The indoor thermal comfort condition results proved that the use of the green roof without a layer of thermal insulation leads to extreme levels of thermal discomfort in the indoor environment.

4.6. THE RESULT OF SCENARIO 5

External walls with thermal insulation thickness of 150mm were examined and a thickness of 150 mm for the roof with a green roof and using the floor with 75 mm thermal insulation to obtain the required level of U-value supposed by Turkish

standard (TS825). According to the results of scenario 2, the glazing ratio of 30% is the most appropriate for the case study and was used with a double glazing system that has low-E panels.

Table 4.8. Annual heating and cooling loads for the retrofitted model by floor area (Kwh/m²).

Loads	Energy use intensive (EUI) kWh/m ²	Total
Heating	57,50	108,91
Cooling	51,41	

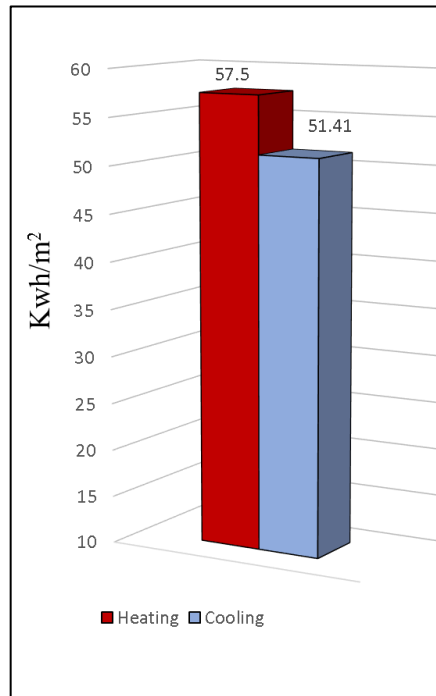


Figure 4.39. Heating and cooling loads for the retrofitted model by floor area (Kwh/m²).

Table 4.8 and Figure 4.39 show the results of Scenario 5. The results of the scenario explained the significant effect of retrofitting the existing building envelope on reducing the thermal loads inside the building. With the proposed retrofit of the building envelope, the heating loads were reduced by 25%. In addition, this scenario achieved a 22% reduction in cooling loads. Moreover, total energy consumption was reduced by 23% compared to the existing building.

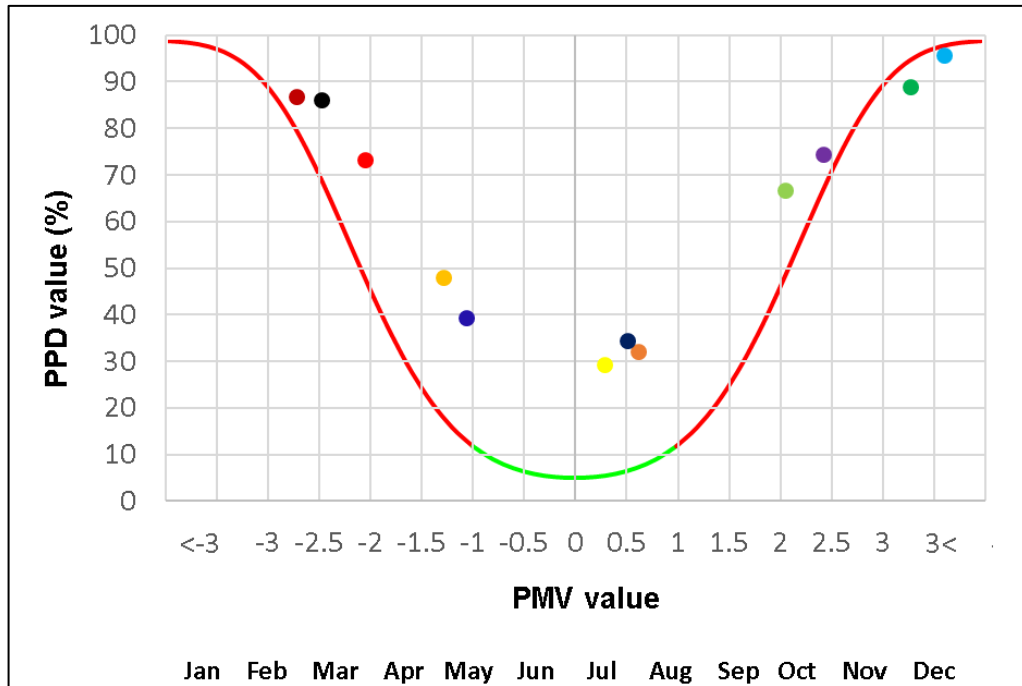


Figure 4.40. PMV and PPD values for the best scenario.

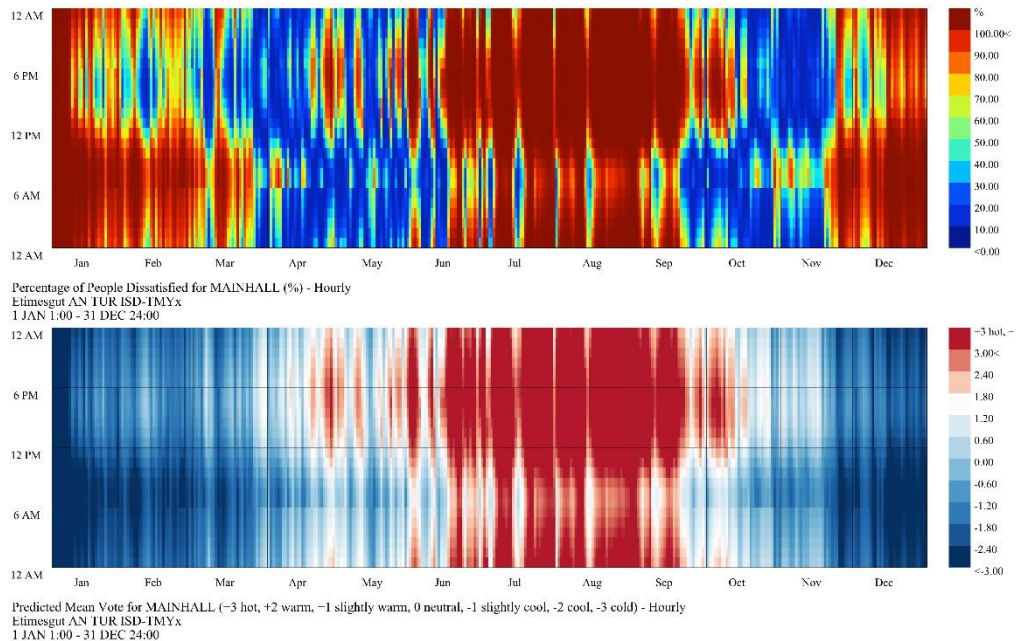


Figure 4.41. Annual PMV and PPD chart for the best scenario.

Also, with the proposed retrofit of the building envelope, the indoor thermal comfort was improved, especially during the winter, as it appears in Figure 4.40. However, this improvement does not reach the level suggested by the ASHRAE standard.

PART 5

CONCLUSION

This research proposed investigating the effectiveness of passive solar design strategies in cold and semi-arid climate areas. The research was conducted in Ankara city in Turkey through the Yaşamkent mosque. The methodology was based on establishing retrofitting strategies in the case study. Retrofitting strategies that have been examined are thermal insulation for walls, floor, and roof, as well as examining various values of glazing ratio and different types of glazing systems, in addition to examining the effectiveness of the green roof. Table 5.1 shows the comparison of retrofitting scenarios and the existing model:

Table 5.1. Comparing the results.

Scenario	Sub	Loads		(-)% decrease (+)% increase	
		Heating	Cooling	Heating	Cooling
Exist model		76,20	65,75		
Walls with 80mm insulation	S1.a	73,84	65,96	-3%	+0.3%
Walls with 100mm insulation	S1.b	72,91	66	-4.3%	+0.3%
Walls with 150mm insulation	S1.c	71,50	66,12	-6%	+0,55%
Walls with 200mm insulation	S1.d	70,71	66,14	-7%	+0,6%
Floor with 75mm insulation	S1.e	76	67.13	-0.25%	+2%
Floor with 100mm insulation	S1.f	75,95	68,51	-0,30%	+4%
Roof with 150mm insulation	S1.g	73,83	65,46	-3%	-0,4%
WWR 75 %	S2.a	76,75	61,84	+0.7%	-6%
WWR 50 %	S2.b	79,51	55,34	+4%	-16%
WWR 30 %	S2.c	82,76	49,89	+8%	-24%
Triple glazing with 6mm cavity	S3.a	71,05	60,19	-7%	-8%
Triple glazing with 10mm cavity	S3.b	71,05	60,19	-7%	-8%
Double glazing with low-E panels	S3.c	55,33	63,73	-27%	-3%
Green roof with 100 mm insulation	S4.a	73,28	66,79	-4%	+1,5%
Green roof with 150 mm insulation	S4.b	71,95	66,31	-6%	+0,85%
Green roof without insulation	S4.c	88,96	71,25	+14%	+8%

According to the results, the glazing ratio significantly impacts increasing and decreasing thermal loads. Yet, the effect is variable according to the climate. In the winter, increasing the glazing ratio can significantly reduce heating loads. On the other hand, the high glazing ratio will cause a significant increase in cooling loads in the summer. Therefore, this point requires more intensive studies to achieve satisfying results, especially in places with cold winters and hot summers. Also, the results reveal that the use of low-emissivity glass has an enormous effect on energy performance, especially heating energy, as it contributed to reducing heating loads by 27% compared to the existing building.

In addition to the above, establishing a green roof to roof without thermal insulation has a negative effect on energy performance, as it increases energy consumption by 11% compared to the existing condition.

The best performance in each scenario has been considered in the fifth scenario for the case study. The results have been compared in Table 5.2.

Table 5.2. Comparing the best performance of retrofiting strategies with the existing model and 1,2,3,4 scenario.

Scenario	Sub	Loads		(-)% decrease (+)% increase	
		Heating	Cooling	Heating	Cooling
Retrofited model (scenario5)		57,50	51,41		
Exist model		76,20	65,75	-25%	-22%
Walls with 80mm insulation	S1.a	73,84	65,96	-22%	-22%
Walls with 100mm insulation	S1.b	72,91	66	-21%	-22%
Walls with 150mm insulation	S1.c	71,50	66,12	-20%	-22%
Walls with 200mm insulation	S1.d	70,71	66,14	-19%	-22%
Floor with 75mm insulation	S1.e	76	67.13	-24%	-23%
Floor with 100mm insulation	S1.f	75,95	68,51	-24%	-25%
Roof with 150mm insulation	S1.g	73,83	65,46	-22%	-21%
WWR 75 %	S2.a	76,75	61,84	-25%	-17%
WWR 50 %	S2.b	79,51	55,34	-28%	-7%
WWR 30 %	S2.c	82,76	49,89	-31%	+3%
Triple glazing with 6mm cavity	S3.a	71,05	60,19	-19%	-15%
Triple glazing with 10mm cavity	S3.b	71,05	60,19	-19%	-15%
Double glazing with low-E panels	S3.c	55,33	63,73	+4%	-19%
Green roof with 100 mm insulation	S4.a	73,28	66,79	-22%	-23%
Green roof with 150 mm insulation	S4.b	71,95	66,31	-20%	-22%
Green roof without insulation	S4.c	88,96	71,25	-35%	-28%

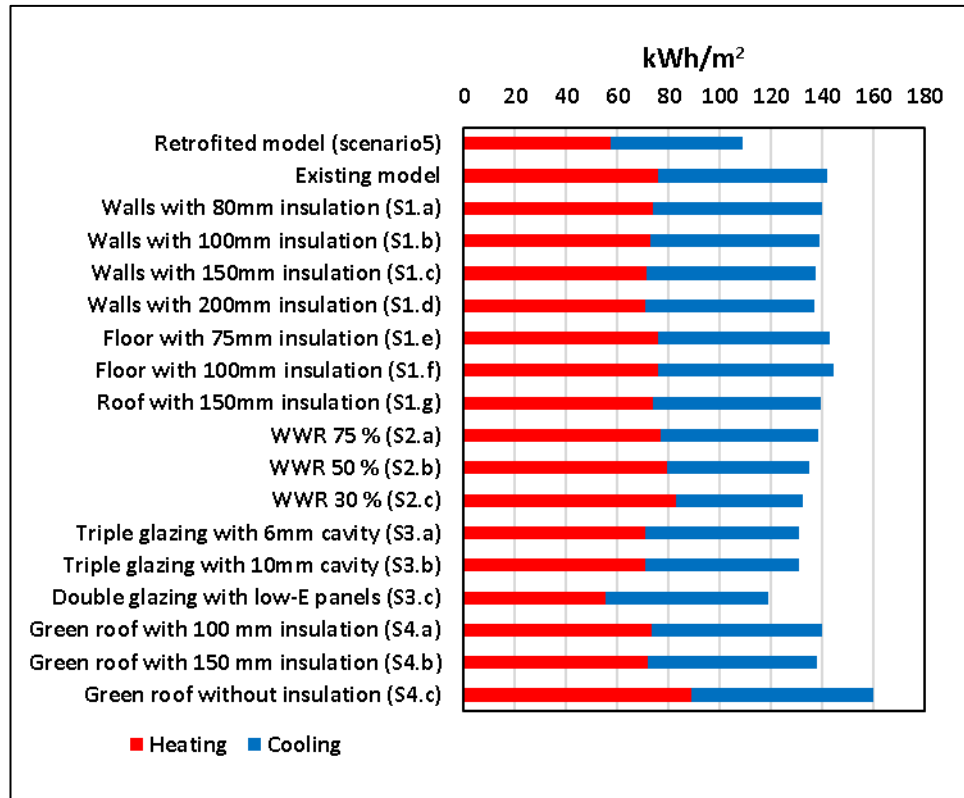


Figure 5.1. Annual heating and cooling loads for each scenario.

According to Table 5.2, the positive effect of retrofitting the building envelope can be observed in reducing heating and cooling loads, except for causing an increase in heating loads by 4% compared to the existing building with low-emissivity glass. This is due to using a 30% transparency ratio on the south facade in the retrofitted building envelope, while in the existing building it is 90% of the south facade, which caused a decrease in the amount of solar energy that is gained during the winter.

In terms of thermal comfort, no improvement was achieved in the level of indoor thermal comfort during scenarios 1, 2, 3, and 4, despite a slight improvement when examining the floor without insulation. However, in the fifth scenario, a weak improvement in the level of indoor thermal comfort was observed, up to 6% compared to the existing model. However, despite the improvement in the level of indoor thermal comfort, it did not reach the required level according to the ASHRAE standard.

Through the proposed retrofitting in Scenario 5, a significant improvement was observed in the level of energy performance in the building, as these improvements contributed to reducing the annual consumption rate by 23% compared to the existing building. (Table 5.3.) provides more details in particular.

Table 5.3. Comparing the annual consumption of retrofitting strategies with the existing model and 1,2,3,4 scenario.

Scenario	Energy use intensive (EUI) kWh/m ²	(-)% decrease (+)% increase
Retrofited model (scenario5)	108.91	
Exist model	141,95	-23%
Walls with 80mm insulation	139,8	-22%
Walls with 100mm insulation	138,91	-22%
Walls with 150mm insulation	137,62	-21%
Walls with 200mm insulation	136,85	-20%
Floor with 75mm insulation	143.13	-24%
Floor with 100mm insulation	144,46	-25%
Floor without insulation	118,43	-8%
Roof with 150mm insulation	139,29	-22%
WWR 75 %	138,59	-21%
WWR 50 %	134,85	-19%
WWR 30 %	132,65	-18%
Triple glazing with 6mm cavity	131,24	-17%
Triple glazing with 10mm cavity	131,24	-17%
Double glazing with low-E panels	119,06	-9%
Green roof with 100 mm insulation	140,07	-22%
Green roof with 150 mm insulation	138,26	-21%
Green roof without insulation	160,21	-32%

Based on the results of this study, it can be stated that the building envelope has a primary impact on indoor thermal comfort and the rate of energy consumption. Retrofitting and improving the building envelope will lead to both improving the level of indoor thermal comfort and reducing energy consumption.

Through this study, the possibility of the retrofitting system in enhancing the performance of the Yaşamkent mosque in terms of reducing thermal loads and improving the level of indoor thermal comfort by using passive design systems has been recognized. However, this study is an exploratory step in the field of studying the development of the performance of mosque buildings in a cold, semi-dry climate.

This study can encourage conducting further studies with a greater focus on specific variables, for example:

1. Studying the effect of integrating the use of passive technique/s and active systems.
2. Conducting a numerical study supported by measurements throughout the year.
3. Conducting an optimization study to determine the optimum window-to-wall ratio (WWR) for the Qibla wall.
4. Studying indoor thermal comfort supported by a questionnaire survey to compare actual and predicted mean votes.
5. Study of different types of thermal insulation materials.
6. Since passive solar design systems require air-tightened building envelopes, studies should be carried out on the effect of these systems on indoor air quality.

Since the construction of the first mosque in Islam in Madina in 622, the design and construction of mosques have witnessed continuous development. The style of mosques in the Middle East has been classified into three styles: Arab style, Persian style, and Ottoman style. Each style has characteristics that distinguish it from others.

Since the establishment of the Republic of Turkey in 1923, mosque architecture in Turkey has witnessed a great development based on the integration of traditional Ottoman architecture with modern ideas. The rectangular shape of the prayer hall, the dome, and the courtyard are elements that represent the traditional Ottoman mosque. The use of solid concrete blocks except for the Qibla wall and the excessive use of glazing are elements that represent modernity in the mosques. Yaşamkent mosque is an example.

The results of the study support this aspect by proving the effectiveness of using a high ratio of glazing surfaces with low-emission double glazing in reducing heating loads. Due to the methodology of the study that adopted the style of retrofitting, the researcher needed to maintain the approach of the designer and the architectural

concept of the mosque. Other building materials were not examined. Also, openings on the East and West sides have not been examined, although Wilson (2012) stated in his study that the presence of openings on the East and West sides has a negative effect on the indoor space and makes it uncomfortable.

Through this study and future studies in this field, it is possible to establish a guideline for constructing sustainable mosques that supports decision-makers and architects in cities located in cold, semi-arid climates.

REFERENCES

- Abergel, T., and Delmastro, C., “Is Cooling The Future Of Heating?”, *the International Energy Agency IEA*, (2020).
- Alabdullatief, A., Omer, S., Elabdein, R. Z., and Alfraidi, S., “Green roof and louvers shading for sustainable mosque buildings in Riyadh, Saudi Arabia. *Proceedings of the First International Conference on Mosques Architecture, Imam Abdulrahman Bin Faisal University*, Dammam, KSA, (2016).
- Alabdullatief, A., Omer, S., “Sustainable techniques for thermal comfort in buildings designed used by worshipers: A case of roof options for mosque buildings in hot arid climate”, *Proceedings of the 16th International Conference on Sustainable Energy Technologies*, Bologna, Italy, (2017).
- Al Anzi, A., and Al-Shammeri, B., “Energy Saving Opportunities Using Building Energy Simulation For a Typical Mosque In Kuwait”, *Proceedings of the ASME-2010 4th International Conference on Energy Sustainability*, Phoenix, AZ, USA, 383–391, (2010).
- Aldawoud, A., “Assessing the energy performance of modern glass facade systems”, *MATEC Web of Conferences*, 120, (2017).
- Alhemiddi, N. A., “Strategies to Reduce the Electricity Energy Consumption in Mosque Buildings: An Analysis Study for Riyadh Mosque Buildings and Arrahmaniyah Mosque in Sakaka City in Saudi Arabia”, *King Saud University, Architecture and Planning Department*, Riyadh, KSA, (2003).
- Al-Homoud, M. S., Abdou, A. A., and Budaiwi, I. M., “Assessment of monitored energy use and thermal comfort conditions in mosques in hot-humid climates”, *Energy and Buildings*, 41(9): 607- 614, (2009).
- Al-Homoud, M. S., “Envelope Thermal Design Optimization of Buildings with Intermittent Occupancy”, *Journal of Building Physics*, 33(1): 65–82, (2009).
- Allen, J. G., Macomber, J. D., “Healthy Buildings: How Indoor Spaces Drive Performance and Productivity”, *Harvard University Press*, (2020).
- Ali, H., Hayat, N., Farukh, F., Imran, S., Kamran, M. S., Ali, H. M., “Key Design Features of Multi-Vacuum Glazing for Windows”, *Thermal Science*, 21(6B): pp 2673-2687, (2017).

Almarzouq, A., and Sakhrieh, A., “Effects Of Glazing Design And Infiltration Rate On Energy Consumption And Thermal Comfort In Residential Buildings”, *Thermal Science*, (2018).

Al-Sanea, S. A., and Zedan, M. F., “Effect of insulation location on thermal performance of building walls under steady periodic conditions”, *International Journal of Ambient Energy*, 22(2): 59-72, (2001).

Andamon, M. M., Williamson, T. J., and Soebarto, V., “Perceptions and Expectations of Thermal Comfort in the Philippines”, *Conference: Challenges for Architectural Science in Changing Climates: Proceedings of the 40th Annual Conference of the Architectural Science Association ANZAScA At University of Adelaide*, South Australia, Australia, (2006).

ANSI/ASHRAE Standard 55-2013, “Thermal Environmental Conditions for Human Occupancy”, *American Society of Heating, Refrigeration and Air Conditioning Engineers*, Atlanta, US, (2013).

Ardabili, N. G., "Parametric Design And Simulation Of A Smart Façade For Hot And Humid Climates Using Biomimetics, PCMs And SMAs: A Case Study In Iran", *The Graduate School Of Natural And Applied Sciences Of Middle East Technical University*, Ankara, Turkey, (2020).

Arens, E., Zhang, H., “The skin's role in human thermoregulation and comfort”, *Thermal and Moisture Transport in Fibrous Materials*, eds N. Pan and P. Gibson, *Woodhead Publishing Ltd*, pp 560-602, (2006).

Arens, E., Humphreys, M., de Dear, R., and Zhang. H., “Are ‘class A’ Temperature Requirements Realistic or Desirable?”, *Building and Environment*, 45(1): 4-10, (2010).

Arıcı, M., and Karabay, H., “Determination of optimum thickness of double-glazed windows for the climatic regions of Turkey”, *Energy and Buildings*, 42(10): 1773-1778, (2010).

ASHRAE, “Handbook of Fundamentals (SI edition)”, *American Society of Heating, Refrigeration and Air Conditioning Engineers*, (2017).

Atmaca, A. B., and Gedik, G. Z., “Determination of thermal comfort of religious buildings by measurement and survey methods: Examples of mosques in a temperate-humid climate”, *Journal of building engineering*, 30, (2020).

Atmaca, A. B., Gedik, G. Z., and Wagner, A., “Determination of Optimum Envelope of Religious Buildings in Terms of Thermal Comfort and Energy Consumption: Mosque Cases”, *Energies*, 14, (2021).

Azmi, N. A., Arıcı, M., and Baharun, A., “A review on the factors influencing energy efficiency of mosque buildings” *Journal of Cleaner Production*, 292, (2021).

- Azmi, N. A., Kandar, M. Z., “Factors contributing in the design of environmentally sustainable mosques”, *Journal of Building Engineering*, 23: 27-37, (2019).
- Bainbridge, D., A., and Haggard, K., “Passive Solar Architecture: Heating, Cooling, Ventilation, Daylighting, and More Using Natural Flows”, *Chelsea Green Publishing*, White River Junction, VT, US, (2011).
- Baker. N., “Modelling and Analysis of Daylight, Solar Heat Gains and Thermal Losses to Inform the Early Stage of the Architectural Process”, Master thesis, *KTH Royal Institute Of Technology*, Stockholm, Sweden, (2017).
- Bazafkan. E., “Assessment Of Usability And Usefulness Of New Building Performance Simulation Tools In The Architectural Design Process”, Master thesis, *Vienna University of Technology*, Vienna, Austria, (2017).
- Boeri, A., Antonini, E., Gaspari, J., and Longo, D., “Energy Design Strategies for Retrofitting. Methodology, Technologies and Applications”, *WIT Press*, Southampton, UK, (2015).
- Bolattürk, A., “Optimum insulation thicknesses for building walls with respect to cooling and heating degree-hours in the warmest zone of Turkey”, *Building and Environment*, 4: 1055-1064, (2008).
- Brdnik, A. P., “Thermal Performance Optimization of Double and Triple Glazing Systems for Slovenian Climate Conditions”, *Sustainability* 2021, 13(21), 11857, (2021).
- Brondzik, W. T., and Kwok, A., G., “Mechanical and Electrical Equipment for Buildings (12th ed.)”: *John Wiley & Sons*, <https://bookshelf.vitalsource.com/#/books/9781118862285/>, Hoboken, NJ, US, (2014).
- Brophy, V., and Lewis, J. O., “A Green Vitruvius: Principles and Practice of Sustainable Architectural Design”, *Earthscan*, Washington, DC, (2011).
- Budaiwi, I. M., and Abdou, A. A., Al-Homoud, M. S., “Envelope retrofit and air-conditioning operational strategies for reduced energy consumption in mosques in hot climates”, *Build. Simulation*, 6(1): 33–50, (2012).
- Bughrara, K. S. M., Arsan, Z.D., and Akkurt, G.G., “Applying underfloor heating system for improvement of thermal comfort in historic mosque: the case study of Salepçioğlu Mosque, Izmir, Turkey”, *Energy Procedia*, 133, 290–299, (2017).
- Büyükalaca. O., Bulut. H., and Yılmaz. T., “Analysis of variable-base heating and cooling degree-days for Turkey”, *Applied Energy*, 69(4): 269-283, (2001).
- Çakır, Ç., “Assessing Thermal Comfort Conditions; A Case Study On The METU Faculty Of Architecture Building”, Master thesis, *The Graduate School Of Natural And Applied Sciences Of Middle East Technical University*, Ankara, (2006).

CanmetENERGY., “Overview of Different Measurement and Verification (M&V) Protocols”, a report from *Natural Resources Canada://www.nrcan.gc.ca*, (2008).

Carlucci, S., “Thermal Comfort Assessment of Buildings” *2013th ed. Springer*, (2013).

Çengel, Y., A., “Heat Transfer: A Practical Approach (2nd ed)”, *McGraw-Hill*, Boston, (2002).

Cole, R. J., and Lorch, R., “Buildings, Culture and Environment: Informing Local and Global Practices”, *Wiley-Blackwell*, (2003).

Crosbie, M. J., “Sustainability by amateurs”, *AIA Architect*, p: 14, (2008).

CSN EN 15251, <https://www.en-standard.eu/csn-en-15251-indoor-environmental-input-parameters-for-design-and-assessment-of-energy-performance-of-buildings-addressing-indoor-air-quality-thermal-environment-lighting-and-acoustics>.

d’Ambrosio Alfano, F. R., Dell’Iola, M., Palella, B. I., Riccio, G., and Russi, A., “On the measurement of the mean radiant temperature and its influence on the indoor thermal environment assessment”, *Building and Environment*, 63: 79-88, (2013).

Detsi, M., Manolitsis, A., Atsonios, I., Mandilaras, I., and Founti, M., “Energy Savings in an Office Building with High WWR Using Glazing Systems Combining Thermochromic and Electrochromic Layers”, *Energies* **2020**, 13(11), 3020, (2020).

Diler, Y., Turhan, C., Arsan, Z. D., and Akkurt, G. G., “Thermal comfort analysis of historical mosques. Case study: The Ulu mosque, Manisa, Turkey”, *Energy and Buildings*, 252, (2021).

Djunaedy. E., Hensen. J., Hopfe. C., Struck. C., Trcka. M., and Yahiaoui. A., “Notes on building performance simulation and the role of IBPSA”, Proceedings of the 11th Brazilian Congress of Thermal Sciences and Engineering, *ENCIT 2006*, (2006).

Doğrusoy, İ. T., “Doğal Aydınlatmanın İşlevsel ve Estetik Boyutları”, *Yapı*, 235: 76-77, (2001).

Donn, M. & Thomas, G., “Designing comfortable homes: Guidelines on the use of glass, mass and insulation for energy efficiency”, *Cement & Concrete Association of New Zealand*, Wellington, N.Z, (2010).

Ekici, C., “A Review Of Thermal Comfort And Method Of Using Fanger’s Pmv Equation”, 5TH International Symposium on Measurement, Conference Paper, *Analysis and Modeling of Human Functions*, Vancouver, (2013).

Energy.gov, “Guide to Passive Solar Home Design”, *U.S. Department of Energy*, https://www.energy.gov/sites/prod/files/guide_to_passive_solar_home_design.pdf, (2010).

- Erlandson, T. M., Cena, K., and de Dear, R., “Gender Differences and Non-Thermal Factors in Thermal Comfort of Office Occupants in a Hot-Arid Climate”, *Elsevier Ergonomics Book Series*,3: 263-268, (2005).
- Ertuş. K., “TS 825 Binalarda Isı Yalıtım Kuralları Standardı”, *Tesisat Mühendisliği*, (2000).
- Faghih, A. K., and Bahadori, M. N., “Thermal performance evaluation of domed roofs”, *Energy and Buildings*, 43(6): 1254–1263 (2011).
- Fang, Y., Hyde, T. J., Hewitt, N., Eames, P. C., and Norton, B., “Thermal Performance Analysis Of An Electrochromic Vacuum Glazing With Low Emittance Coatings”, *Solar Energy*, 84(4): 516-525, (2010).
- Fanger, P. O., “Thermal Comfort: Analysis and Applications in Environmental Engineering”, *McGraw-Hill Inc*, US, (1970).
- Fanger, P., O., “Thermal Comfort”, *McGraw-Hill Inc*, US, (1973).
- Freire Castro, UA., “Climate in architecture: revision of early origins”, https://digitalrepository.unm.edu/ltam_etds/49, (2019).
- Fugate, J., R., “A Passive Solar Retrofit in a Gloomy Climate”, Master Thesis, *Rochester Institute of Technology*, New York, (2018).
- Gabril, N, M, S., “Thermal Comfort and Building Design Strategies for Low Energy Houses in Libya”, Ph.D. thesis, *University of Westminster*, London, (2014).
- Gameiro da Silva, M., C., “Spreadsheets For The Calculation Of Thermal Comfort Indices PMV And PPD”, *Working Paper*, (2013).
- Ghosh. S., and Neogi. S., “Advance Glazing System - Energy Efficiency Approach for Buildings a Review”, *Energy Procedia*, 54: 352-358, (2014).
- Ghouchani, M., Taji, M., and Kordafshari, F., “The effect of qibla direction on the hierarchy of movement in mosque: A case study of mosques in Yazd, Iran”, *Frontiers of Architectural Research*, (2019).
- Güçyeter. B., “Calibration Of A Building Energy Performance Simulation Model Via Monitoring Data”, *Building Performance Analysis Conference and SimBuild*, (2018).
- Harris, J. C., Rumack, B. H., and Aldrich, F. D., “Toxicology of Urea-Formaldehyde and Polyurethane Foam Insulation”, *Journal of the American Medical Association*, Volume. 245, Issue. 3, (1981).
- Hensen, J., and Lamberts, R., “Building performance simulation for design and operation”, *Routledge*, (2011).

Holladay, M., “All About Glazing Options” *Green Building Advisor*, <http://www.greenbuildingadvisor.com/blogs/dept/musings/all-about-glazing-options>, (2016).

Holladay, M., “All About Thermal Mass”, <http://www.greenbuildingadvisor.com/blogs/dept/musings/all-about-thermal-mass>, *Green Building Advisor*, (2013).

Hong, T., Chou, S. and Bong, T., “Building simulation: an overview of developments and information sources”, *Building and Environment*, 35 (4): 347-361 (2000).

Hosey, L., “The Shape of Green: Aesthetics, Ecology, and Design”, Island Press, Washington D.C, (2012).

HSE.gov, The health and safety commission and the health and safety executive. <http://www.hse.gov.uk/temperature/thermal/factors.htm>.
<https://www.smarterhomes.org.nz/smart-guides/heating-cooling-and-insulation/insulating-your-home/>.

Ibrahim, S. H., Baharun, A., Nawi, M. N. M., and Junaidi, E., “Assessment of thermal comfort in the mosque in Sarawak, Malaysia”, *Energy and Environment*, 5(3): 327–334, (2014).

IEA, “Energy Efficiency Requirements in Building Codes, Energy Efficiency Policies for New Buildings”, Report, *International Energy Agency*, (2008).

IEA, “Turkey 2021: Energy Policy Review”, Report, *International Energy Agency*, (2021).

IEA, *International Energy Agency*, Retrofitted from: <https://www.iea.org/reports/tracking-buildings-2020>.

İlçi, V., Ozulu, İ. M., Arslan, E., and Alkan, R. M. “Investigation on the Accuracy of Existing Qibla Directions of the Mosques from Different Periods: A Case Study in Çorum City, Turkey”, *Tehnicki vjesnik - Technical Gazette*, (2018).

IPCC., “Climate Change 2014–Synthesis Report”, Intergovernmental Panel on Climate Change, *Cambridge University Press*, (2014).

ISO 7730, “Moderate thermal environments-Determination of the PMV and PPD indices and specification of the conditions of Thermal Comfort”, 2nd ed, *International Standards Organization*, Geneva, (2005).

Karjalainen, S., “Thermal Comfort and Gender: A Literature Review”, *Indoor Air*, 22(2): 96-109, (2012).

Karwowski, W., “International Encyclopedia of Ergonomics and Human Factors”, Second Edition-3 Volume set, *CRC Press*, (2010).

Kaynaklı, .Ö., and Kaynaklı, F., “Determination Of Optimum Thermal Insulation Thicknesses For External Walls Considering The Heating, Cooling And Annual Energy Requirements”, *Uludağ University Journal of The Faculty of Engineering*, 21(1): 227-242, (2016).

Kaynakli, O., “A study on residential heating energy requirement and optimum insulation thickness”, *Renewable Energy*, 33: 1164-1172, (2008).

Kılıçarslan, D., “Optimizing The Fenestration of Typical Turkish School Building With Respect to Daylight and Thermal Performance”, Master thesis, *The Graduate School Of Natural And Applied Sciences Of Middle East Technical University*, Ankara, (2013).

Konis, K., Gamas, A., and Kensek, K., "Passive performance and building form: an optimization framework for early-stage design support", *Solat Energy*, 125: 161–179, (2016).

Köppen, W, “Köppen World Map of BSk Climates”, *Wikimedia. 2019*. Available online: https://en.wikipedia.org/wiki/Semi-arid_climate#/media/File:Köppen-Geiger_Map_BSk_present.svg.

Kumar, S., Singh, M.K., Mathur, A., Mathur, S., and Mathur, J., “Thermal performance and comfort potential estimation in low-rise high thermal mass naturally ventilated office buildings in India: An experimental study”, *Journal of Building Engineering*, 20: 569-584, (2018).

Lechner, N., “Heating, Cooling, Lighting: Sustainable Design Methods For Architects”, 4th Edition, *Wiley*, New Jersey, US, (2014).

Lentz, T. R., “Analysis Of The Passive Design And Solar Collection Techniques Of The Houses in The 2009 U.S. Department of Energy’s Solar Decathlon Competition”, Master thesis, *Graduate Faculty Of Iowa State University*, Iowa (2010).

Lohia. S., and Dixit. S., “Energy Conservation using Window Glazing in India”, *International Journal of Advanced Research in Electrical, Electronics and Instrumentation Engineering*, 4(11), (2015).

Luo, M., Wang, Z., Ke, K., Cao, B., Zhai, Y., and Zhou, X., “Human metabolic rate and thermal comfort in buildings: The problem and challenge”, *Building and Environment*, 131: 44-52, (2018).

Maarof, S., “Roof designs and affecting thermal comfort factors in a typical naturally ventilated Malaysian mosque”, PhD Thesis, *Cardiff University*, Cardiff, UK, (2014).

Manz. H., Brunner. S., and Wulschleger. L., “Triple Vacuum Glazing: Heat Transfer and Basic Mechanical Design Constraints”, *Solar Energy*, 80(12): 1632-1642, (2006).

Mathews, D, “Nifty Walls Remain Just Around the Corner”, <http://earthtechling.com/2013/04/nifty-walls-remain-just-around-the-corner/>, *Earth Techling*, (2013).

Mazria, E., “It’s the architecture, stupid!”, Article, *Solar Today May/June 2003*, (2003).

Metz, F., Pielert, J., Cooke, P., and Walton, W., “Health and Safety Considerations for Passive Solar Heated and Cooled Buildings”, NIST Interagency/Internal Report (NISTIR), *National Institute of Standards and Technology*, Gaithersburg, MD, US, (1982).

Mode Lab, “The Grasshopper Primer Third Edition V3.3”, *Robert McNeel and Associates*, <http://grasshopperprimer.com>, (2015).

Mushtaha, E., and Helmy, O., “Impact of building forms on thermal performance and thermal comfort conditions in religious buildings in hot climates: a case study in Sharjah city”, *International Journal of Sustainable Energy*, 36(10), (2016).

Nahar, N., M., Sharma, P., and Purohit, M. M., “Performance of Different Passive Techniques for Cooling of Buildings in Arid Regions”, *Building and Environment*, 38: 109-116, (2003).

Nicol, F., “Adaptive Thermal Comfort Standards in the Hot-Humid Tropics”, *Energy and Buildings*, (2004).

Nicol, F., and Humphreys, M. A., “A stochastic approach to thermal comfort, occupant behavior and energy use in buildings”, *ASHRAE Transactions*, 110(2): 554-568, (2004).

Nicol, F., and Wilson, M., “A critique of European Standard EN 15251:strengths, weaknesses and lessons for future standards” *Building Research & Information*, 39(2): 183-193, (2011).

Nicol, F., Humphreys, M., and Roaf, S., “Adaptive Thermal Comfort: Principles and Practice”, *Routledge*, London, (2012).

Nikoofard, S., Ugursal, I., and Beausoleil-Morrison, I., "Effect of window modifications on household energy requirement for heating and cooling in Canada", *Proceedings of eSim 2012: The Canadian Conference on Building Simulation*, Halifax, Canada, pp 324-337, (2012).

Olesen B. W., and Parsons, K. C., “Introduction to thermal comfort standards and to the proposed new version of EN ISO 7730”, *Energy and Buildings*,34(6): 537-548, (2002).

Olesen, B. W., and Brager, G. S., “A Better Way to Predict Comfort: The New ASHRAE Standard 55- 2004”, *UC Berkeley: Center for the Built Environment*, Retrieved from <https://escholarship.org/uc/item/2m34683k>, (2004).

Parsons, K., C., “The Effects of Gender, Acclimation State, the Opportunity to Adjust Clothing and Physical Disability on Requirements for Thermal Comfort”, *Energy and Buildings*, 34(6), (2002).

Parsons, K., “Thermal Comfort in Buildings”, published in “Materials for Energy Efficiency and Thermal Comfort in Buildings” edited by Matthew R. Hall, 127-147. *Woodhead Publishing Series in Energy*, (2010).

Pearlmutter, D., “Architecture and Climate: The Environmental Continuum” Article, *Geography Compass*, 1(4): 752-778, (2007).

Pudke, A., M., Shire, K., S., and, Borkar, Y., R., “Comparative Study on Passive Solar Building”, *IARJSET*, (International Advanced Research Journal in Science, Engineering, and Technology), 4(3), Yavatmal, India, (2017).

Pusat, S., and Ekmekci, I., “A Study On Degree-Day Regions Of Turkey”, *Energy Efficiency*, (2015).

Roudsari, M. S., Pak, M., “Ladybug: A Parametric Environmental Plugin For Grasshopper To Help Designers Create An Environmentally-Conscious Design”, in *13th Conference of International Building Performance Simulation Association, IBPSA*, Chambery, France, pp: 3128-3135, (2013).

Ruiz. G. R., and Bandera. C. F., “Validation of Calibrated Energy Models: Common Errors”, *Energies*, 10: 1-19, (2017).

Sadineni, S. B., Madala, S., and Boehm, R. F., “Passive building energy savings: A review of building envelope components”, *Renewable and Sustainable Energy Reviews*, 15: 3617-3631, (2011).

Sanusi, A. N. Z., Abdullah, F., Azmin, A. K., and Kassim, M. H., “Passive Design Strategies of Colonial Mosques in Malaysia”, *Green Buildings and Renewable Energy, Med Green Forum 2019 - Part of World Renewable Energy Congress and Network*, 247–262, (2020).

Sbar, N. L., Podbelski, L., Yang, H. M., and Pease, B., “Electrochromic dynamic windows for office buildings”, *International Journal of Sustainable Built Environment*, 1(1): 125-139, (2012).

Shohan, A. A. A., and Gadi, M. B., “Evaluation of thermal and energy performance in mosque buildings for current situation (simulation study) in mountainous climate of Abha city”, *Sustainability*, 12, 4014, (2020).

Toutou, A., Fikry, M., and Mohamed, W., “The parametric based optimization framewor daylighting and energy performance in residential buildings in hot arid zone”, *Alexandria Engineering Journal*, 57(4): 3595–3608, (2018).

Trubiano, F., “Design and Construction of High-Performance Homes: Building Envelopes, Renewable Energies, and Integrated Practice”, *Routledge*, New York, (2013).

TS 825, “Thermal insulation requirements for buildings”, Turkish Standard, http://www1.mmo.org.tr/resimler/dosya_ekler/cf3e258bdf3eb7_ek.pdf, (2008).

TÜİK, Türkiye İstatistik Kurumu (Turkish Standard Institute), Retrieved from <https://www.haber365.com.tr/tuik-verilerine-gore-turkiyede-kac-camii-var-g58620>.

U.S. Department of Energy, <https://www.energy.gov/energysaver/energy-efficient-home-design/passive-solar-home-design>.

Ucar. A., and Balo. F., “Effect of fuel type on the optimum thickness of selected insulation materials for the four different climatic regions of Turkey”, *Applied Energy*, 86(5): 730-736, (2009).

United Nations Population Division, “World Urbanization Prospects: The 2018 Revision”, *United Nations*, NewYork, (2019).

Ürey, Ö., “Use Of Traditional Elements In Contemporary Mosque Architecture In Turkey”, Master thesis, *The Graduate School Of Natural And Applied Sciences Of Middle East Technical University*, Ankara, Turkey, (2010).

Voss, K., Herkel, S., Pafafferott, J., and Loehnert, G., “Energy efficient office buildings with passive cooling – Results and experiences from a research and demonstration programme”, *Solar Energy*, 81(3): 424-434, (2007).

Wagner, A., Gossauer, E., Moosmann, C., Gropp, T., and Leonhart, R., “Thermal comfort and workplace occupant satisfaction Results of field studies in German low energy office buildings”, *Energy and Buildings*, 39(7): 758-769, (2007).

Wilson, A., “Passive Solar Heating”, <https://www.buildinggreen.com/feature/passive-solar-heating>, *BuildingGreen.com*, (2012).

Wright, D., Andrejko, D. A., and Cook, J., “The Passive Solar Primer: Sustainable Architecture”, *Schiffer Pub Ltd*, Pennsylvania, (2008).

Yamtraipat, N., Khedari, J., and Hirunlabh, J., “Thermal Comfort Standards for Air Conditioned Buildings in Hot and Humid Thailand Considering Additional Factors of Acclimatization and Education Level”, *Solar Energy*, 78(4): 504-517, (2005).

Yüksel, A. N., Arıcı, M., Krajčák, M., and Karabay, H., “Experimental investigation of thermal comfort and CO₂ concentration in mosques: A case study in warm temperate climate of Yalova, Turkey”, *Sustainable Cities and Society*, 52, (2020).

URL1., http://climate.onebuilding.org/WMO_Region_6_Europe/TUR_Turkey/AN_Ankara/TUR_AN_Etimesgut.171290_TMYx.zip.

URL2., <https://www.ladybug.tools>.

URL3., <https://github.com/ladybug-tools/honeybee-wiki>.

URL4., <https://www.food4rhino.com/en/app/ladybug-tools>.

URL5., <https://www.ladybug.tools/epwmap>.

URL6., <https://www.food4rhino.com/en/app/ladybug-tools>.

URL7., http://hydrashare.github.io/hydra/viewer?owner=chriswmackey&fork=hydra_2&id=Green_Roof_In_Energy_Model&slide=0&scale=1&offset=0,0.

URL8., <https://comfort.cbe.berkeley.edu/>.

URL9., <https://mosqpedia.org/en/mosque/298>.

URL10., <http://atarim.com.tr/tr/proje/yasamkent-camii>.

APPENDICES

APPENDIX A: OBSERVED AND SIMULATED TEMPERATURE DATA

Table Appendix A.1. Observed temperature data.

No	Time	Temperature°C	No	Time	Temperature°C
1	11/28/20 0:00	17.5	30	11/29/20 5:00	17.2
2	11/28/20 1:00	17.4	31	11/29/20 6:00	17.1
3	11/28/20 2:00	17.4	32	11/29/20 7:00	17
4	11/28/20 3:00	17.4	33	11/29/20 8:00	17
5	11/28/20 4:00	17.3	34	11/29/20 9:00	17.2
6	11/28/20 5:00	17.3	35	11/29/20 10:00	18.2
7	11/28/20 6:00	17.3	36	11/29/20 11:00	19.3
8	11/28/20 7:00	17.4	37	11/29/20 12:00	20.3
9	11/28/20 8:00	17.3	38	11/29/20 13:00	20.5
10	11/28/20 9:00	17.3	39	11/29/20 14:00	20.4
11	11/28/20 10:00	17.7	40	11/29/20 15:00	20.2
12	11/28/20 11:00	18.8	41	11/29/20 16:00	19.9
13	11/28/20 12:00	19.7	42	11/29/20 17:00	19.4
14	11/28/20 13:00	20	43	11/29/20 18:00	19
15	11/28/20 14:00	20.1	44	11/29/20 19:00	18.7
16	11/28/20 15:00	20.5	45	11/29/20 20:00	18.5
17	11/28/20 16:00	20	46	11/29/20 21:00	18.2
18	11/28/20 17:00	19.6	47	11/29/20 22:00	18
19	11/28/20 18:00	19.1	48	11/29/20 23:00	17.9
20	11/28/20 19:00	18.9	49	11/30/20 0:00	17.7
21	11/28/20 20:00	18.5	50	11/30/20 1:00	17.6
22	11/28/20 21:00	18.3	51	11/30/20 2:00	17.5
23	11/28/20 22:00	18.1	52	11/30/20 3:00	17.4
24	11/28/20 23:00	17.9	53	11/30/20 4:00	17.3
25	11/29/20 0:00	17.8	54	11/30/20 5:00	17.2
26	11/29/20 1:00	17.6	55	11/30/20 6:00	17.1
27	11/29/20 2:00	17.5	56	11/30/20 7:00	17.1
28	11/29/20 3:00	17.4	57	11/30/20 8:00	17.1
29	11/29/20 4:00	17.3	58	11/30/20 9:00	17.2

No	Time	Temperature°C	No	Time	Temperature°C
59	11/30/20 10:00	18	102	12/2/20 5:00	17.3
60	11/30/20 11:00	19	103	12/2/20 6:00	17.3
61	11/30/20 12:00	19.7	104	12/2/20 7:00	17.4
62	11/30/20 13:00	20	105	12/2/20 8:00	17.3
63	11/30/20 14:00	19.9	106	12/2/20 9:00	17.3
64	11/30/20 15:00	19.9	107	12/2/20 10:00	17.7
65	11/30/20 16:00	19.5	108	12/2/20 11:00	18.8
66	11/30/20 17:00	19.2	109	12/2/20 12:00	19.7
67	11/30/20 18:00	18.9	110	12/2/20 13:00	20
68	11/30/20 19:00	18.7	111	12/2/20 14:00	20.1
69	11/30/20 20:00	18.4	112	12/2/20 15:00	20.1
70	11/30/20 21:00	18.2	113	12/2/20 16:00	19.8
71	11/30/20 22:00	18	114	12/2/20 17:00	19.5
72	11/30/20 23:00	17.9	115	12/2/20 18:00	19.1
73	12/1/20 0:00	17.8	116	12/2/20 19:00	19
74	12/1/20 1:00	17.7	117	12/2/20 20:00	18.7
75	12/1/20 2:00	17.6	118	12/2/20 21:00	18.4
76	12/1/20 3:00	17.6	119	12/2/20 22:00	18.3
77	12/1/20 4:00	17.5	120	12/2/20 23:00	18.1
78	12/1/20 5:00	17.5	121	12/3/20 0:00	18
79	12/1/20 6:00	17.4	122	12/3/20 1:00	17.9
80	12/1/20 7:00	17.5	123	12/3/20 2:00	17.8
81	12/1/20 8:00	17.5	124	12/3/20 3:00	17.7
82	12/1/20 9:00	17.4	125	12/3/20 4:00	17.6
83	12/1/20 10:00	17.4	126	12/3/20 5:00	17.5
84	12/1/20 11:00	17.5	127	12/3/20 6:00	17.4
85	12/1/20 12:00	17.6	128	12/3/20 7:00	17.5
86	12/1/20 13:00	17.8	129	12/3/20 8:00	17.4
87	12/1/20 14:00	17.9	130	12/3/20 9:00	17.6
88	12/1/20 15:00	17.9	131	12/3/20 10:00	18.5
89	12/1/20 16:00	17.8	132	12/3/20 11:00	19.5
90	12/1/20 17:00	17.7	133	12/3/20 12:00	20.4
91	12/1/20 18:00	17.7	134	12/3/20 13:00	20.7
92	12/1/20 19:00	17.8	135	12/3/20 14:00	20.6
93	12/1/20 20:00	17.7	136	12/3/20 15:00	20.1
94	12/1/20 21:00	17.6	137	12/3/20 16:00	19.8
95	12/1/20 22:00	17.5	138	12/3/20 17:00	19.5
96	12/1/20 23:00	17.9	139	12/3/20 18:00	19.1
97	12/2/20 0:00	17.5	140	12/3/20 19:00	19
98	12/2/20 1:00	17.4	141	12/3/20 20:00	18.7
99	12/2/20 2:00	17.4	142	12/3/20 21:00	18.4
100	12/2/20 3:00	17.4	143	12/3/20 22:00	18.3
101	12/2/20 4:00	17.3	144	12/3/20 23:00	18.1

Table Appendix A.2. Simulated temperature data.

No	Time	Temperature°C	No	Time	Temperature°C
1	11/28/20 0:00	18.43	36	11/29/20 11:00	17.9
2	11/28/20 1:00	17.67	37	11/29/20 12:00	19.3
3	11/28/20 2:00	17.01	38	11/29/20 13:00	21.6
4	11/28/20 3:00	16.40	39	11/29/20 14:00	23.4
5	11/28/20 4:00	15.85	40	11/29/20 15:00	24.2
6	11/28/20 5:00	15.35	41	11/29/20 16:00	24.4
7	11/28/20 6:00	15.14	42	11/29/20 17:00	24.1
8	11/28/20 7:00	15.13	43	11/29/20 18:00	23.4
9	11/28/20 8:00	15.57	44	11/29/20 19:00	22.7
10	11/28/20 9:00	16.44	45	11/29/20 20:00	21.9
11	11/28/20 10:00	17.81	46	11/29/20 21:00	21.1
12	11/28/20 11:00	19.50	47	11/29/20 22:00	20.1
13	11/28/20 12:00	21.24	48	11/29/20 23:00	18.9
14	11/28/20 13:00	23.46	49	11/30/20 0:00	17.9
15	11/28/20 14:00	24.87	50	11/30/20 1:00	17.1
16	11/28/20 15:00	25.34	51	11/30/20 2:00	16.3
17	11/28/20 16:00	25.35	52	11/30/20 3:00	15.6
18	11/28/20 17:00	24.89	53	11/30/20 4:00	15.1
19	11/28/20 18:00	24.09	54	11/30/20 5:00	14.6
20	11/28/20 19:00	23.29	55	11/30/20 6:00	14.4
21	11/28/20 20:00	22.46	56	11/30/20 7:00	14.4
22	11/28/20 21:00	21.67	57	11/30/20 8:00	14.9
23	11/28/20 22:00	20.58	58	11/30/20 9:00	15.6
24	11/28/20 23:00	19.41	59	11/30/20 10:00	16.5
25	11/29/20 0:00	18.39	60	11/30/20 11:00	17.5
26	11/29/20 1:00	17.52	61	11/30/20 12:00	18.7
27	11/29/20 2:00	16.75	62	11/30/20 13:00	20.3
28	11/29/20 3:00	16.06	63	11/30/20 14:00	21.8
29	11/29/20 4:00	15.43	64	11/30/20 15:00	22.9
30	11/29/20 5:00	14.85	65	11/30/20 16:00	23.3
31	11/29/20 6:00	14.61	66	11/30/20 17:00	23.3
32	11/29/20 7:00	14.60	67	11/30/20 18:00	22.8
33	11/29/20 8:00	15.06	68	11/30/20 19:00	22.2
34	11/29/20 9:00	15.79	69	11/30/20 20:00	21.6
35	11/29/20 10:00	16.73	70	11/30/20 21:00	21.1

No	Time	Temperature°C	No	Time	Temperature°C
71	11/30/20 22:00	20.3	108	12/2/20 11:00	17.92
72	11/30/20 23:00	19.5	109	12/2/20 12:00	18.69
73	12/1/20 0:00	18.9	110	12/2/20 13:00	19.85
74	12/1/20 1:00	18.4	111	12/2/20 14:00	20.88
75	12/1/20 2:00	17.9	112	12/2/20 15:00	21.42
76	12/1/20 3:00	17.4	113	12/2/20 16:00	21.74
77	12/1/20 4:00	16.9	114	12/2/20 17:00	21.68
78	12/1/20 5:00	16.6	115	12/2/20 18:00	21.19
79	12/1/20 6:00	16.4	116	12/2/20 19:00	20.65
80	12/1/20 7:00	16.3	117	12/2/20 20:00	20.06
81	12/1/20 8:00	16.7	118	12/2/20 21:00	19.37
82	12/1/20 9:00	17.4	119	12/2/20 22:00	18.51
83	12/1/20 10:00	18.1	120	12/2/20 23:00	17.62
84	12/1/20 11:00	18.9	121	12/3/20 0:00	16.75
85	12/1/20 12:00	20.0	122	12/3/20 1:00	16.05
86	12/1/20 13:00	21.3	123	12/3/20 2:00	15.49
87	12/1/20 14:00	22.5	124	12/3/20 3:00	15.03
88	12/1/20 15:00	23.0	125	12/3/20 4:00	14.64
89	12/1/20 16:00	23.1	126	12/3/20 5:00	14.30
90	12/1/20 17:00	22.8	127	12/3/20 6:00	14.20
91	12/1/20 18:00	22.1	128	12/3/20 7:00	14.21
92	12/1/20 19:00	21.5	129	12/3/20 8:00	14.41
93	12/1/20 20:00	20.9	130	12/3/20 9:00	14.71
94	12/1/20 21:00	20.2	131	12/3/20 10:00	15.01
95	12/1/20 22:00	19.4	132	12/3/20 11:00	15.35
96	12/1/20 23:00	18.6	133	12/3/20 12:00	15.83
97	12/2/20 0:00	17.9	134	12/3/20 13:00	16.61
98	12/2/20 1:00	17.2	135	12/3/20 14:00	17.45
99	12/2/20 2:00	16.7	136	12/3/20 15:00	18.05
100	12/2/20 3:00	16.3	137	12/3/20 16:00	18.32
101	12/2/20 4:00	15.9	138	12/3/20 17:00	18.25
102	12/2/20 5:00	15.6	139	12/3/20 18:00	17.90
103	12/2/20 6:00	15.4	140	12/3/20 19:00	17.47
104	12/2/20 7:00	15.4	141	12/3/20 20:00	17.05
105	12/2/20 8:00	15.9	142	12/3/20 21:00	16.64
106	12/2/20 9:00	16.6	143	12/3/20 22:00	16.24
107	12/2/20 10:00	17.2	144	12/3/20 23:00	15.86

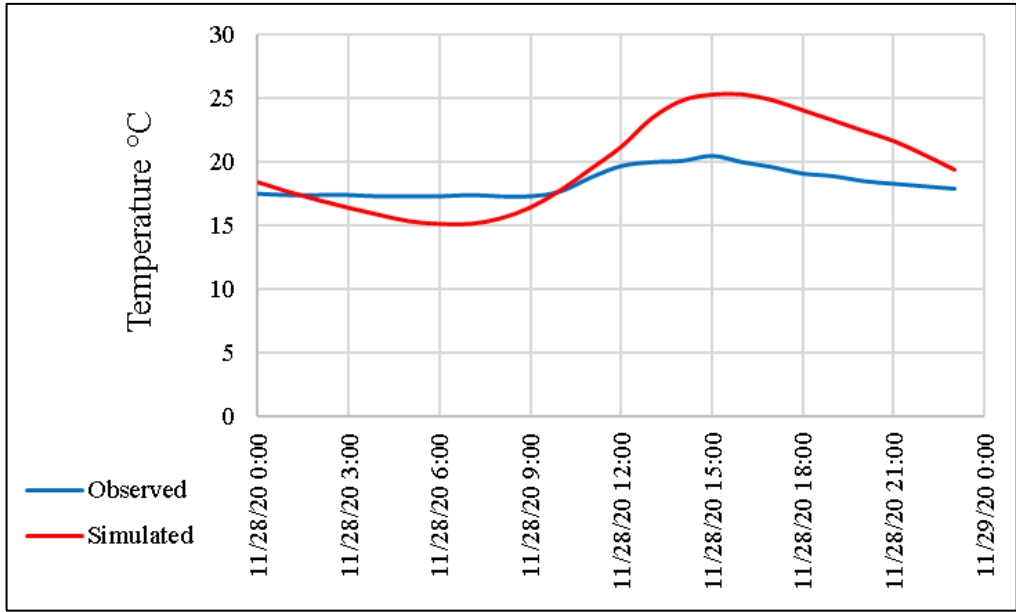


Figure Appendix A.1. Hourly observed and simulated temperature data on 28 Nov 2020.

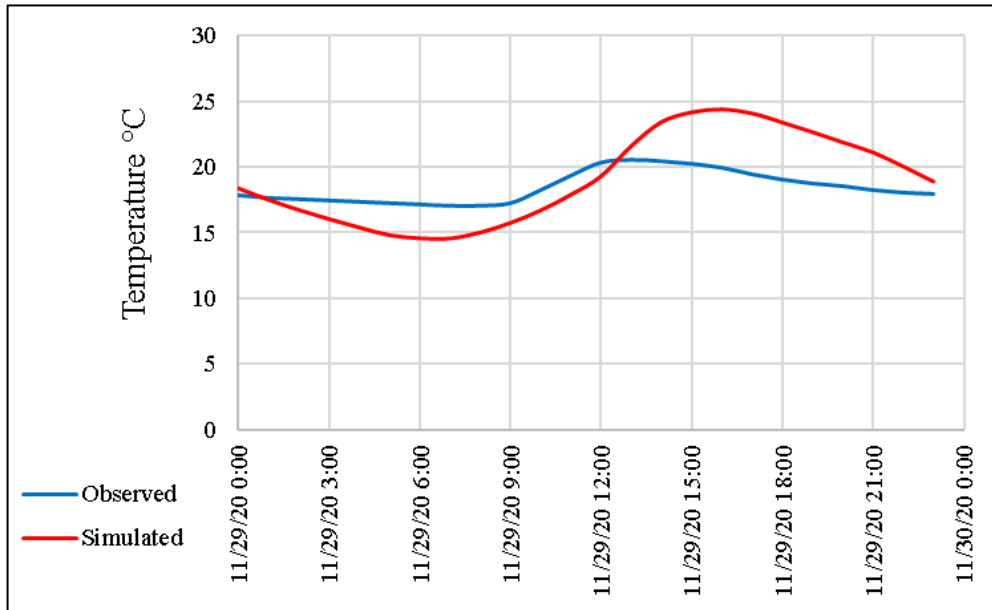


Figure Appendix A.2. Hourly observed and simulated temperature data on 29 Nov 2020.

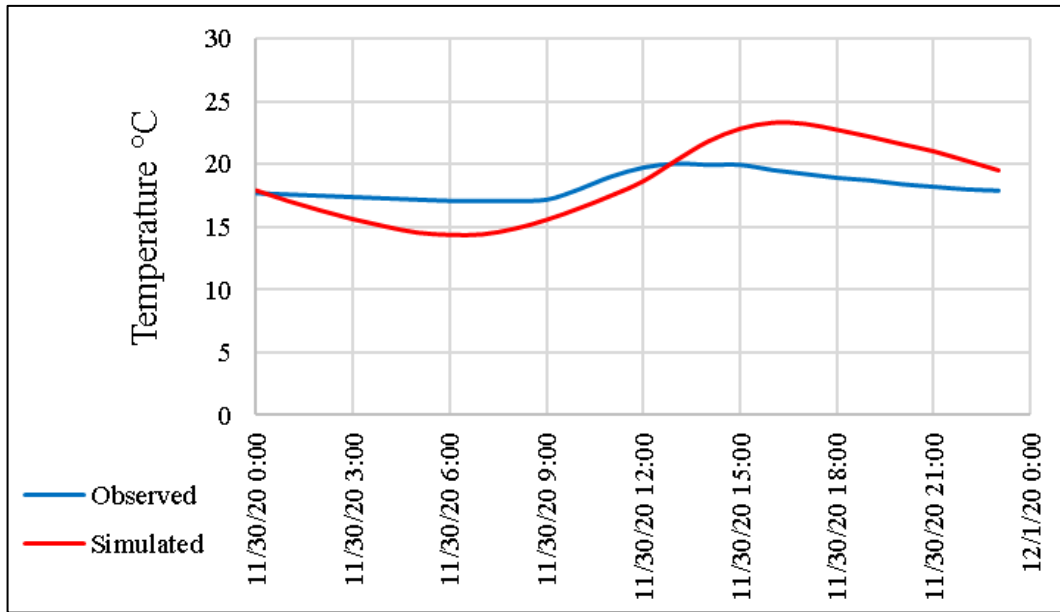


Figure Appendix A.3. Hourly observed and simulated temperature data on 30 Nov 2020.

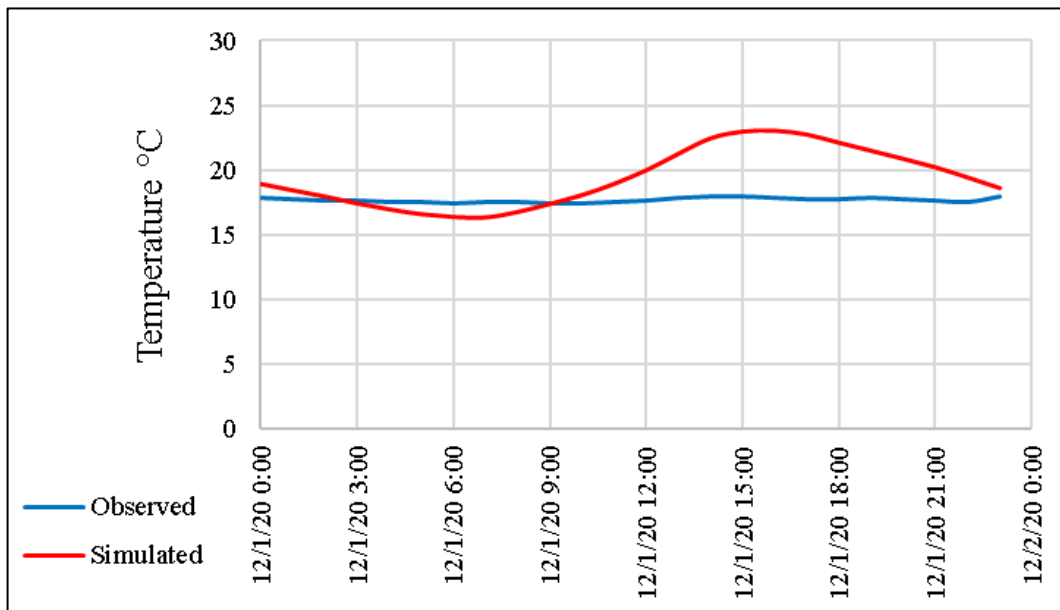


Figure Appendix A.4. Hourly observed and simulated temperature data on 01 Dec 2020.

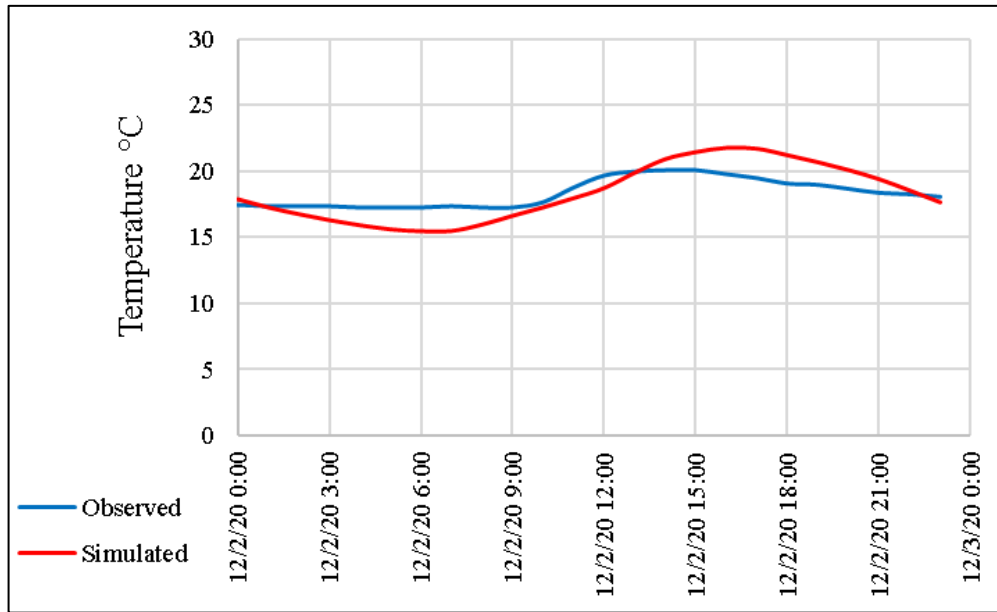


Figure Appendix A.5. Hourly observed and simulated temperature data on 02 Dec 2020.

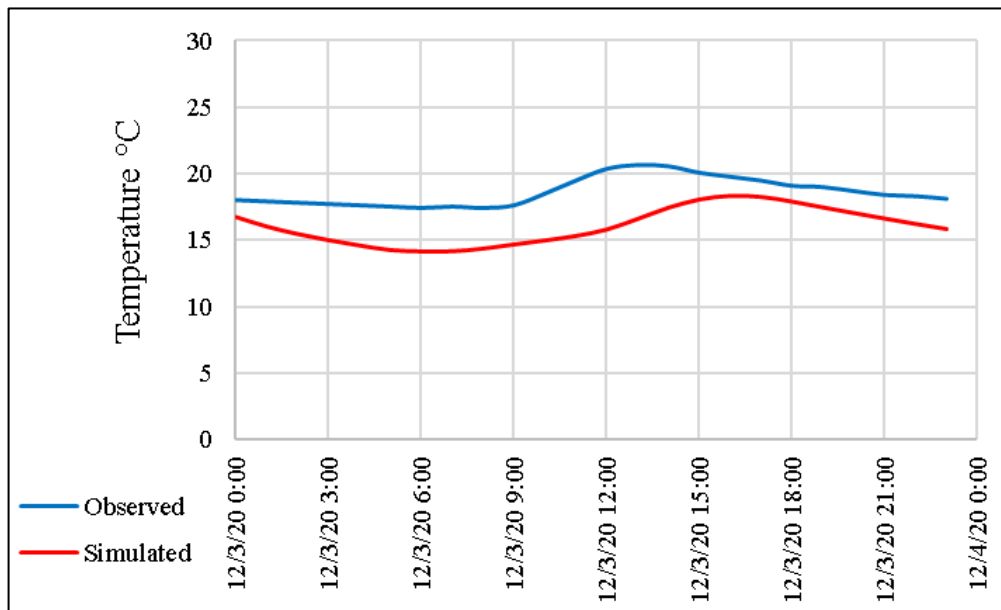


Figure Appendix A.6. Hourly observed and simulated temperature data on 03 Dec 2020.

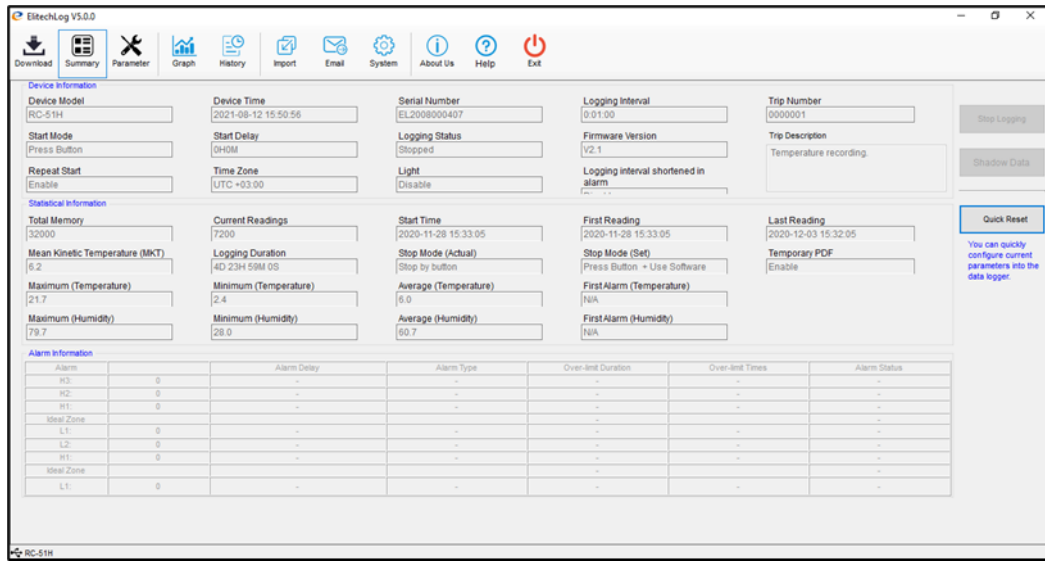


Figure Appendix A.7. ElitechLogWin software

APPENDIX B: WORKFLOW TO CREATE ENERGY MODEL IN THE SIMULATION SOFTWARE

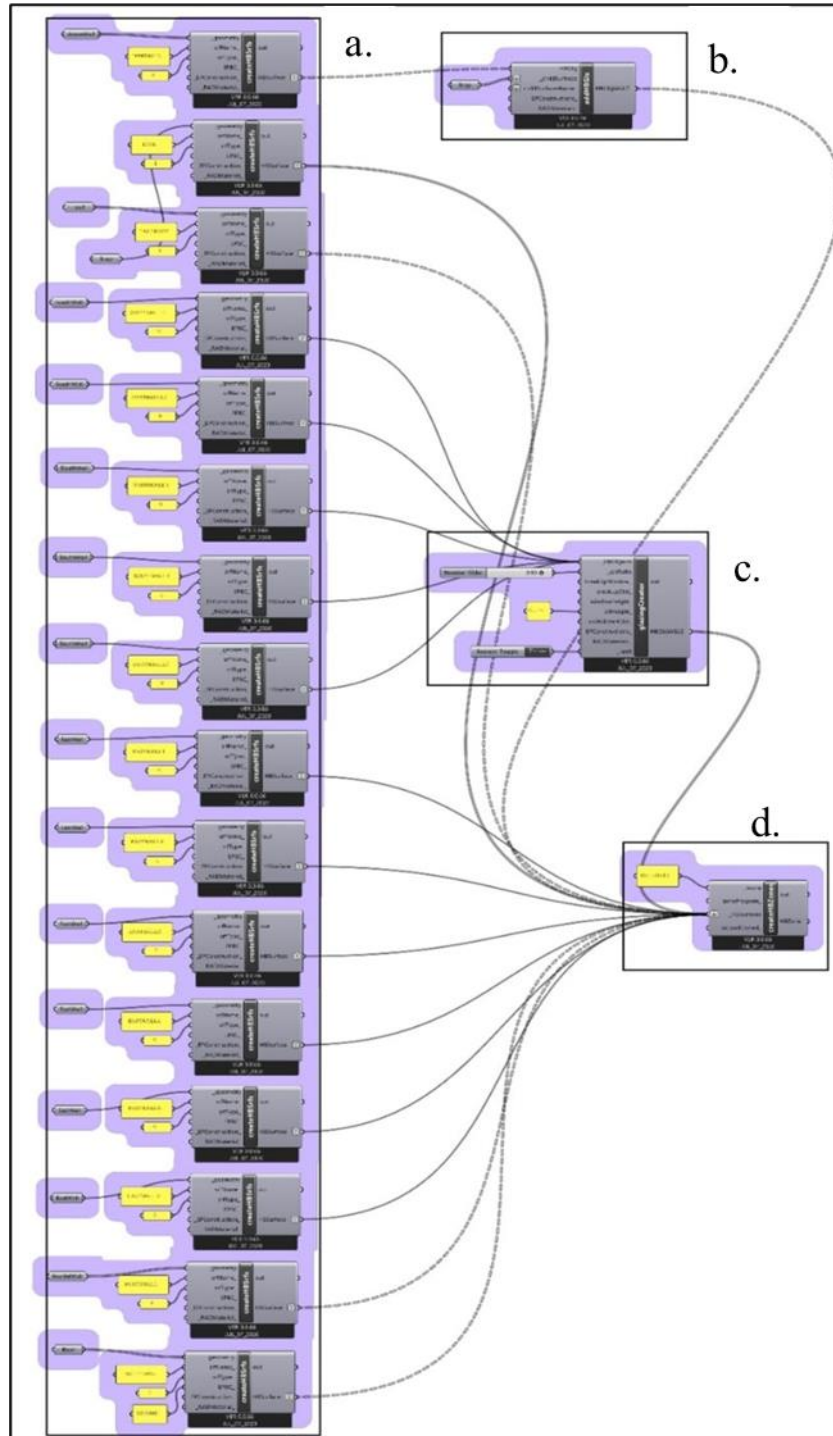


Figure Appendix B.1. Creating Honeybee Zone: a. Create surfaces, b. Set the window, c. Set glazing ratio, d. United all components to make HB Zone.

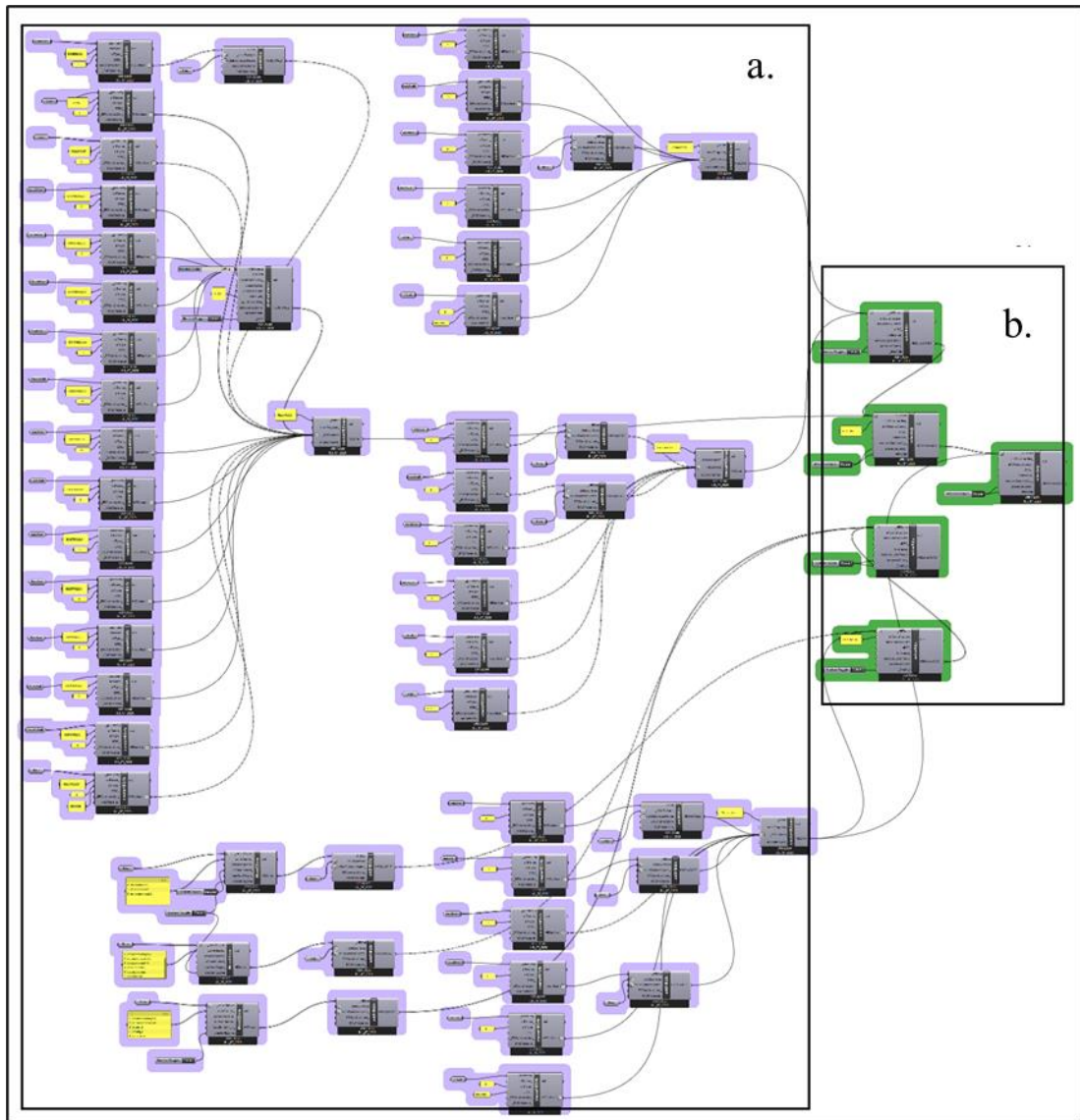


Figure Appendix B.2. Creating the Honeybee energy model, a. Create building zones, b. unite and adjoin all zones to create the energy model.

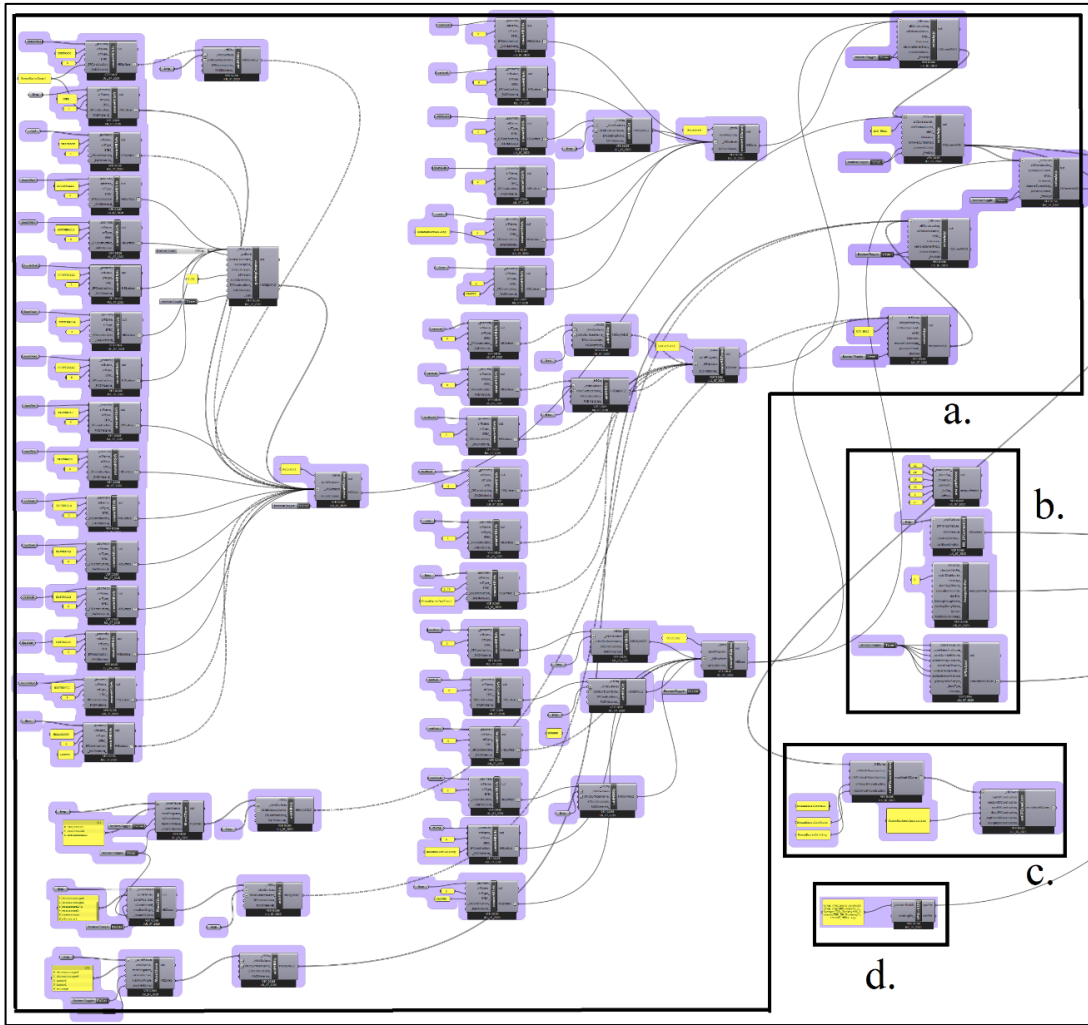


Figure Appendix B.3. Preparing the energy model to be simulated, a. Create energy model, b. simulation parameters, c. Construction materials, d. Weather file.

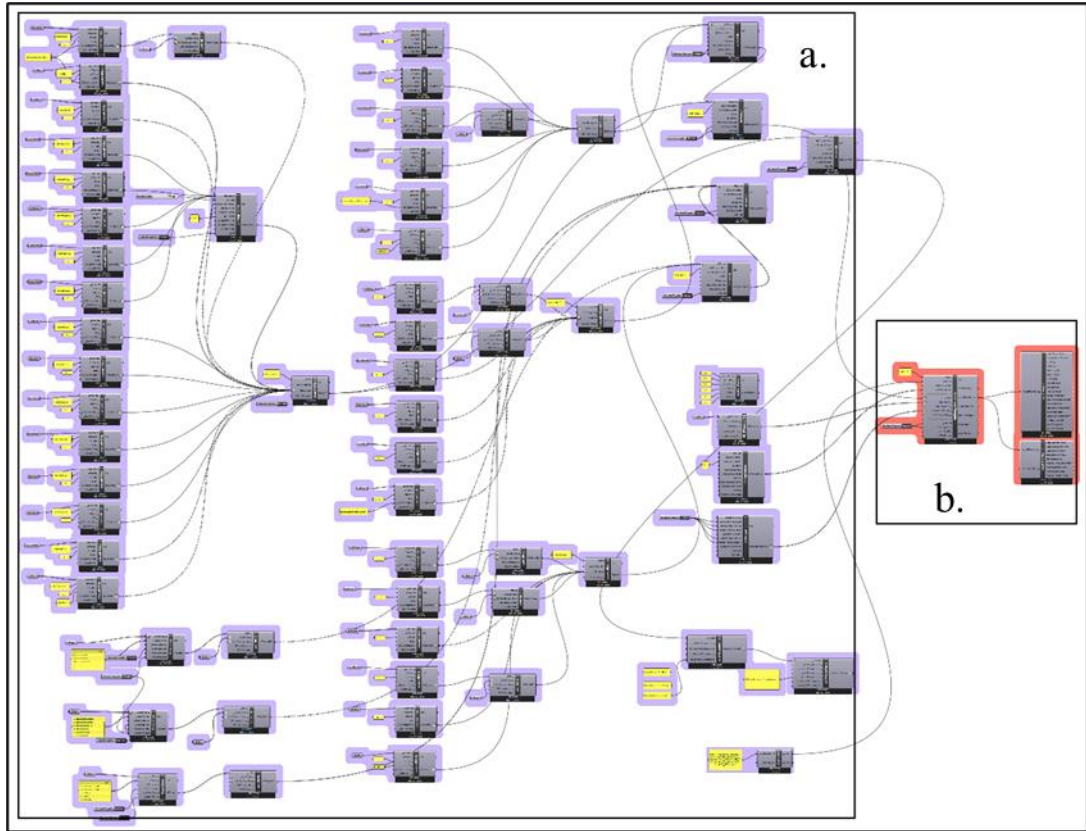


Figure Appendix B.4. Preparing the energy model to be simulated, a. Create energy model, b. Running the simulation and presenting the results.

APPENDIX C: TABLES OF MONTHLY AVERAGE OF PMV&PPD

Table Appendix C.1. Monthly average PMV&PPD the existing model.

	PMV	PPD
Jan	-3.18555	87.42083
Feb	-2.36022	77.33739
Mar	-1.46668	58.09394
Apr	0.344757	37.97127
May	0.685627	37.66011
Jun	1.935252	63.53005
Jul	2.958429	85.76478
Aug	3.361144	92.64868
Sep	2.511287	74.41519
Oct	0.826765	43.74141
Nov	-1.12137	49.80264
Dec	-3.07953	92.11216

Table Appendix C.2. Monthly average PMV&PPD wall with 80mm insulation.

	PMV	PPD
Jan	-3.12568	86.56931
Feb	-2.29598	76.04895
Mar	-1.4072	56.91627
Apr	0.397695	38.49921
May	0.733586	38.53661
Jun	1.975471	64.40931
Jul	2.994486	86.20577
Aug	3.403549	93.0112
Sep	2.560499	75.30164
Oct	0.884917	44.46291
Nov	-1.05703	49.10892
Dec	-3.02907	91.3662

Table Appendix C.3. Monthly average PMV&PPD wall with 100mm insulation.

	PMV	PPD
Jan	-3.10166	86.22783
Feb	-2.26997	75.52671
Mar	-1.38374	56.46274
Apr	0.419188	38.69902
May	0.752501	38.87385
Jun	1.991703	64.76433
Jul	3.00907	86.38763
Aug	3.420431	93.16108
Sep	2.580463	75.66596
Oct	0.907166	44.72957
Nov	-1.03215	48.84801
Dec	-3.00843	91.05399

Table Appendix C.4. Monthly average PMV&PPD wall with 150mm insulation.

	PMV	PPD
Jan	-3.06481	85.70503
Feb	-2.22897	74.68543
Mar	-1.34847	55.77324
Apr	0.451794	38.99725
May	0.781304	39.37844
Jun	2.016587	65.31108
Jul	3.031553	86.67635
Aug	3.446387	93.40017
Sep	2.611192	76.23335
Oct	0.941749	45.14745
Nov	-0.99399	48.43469
Dec	-2.97643	90.5652

Table Appendix C.5. Monthly average PMV&PPD wall with 200mm insulation.

	PMV	PPD
Jan	-3.04441	85.41721
Feb	-2.207	74.24485
Mar	-1.32947	55.38914
Apr	0.4692	39.14162
May	0.796483	39.63525
Jun	2.02932	65.59466
Jul	3.042689	86.82638
Aug	3.459352	93.52529
Sep	2.62641	76.52626
Oct	0.96012	45.36238
Nov	-0.97319	48.20233
Dec	-2.95882	90.29988

Table Appendix C.6. Monthly average PMV&PPD floor with 75mm insulation.

	PMV	PPD
Jan	-3.27924	88.15546
Feb	-2.42203	78.35066
Mar	-1.48800	58.80551
Apr	0.38605	39.03888
May	0.74281	39.17487
Jun	2.03396	65.62358
Jul	3.09676	87.39011
Aug	3.51788	94.09017
Sep	2.62565	76.36549
Oct	0.87650	44.92017
Nov	-1.14101	50.48368
Dec	-3.14913	92.66316

Table Appendix C.7. Monthly average PMV&PPD floor with 100mm insulation.

	PMV	PPD
Jan	-3.26143	87.69413
Feb	-2.37779	77.50972
Mar	-1.44541	58.1702
Apr	0.463303	39.82939
May	0.806903	40.18184
Jun	2.114076	67.32683
Jul	3.197309	88.62531
Aug	3.642294	95.12571
Sep	2.753096	78.57462
Oct	0.9806	46.20425
Nov	-1.06307	49.72349
Dec	-3.14913	92.66316

Table Appendix C.8. Monthly average PMV&PPD roof with 150mm insulation.

	PMV	PPD
Jan	-3.13222	86.73564
Feb	-2.30398	76.29834
Mar	-1.4256	57.24918
Apr	0.380838	38.06731
May	0.707363	37.75437
Jun	1.950101	63.88852
Jul	2.971052	86.05033
Aug	3.382392	92.92996
Sep	2.551261	75.23238
Oct	0.879114	44.14559
Nov	-1.05947	48.98874
Dec	-3.02975	91.46428

Table Appendix C.9. Monthly average PMV&PPD WWR 75%.

	PMV	PPD
Jan	-3.30194	90.04484
Feb	-2.52005	81.28596
Mar	-1.60601	60.11147
Apr	0.20421	35.30852
May	0.589421	35.06199
Jun	1.859928	62.05525
Jul	2.876074	85.12181
Aug	3.230702	92.03027
Sep	2.314174	71.50117
Oct	0.638927	40.31534
Nov	-1.30778	50.48587
Dec	-3.16754	94.0335

Table Appendix C.10. Monthly average PMV&PPD WWR 50%.

	PMV	PPD
Jan	-3.53502	95.30733
Feb	-2.82208	89.54501
Mar	-1.85249	64.80385
Apr	-0.06162	31.50426
May	0.42229	31.0063
Jun	1.719873	58.9576
Jul	2.717586	83.36312
Aug	3.000836	90.54635
Sep	2.000116	65.53341
Oct	0.272531	33.46081
Nov	-1.62988	54.54194
Dec	-3.30671	96.39142

Table Appendix C.11. Monthly average PMV&PPD WWR 30%.

	PMV	PPD
Jan	-3.68618	97.73276
Feb	-3.02374	94.22902
Mar	-2.03542	69.64334
Apr	-0.24125	30.10876
May	0.282644	28.01823
Jun	1.599131	55.95234
Jul	2.582195	81.47928
Aug	2.809933	88.81956
Sep	1.771814	60.12249
Oct	0.028417	29.46884
Nov	-1.85735	59.81296
Dec	-3.41992	97.69791

Table Appendix C.12. Monthly average PMV&PPD triple glazing with 6mm cavity.

	PMV	PPD
Jan	-3.19335	88.59625
Feb	-2.40446	79.02463
Mar	-1.52221	58.14209
Apr	0.277856	35.07111
May	0.637326	35.15785
Jun	1.895145	63.10922
Jul	2.905508	85.9131
Aug	3.275969	92.87128
Sep	2.393219	73.4852
Oct	0.739928	41.10567
Nov	-1.18892	48.32392
Dec	-3.07779	93.00073

Table Appendix C.13. Monthly average PMV&PPD triple glazing with 10mm cavity.

	PMV	PPD
Jan	-3.19335	88.59625
Feb	-2.40446	79.02463
Mar	-1.52221	58.14209
Apr	0.277856	35.07111
May	0.637326	35.15785
Jun	1.895145	63.10922
Jul	2.905508	85.9131
Aug	3.275969	92.87128
Sep	2.393219	73.4852
Oct	0.739928	41.10567
Nov	-1.18892	48.32392
Dec	-3.07779	93.00073

Table Appendix C.14. Monthly average PMV&PPD double glazing with low-E panels.

	PMV	PPD
Jan	-2.73789	80.34755
Feb	-1.83113	66.6541
Mar	-1.01748	48.84074
Apr	0.817264	41.28765
May	1.04105	42.55223
Jun	2.297336	72.5043
Jul	3.321664	91.36162
Aug	3.789397	97.04235
Sep	3.059092	84.9927
Oct	1.382812	50.96138
Nov	-0.58021	43.23672
Dec	-2.68336	86.01192

Table Appendix C.15. Monthly average PMV&PPD Green roof with 100 mm insulation.

	PMV	PPD
Jan	-3.1098	86.30307
Feb	-2.26632	75.59224
Mar	-1.39739	56.75435
Apr	0.412198	38.1831
May	0.762356	38.20213
Jun	2.008991	65.20897
Jul	3.03137	87.08511
Aug	3.436965	93.53899
Sep	2.597724	76.05498
Oct	0.919317	44.54121
Nov	-1.02966	48.75053
Dec	-3.02374	91.33849

Table Appendix C.16. Monthly average PMV&PPD Green roof with 150 mm insulation.

	PMV	PPD
Jan	-3.08205	85.93559
Feb	-2.23832	75.05377
Mar	-1.37837	56.35928
Apr	0.428598	38.28575
May	0.762209	38.20275
Jun	2.003355	65.08873
Jul	3.02369	86.9608
Aug	3.439696	93.55556
Sep	2.613233	76.37301
Oct	0.943556	44.75586
Nov	-0.99559	48.31964
Dec	-2.99182	90.90091

Table Appendix C.17. Monthly average PMV&PPD Green roof without insulation.

	PMV	PPD
Jan	-3.40368	89.76222
Feb	-2.55157	80.95704
Mar	-1.59866	60.83224
Apr	0.243736	36.76264
May	0.761464	37.73832
Jun	2.061549	66.38199
Jul	3.102619	88.60878
Aug	3.393799	93.48756
Sep	2.435983	72.85189
Oct	0.669137	42.22781
Nov	-1.37949	53.60552
Dec	-3.33944	94.94085

Table Appendix C.18. Monthly average PMV&PPD Retrofitted model (SC5).

	PMV	PPD
Jan	-2.715488	86.806218
Feb	-2.048158	73.056345
Mar	-1.282481	47.884986
Apr	0.290296	29.24477
May	0.616734	32.005354
Jun	2.050743	66.579447
Jul	3.268681	88.921831
Aug	3.603215	95.677356
Sep	2.422016	74.327348
Oct	0.514855	34.287785
Nov	-1.06546	39.210763
Dec	-2.48221	86.247599

APPENDIX D: PHOTOGRAPHS OF SOME OF THE MODERN MOSQUES IN TURKEY

All photos were retrieved from Abdullatif Alfozan Award For Mosque Architecture website (<https://mosqpedia.org/>).



Figure Appendix D.1. Alacaatlı Uluyol Mosque, Ankara, Turkey.



Figure Appendix D.2. Mogan Gölü Mosque, Ankara, Turkey.



Figure Appendix D.3. Fatih Üniversitesi Mehmet Hasircilar Mosque, Istanbul, Turkey.

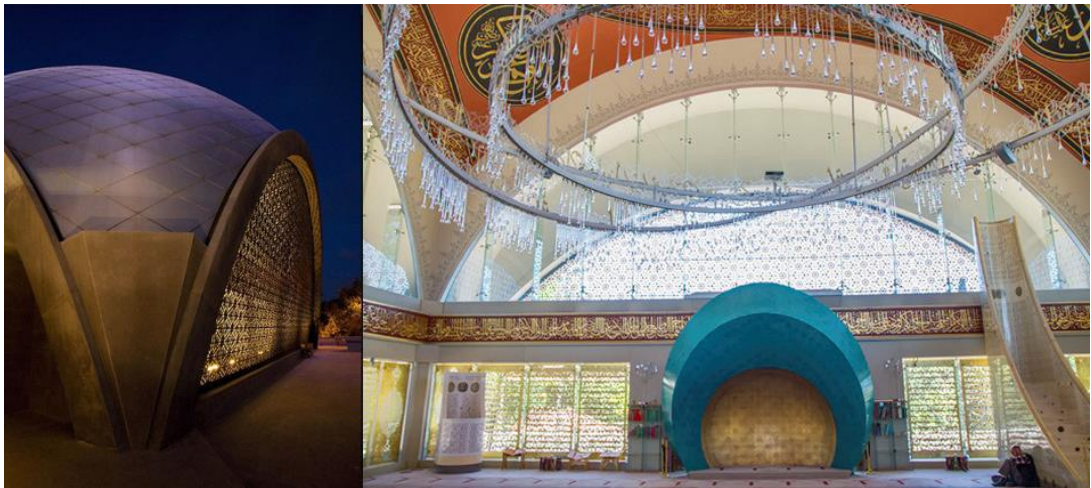


Figure Appendix D.4. Şakirin Mosque, Istanbul, Turkey.



Figure Appendix D.5. Marmara Theology Mosque, Istanbul, Turkey.



Figure Appendix D.6. GOSB Mosque, Kocaeli, Turkey.



Figure Appendix D.7. Alaçatı Süreyya ve Muzaffer Baskıncı Mosque, Izmir, Turkey.



Figure Appendix D.8. Pezberg Mosque, Penzberg, Germany.

RESUME

Hosam Mohamed Abdulsalam DWELA is a Libyan citizen. He was born in Libya in 1983. He completed his primary and secondary education in his hometown of Zintan, after that, he started the undergraduate program in Aljabal Algharbi University Department of Architecture in 2002. Then in 2019, to start his M. Sc. education, he moved to Karabük University.